Université de Montréal

Synthesis and Characterization of Main-Chain Bile Acid-Based Degradable Polymers

par

Jie Zhang

Département de chimie

Faculté des arts et des sciences

Mémoire de Maîtrise présenté à la Faculté des études supérieures en vue de l'obtention du grade de Maîtrise en chimie

Mars 2010

Université de Montréal

Faculté des études supérieures

Ce mémoire intitulé

Synthesis and Characterization of Main-Chain Bile Acid-Based Degradable Polymers

présenté par

Jie Zhang

a été évalué par un jury composé des personnes suivantes :

Richard Martel，président-rapporteur

Julian X. Zhu，directeur de recherche

Robert E. Prud'homme，membre du jury

Mémoire accepté le :

RÉSUMÉ

Les acides biliaires sont des composés naturels existants dans le corps humain. Leur biocompatibilité, leur caractère amphiphile et la rigidité de leur noyau stéroïdien, ainsi que l'excellent contrôle de leurs modifications chimiques, en font de remarquables candidats pour la préparation de matériaux biodégradables pour le relargage de médicaments et l'ingénierie tissulaire.

Nous avons préparé une variété de polymères à base d'acides biliaires ayant de hautes masses molaires. Des monomères macrocycliques ont été synthétisés à partir de dienes composés de chaînes alkyles flexibles attachées à un noyau d'acide biliaire via des liens esters ou amides. Ces synthèses ont été réalisées par la fermeture de cycle par métathèse, utilisant le catalyseur de Grubbs de première génération. Les macrocycles obtenus ont ensuite été polymérisés par ouverture de cycle, entropiquement induite le catalyseur de Grubbs de seconde génération. Des copolymères ont également été préparés à partir de monolactones d'acide ricinoléique et de monomères cycliques de triester d'acide cholique via la même méthode.

Les propriétés thermiques et mécaniques et la dégradabilité de ces polymères ont été étudiées. Elles peuvent être modulées en modifiant les différents groupes fonctionnels décorant l'acide biliaire et en ayant recours à la copolymérisation. La variation des caractéristiques physiques de ces polymères biocompatibles permet de moduler d'autres propriétés utiles, tel que l'effet de mémoire de forme qui est important pour des applications biomédicales.

Mots-clés : Acide biliaire, biocompatibilité, caractère amphiphile, métathèse par fermeture de cycle, polymérisation par ouverture de cycle.

ABSTRACT

Bile acids are natural compounds in the body. Their biocompatibility, facial amphiphilicity, rigidity of steroid nucleus, and ease of chemical modification make them excellent candidates as building blocks for making biodegradable materials used in drug delivery and tissue engineering applications.

We have prepared main-chain bile acid-based polymers having high molecular weights. Macrocyclic monomers were synthesized from dienes, which consist of flexible alkyl chains attached to a bile acid core through either ester or amide linkages, via ring closing metathesis using first-generation Grubbs catalyst. They were polymerized using entropy-driven ring-opening metathesis polymerization using second-generation Grubbs catalyst. Copolymers were also prepared from monolactone of ricinoleic acid and cholic acid-based cyclic triester monomer via the same method.

The thermal and mechanical properties and degradation behaviours of these polymers have been investigated. The properties can be tuned by varying the chemical linking with the bile acid moiety and by varying the chemical composition of the polymers such as copolymerization with ricinoleic acid lactones. The tunability of the physical properties of these biocompatible polymers gives access to a range of interesting attributes. For example, shape memory properties have been observed in some samples. This may prove useful in the design of materials for biomedical applications.

Keywords : Bile acids, biocompatibility, amphiphilicity, ring closing metathesis, ring opening metathesis polymerization

TABLE OF CONTENTS

LIST OF FIGURES

LIST OF TABLES

LIST OF SYMBOLS AND ABBREVIATIONS

ADMET	Acyclic diene metathesis polymerization
CAC	Critical aggregation concentration
CM	Cross-metathesis
DCM	Dichoromethane
DMA	Dynamic mechanical analysis
COSY	COrrelated SpectroscopY
DS	Degree of substitution
DSC	Differential scanning calorimetry
E	Young's modulus
ED-ROMP	Entropy-driven ring-opening metathesis polymerization
FDA	Food and Drug Administration (USA)
GPC	Gel permeation chromatography
HMQC	Heteronuclear multiple quantum correlation
IR	Infrared spectroscopy
LC	Liquid crystalline
LS	Light scattering
MALDI-TOF	Matrix-assisted laser desorption/ionization time-of-flight
MS	Mass spectrometry
NHC	N-heterocyclic carbine
NMR	Nuclear magnetic resonance spectroscopy
PDI	Polydispersity index
PGA	Polyglycolides
PLA	Polylactides
POM	Polarizing optical microscopy
PSA	Poly(sebacic anhydride)
RCA	Ricinoleic acid
RCM	Ring-closing metathesis

R_f	Strain fixity
RMS	root-mean-square
ROMP	Ring opening metathesis polymerization
R_r	Strain recovery
SEC	Size exclusion chromatography
T_g	Glass transition temperature
TGA	Thermogravimetric analysis
THF	Tetrahydrofuran
TLC	Thin layer chromatography
ε_m	Maximum strain
ε_p	Strain after recovery above T_g
ε_u	Strain after relaxation below T_g

ACKNOWLEDGEMENTS

This Mémoire is so far the most important and difficult achievement in my life. Many people gave me generous help when I had difficulties. I could not accomplish it without them.

First of all, I would like to thank my research supervisor, Professor Julian X. X. Zhu of the Chemistry Department at Université de Montréal. His diligence, erudition and scientific rigor inspired me to make the right choice when I faced difficulties and he helped me to develop good research habits. This will be very beneficial in my future life and career.

I wish to thank Dr. Julien E. Gautrot for helping me understanding the general concepts about this project. I am very grateful to Professor Qiang Wu from Nankai University in China for his help and cooperation. I also want to thank Dr. Yu Shao for his help in my synthesis work. I sincerely thank Dr. Kimberly Metera for correcting this Mémoire. I also wish to thank Dr. Qian Zhang for his kind help when I studied the liquid crystalline properties of one of my polymers and for correcting the liquid crystalline part in my Mémoire.

I want to thank all my friends in the group: Dr. Marc Gauthier, Dr. Huiyou Liu, Dr. Stephen G. Holden, Dr. Cédric Malveau, Dr. Héloïse Thérien-Aubin, Dr. Xin Jia, Dr. Tarek Kassem, Dr. Kai Wu, Dr. Ning Zhao, Gwénaëlle Bazin, Guillaume Giguère**,** Yujuan Wang, Sam Ge, Florence Janvier, Shanshan Chen, Yilong Chen, Bao Toan Nguyen…

My family gave me the spiritual support, which is very important to inspire me to continue and finish my study. I thank my wife Yunxia Wu and my two sons Lei and Fan.

1 Introduction

For several decades now, drug delivery and tissue engineering, two important areas in the field of biomedical engineering, have drawn much research interest. Scientists made great effort to find materials that could deliver pharmaceutical substances to targeted areas in the body in a controlled way, or materials that could support and stimulate cell growth. In both cases, the materials should be biocompatible to avoid triggering a strong immune response, and sometimes biodegradable in order to degrade after accomplishing their tasks.[1]

Suitable materials having these properties can be divided into two main classes: natural[2-4] and synthetic polymers.[2,3,5-9] Natural polymers may be the most promising candidates for biomedical applications due to their inherent advantages.[10] However, natural polymers still have some short-comings: they may trigger immune responses at the implantation site;[11,12] their stability and mechanical properties are often relatively poor;[4,13] and their toxicity may be a problem.[1] In comparison with natural polymers, synthetic polymers possess better qualities, such as the ease in processing and good mechanical properties.[1]

Bile acids are natural compounds that exist in the bile of most animals. Materials based on bile acids, when used for biomedical purposes, present lower toxicity for their degradation products.[14] Thus, these materials show great promise in drug delivery and tissue engineering.[15]

1.1 Bile acids

Bile acids are compounds in the steroid family that help during the digestion of fat by forming micellar aggregates. Biosynthesized from cholesterol by the liver, bile acids are conjugated with taurine or glycine and stored in the gallbladder. Taurocholic acid and glycocholic acid (derivatives of cholic acid) account for eighty percent of all bile acids in a human body.[16]

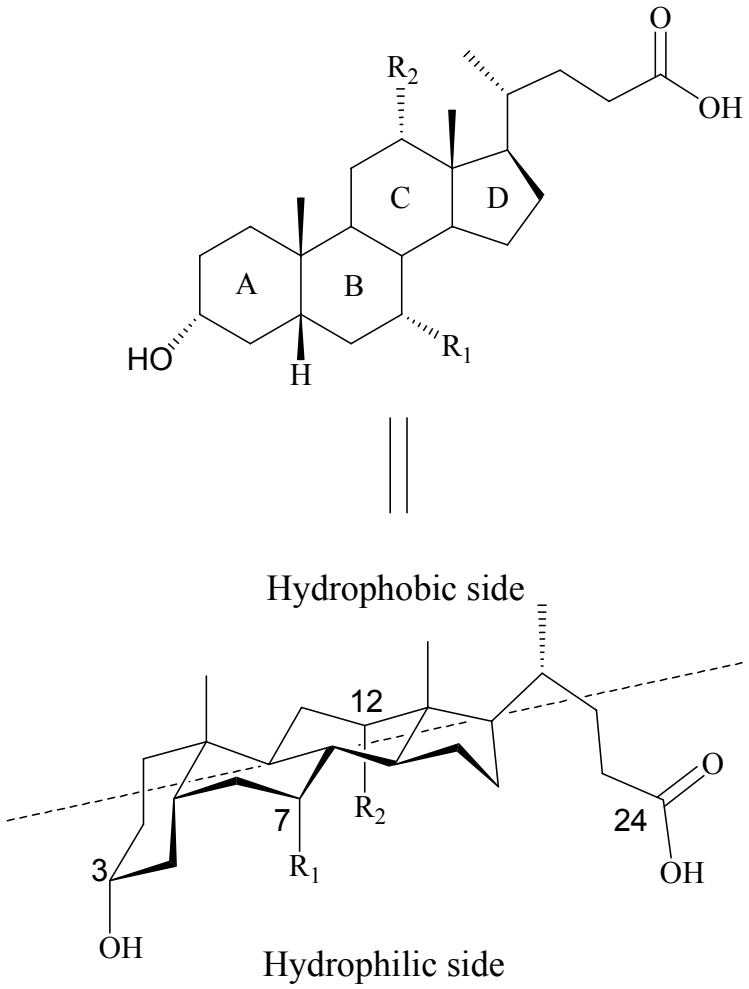

Bile acid	R_1	R_2
Cholic acid	OH	OH
Deoxycholic acid	H	OH
Chenodeoxycholic acid	OH	H
Lithocholic acid	H	H

Figure 1.1. Chemical structure of bile acids.

Bile acids contain a rigid steroid nucleus and a short aliphatic side chain (shown in Figure 1.1). The steroid nucleus consists of three six-membered rings (A, B and C) and a five-membered ring (D). In contrast to the cholestane steroids, which are trans isomers, the cis connection between rings A and B bends the steroid skeleton, and results in the formation of a cavity[17] and two faces having different properties. The face with the carboxylic group at position 24 and several hydroxyl groups directed toward the cavity is hydrophilic. The other face is hydrophobic and contains three methyl groups. Because of its facial amphiphilicity, bile acids can form micelles with back-to-back hydrophobic interactions.[18,19]

Bile acids possess several chiral centers and have two to four functional groups that can be used to form chemical links with other molecules (Figure 1.1). An ester or ether bond can be formed from the hydroxyl group at position 3. Ester or ether bonds can also be formed from the hydroxyl groups at positions 7 and 12, although the reactivity of the axial hydroxyl groups is much lower than the equatorial one at position 3. Furthermore, an ester or amide bond can be formed from the carboxylic group at position 24.[1,17]

The interesting properties of bile acids make them useful building blocks in the design of new polymeric materials. These materials may retain some of the properties of bile acids, such as the rigidity, chemical stability, chirality, facial amphiphilicity, capacity of self-assemble and reactivity of functional groups. In general, polymers based on bile acids include bile acids in the main chain,[15,20,21] bile acids as pendent groups,[22-26] and star-shaped polymers with bile acids as the core.[27-34]

1.2 Biodegradable polymers based on bile acids

In the last 30 years, biodegradable biomaterials have been developed for related applications.[10,35] Based on the current trend, it has been predicted that, in the near future, most of prosthetic devices for temporary use will be made from biodegradable polymers.[10]

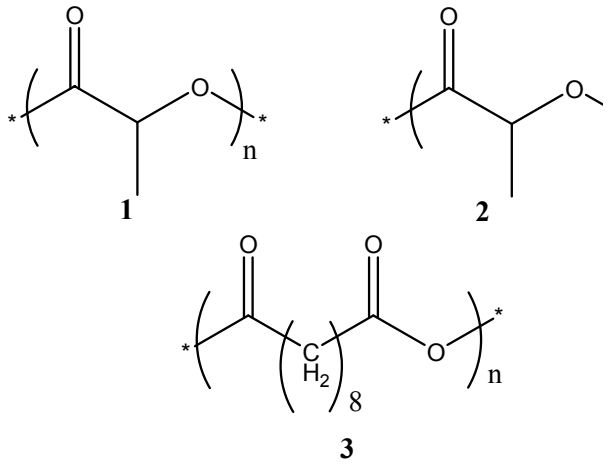

Figure 1.2. Structures of selected biodegradable polymers: (1) Polylactides; (2) Polyglycolides; (3) Polysebacic anhydrides.

Biodegradable polymers can be divided into natural polymers such as polysaccharides (starch, cellulose, chitin, chitosan and alginic acid), polypeptides of natural origin and bacterial polyesters, and synthetic polymers such as polyesters, polyamides and polyanhydrides.[36] In comparison with natural polymers, synthetic polymers are more versatile in chemical structure and their mechanical and biodegradable biocompatible properties can be easily tuned.[1] Several synthetic polymers, such as polylactides (PLA), polyglycolides (PGA) and polysebacic anhydrides (PSA, Figure 1.2), approved by the USA Food and Drug Administration (FDA), are subjects of intensive reseach[37-41] and show promise for biomaterial applications. However, these polymers are based on small aliphatic molecules that induce a high level of crystallinity. As a result, their mechanical and degradable properties still need to be improved. Therefore, it is necessary to introduce comonomers such as ricinoleic acid to improve the properties of these polymers. Furthermore, the acidic degradation products of these polymers may cause adverse tissue reactions.[42]

When incorporated into a polymer, bile acids add new properties, such as the tuning of the hydrophobicity and increased rigidity of the polymer chain. The tuning of the polymer properties can make it more suitable for use in the fields of drug delivery and tissue engineering.

1.2.1 Grafting of bile acids onto degradable polymers

Bile acids can be grafted to degradable polymers via their carboxylic acid group at position 24[43,44] or their hydroxyl group at position 3[45]; thus the use of an ester or amide linker at those positions improve the hydrophobicity, biocompatibility and aggregation properties of the polymers.[46-48] Many natural polymers, including polysaccharides (chitosan[47-49], glycol chitosan[50-53], heparin[54], dextran[43-45] or agarose[55]) and proteins (bovine serum albumin[56,57]) have been modified in this way with bile acids.

Kwon and co-workers studied core-shell spheres made from degradable polymers such as chitosan and glycol chitosan. They grafted bile acids onto these polymers to increase their hydrophobicity[47-49] and induce aggregation in the form of nanometer-sized core-shell spheres. When deoxycholic acid-derivatized chitosan (Figure 1.3, **1**) forms such core-shell spheres, the hard hydrophobic core contains deoxycholic acid and the soft hydrophilic shell has the chitosan chain.

Nichifor et al. attached cholic acid and deoxycholic acid as pendant groups to dextran using the carboxylic group of cholic acid via an ester linker (Figure 1.3, **2**).[43,44] It was found that the critical aggregation concentration (CAC) decreases with increasing degree of substitution (DS), which is similar to the chitosan case. Meanwhile, the CAC measured for modified dextran was one order of magnitude lower than that measured for modified chitosan because chitosan is more hydrophilic than dextran. Nichifor et al. also attached cholic acid as pendant group to dextran using the hydroxyl group at position 3 of cholic acid (Figure 1.3, **3**) to increase the solubility of dextran in aqueous solution.[45] This polymer is still water-soluble even with a DS as high as 25%.

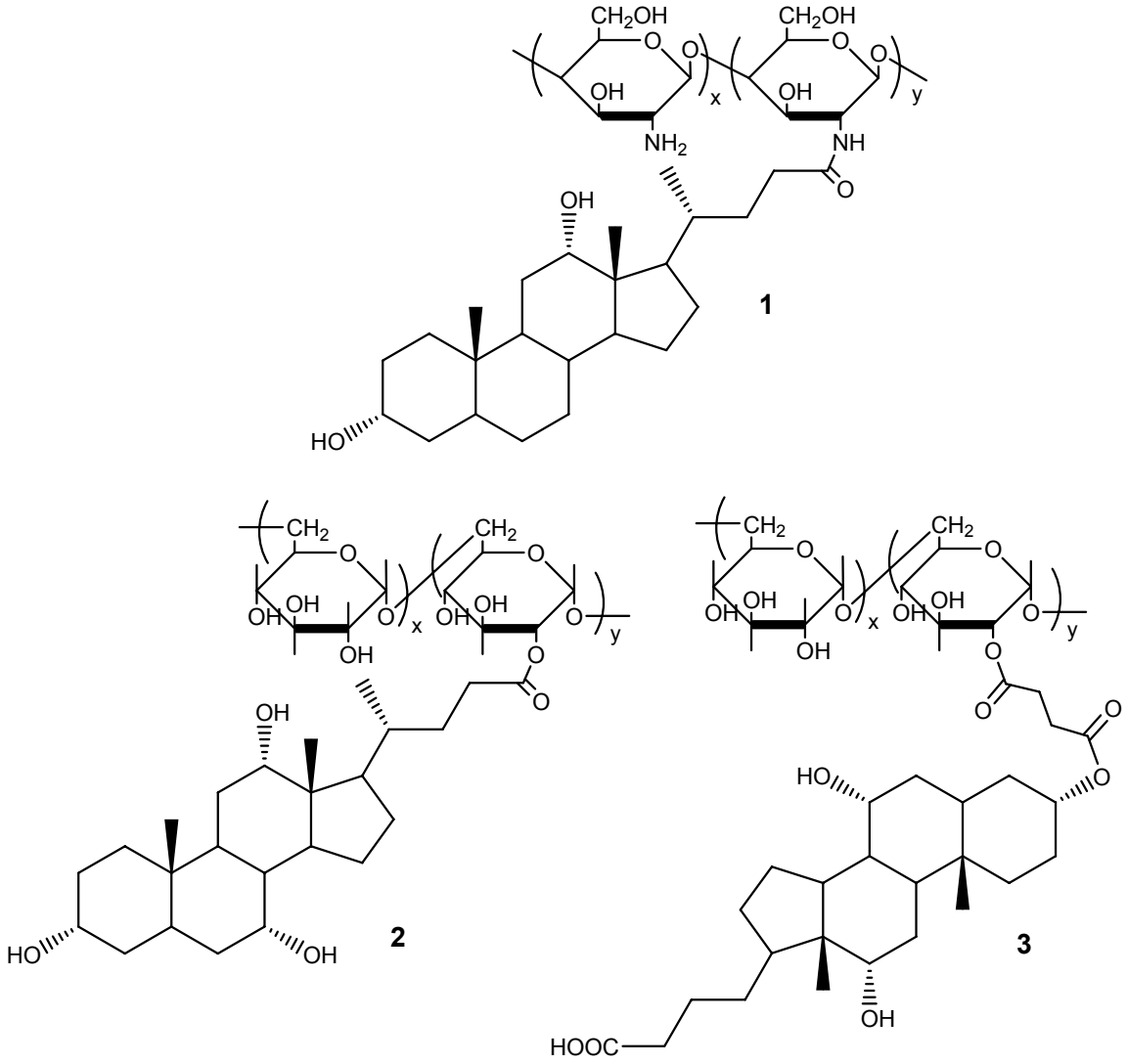

Figure 1.3. The structure of bile-acid-modified polysaccharides: (1) chitosan modified with deoxycholic acid; (2) dextran modified with cholic acid via the carboxylic group at position 24; (3) dextran modified with cholic acid via the hydroxyl group at position 3.

1.2.2 Degradable synthetic polymers based on bile acids

Bile acids can be incorporated into the backbone of synthetic polymers through an ester, anhydride or amide linkage using either polycondensation or ring-opening metathesis. However, the preparation of bile-acid-based polyesters is still a challenge and

reports on bile-acid-based polyesters are scarce. Ahlheim and Hallenleben used p-toluenesulfonic acid as a catalyst and high reaction temperature to obtain main-chain cholic acid-based and deoxycholic acid-based polyesters.[58] The polyesters obtained had low molecular weights and poor solubility in organic solvents. In other attempts to synthesize main-chain bile acid-based polyesters, Noll and Ritter used a lipase enzyme as the catalyst[59] and Zuluaga et al. used N,N-(dimethylamino)pyridine and p-toluenesulfonic acid as catalyst.[60] Polyesters with quite high molecular weights, ranging from 2.0 to 6.0 × 10^4, have been obtained by these methods at room temperature.

Three different methods can be used to prepare bile-acid-based polyanhydrides. The first developed in our group involved a selective hydrolysis of 3α-lithocholic acid methyl ester dimers, previously synthesized by linking two lithocholate methyl ester molecules with sebacoyl chloride, yielded carboxylic acid dimer (Figure 1.4, **1**).[20] After refluxing in acetic anhydride, the carboxylic acid dimer was transformed to dianhydride (Figure 1.4, **2**). This dianhydride was then polycondensed or with a comonomer such as sebacic acid to get homo- or co-polymers with various bile acid contents. The second method to prepare lithocholic-acid-based polyanhydrides, developed by Domb and co-workers, consists of using lithocholic acid as starting material for a reaction with a sebacic anhydride pre-polymer to form a diacid, which contained a lithocholic acid moiety and sebacic acid moiety linked by an ester.[61] This diacid polycondensed with varying amounts of sebacic anhydride pre-polymer, and resulted in copolymers with various contents of lithocholic acid was obtained. The molecular weight measured was from 1.2 to 6.7 × 10^4. A third method was also developed in our group involving the polycondensation of acid dimer (Figure 1.4, compound **1**) and sebacoyl chloride, and this research is still ongoing.

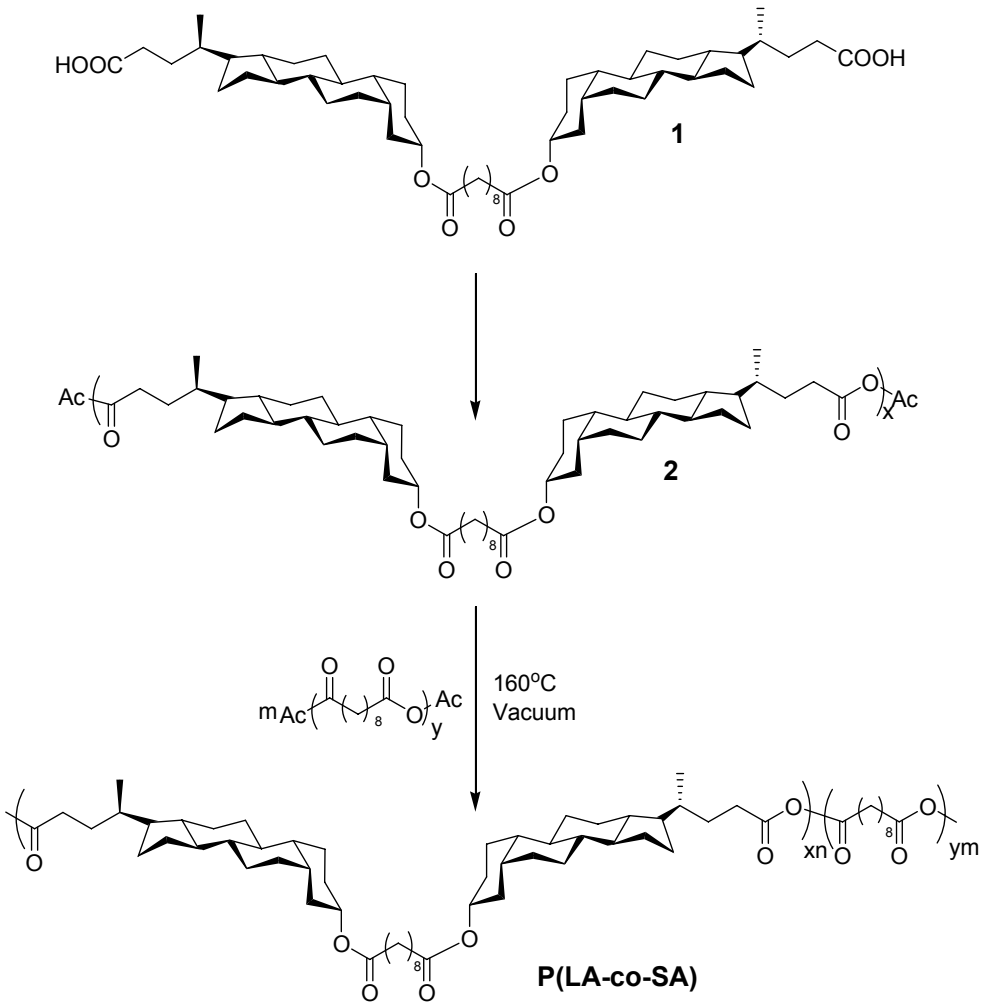

Figure 1.4. Synthesis of lithocholic acid-based polyanhydrides.

Although these polymers can be prepared by polycondensation as discussed above, their molecular weights are still relatively low. The preparation of bile acid-based degradable polymers is still a challenge to the organic chemists.

1.3 Olefin metathesis

Ring opening metathesis polymerization (ROMP) is one of the useful applications of olefin metathesis and a powerful tool for preparing polymers with high molecular weights. The word "metathesis" is derived from the Greek word for "transposition". Calderon et al. first introduced the term "olefin metathesis" in the 1960s[62-64]. The

generally accepted mechanism of olefin metathesis (shown in Figure 1.5) was originally reported by Hérisson and Chauvin in 1971[65], and subsequently validated with key experimental evidences by the Casey[66], Katz[67] and Grubbs' groups.[68-70] The revolution of synthetic chemistry caused by olefin metathesis led to the 2005 Nobel Prize in Chemistry awarded to Yves Chauvin, Robert H. Grubbs, and Richard R. Schrock.[71-73]

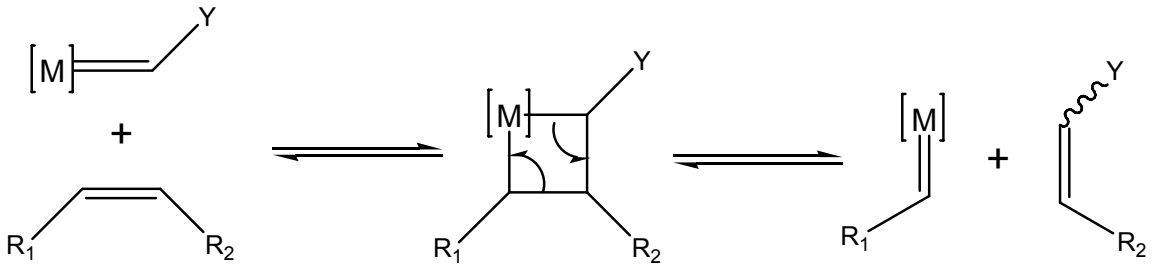

Figure 1.5. Olefin metathesis mechanism proposed by Chauvin.[65]

Olefin metathesis is a fundamental chemical reaction involving the metal-catalyzed redistribution of carbon-carbon double bonds. It can be used to couple, cleave, or polymerize olefinic molecules.[74] As shown in Figure 1.6, olefin metathesis can be applied in different ways including ring-closing metathesis (RCM), ring-opening metathesis (ROM), ring-opening metathesis polymerization (ROMP), acyclic diene metathesis polymerization (ADMET), and cross-metathesis (CM).[75] The catalyst plays a crucial role in these reactions. The early catalytic systems, such as WCl_6/Bu_4Sn, $WOCl_4/EtAlCl_2$, MoO_3/SiO_2 and Re_2O_7/Al_2O_3, are easy to prepare and cheap. Thus, these catalytic systems are used in important commercial applications of olefin metathesis[75], but they are not tolerant to most functional groups, and the reactions catalyzed by these systems are difficult to initiate or control because very few active species are formed in the catalytic mixture.[75]

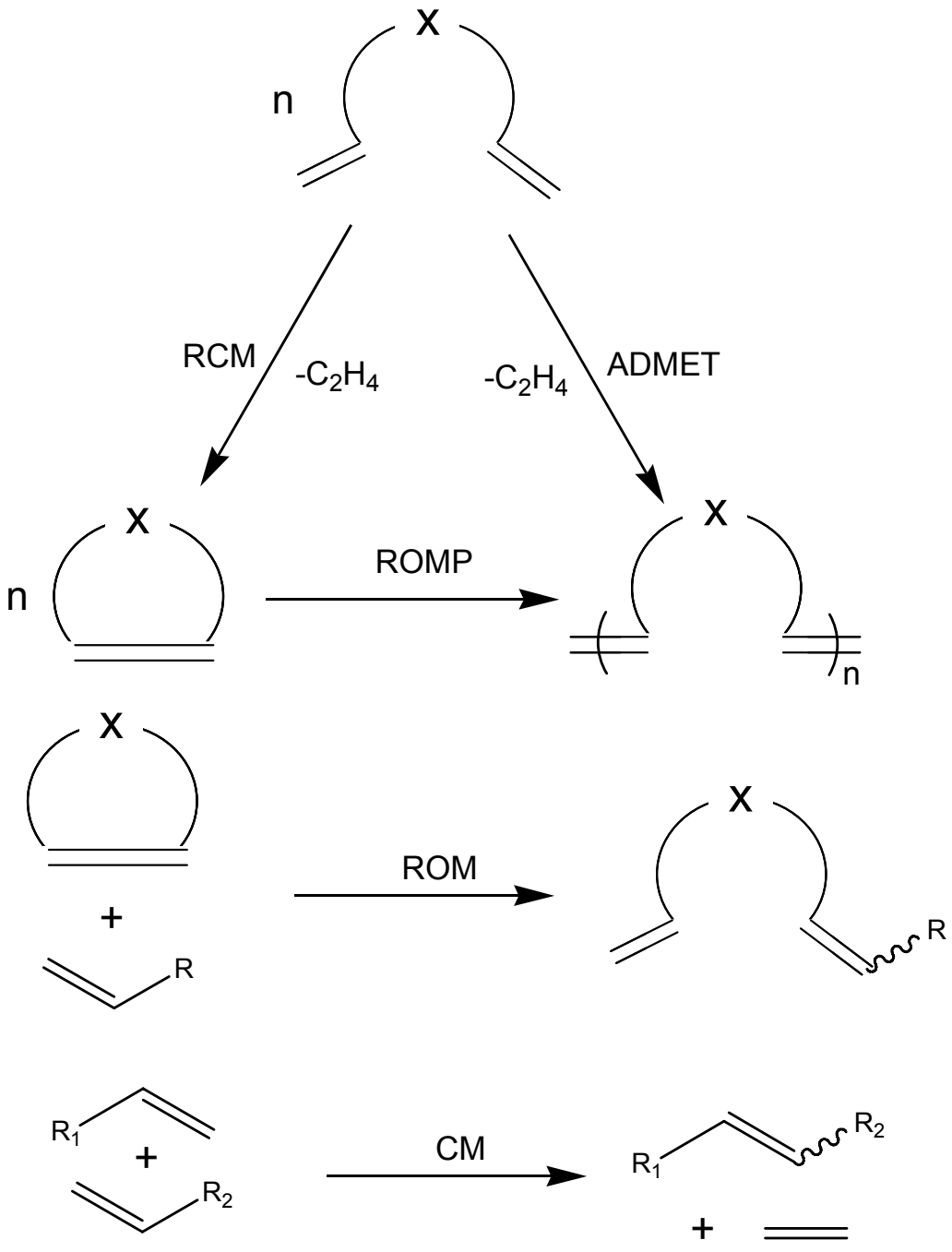

Figure 1.6. Various olefin metathesis reactions including ring-closing metathesis (RCM), ring-opening metathesis polymerization (ROMP), acyclic diene metathesis polymerization (ADMET), ring-opening metathesis (ROM), and cross-metathesis (CM).

The first single-component catalysts for metathesis, based on molybdenum and tungsten, have a general formula $(NAr)(OR')_2M=CHR$, where Ar is aryl group, and R and R′ are different alkyl groups.[76] They have greater activity under milder reaction conditions and provide moderate functional group tolerance.[76] However, they are extremely sensitive to oxygen and moisture, and can only be used in an inert atmosphere and with vigorously purified, dried and degassed solvents and reagents.[76]

The ruthenium-based metathesis catalysts (Figure 1.7) provide a high tolerance to functional groups and allow researchers to work outside the glovebox as they do not require a strictly inert atmosphere.[76] It should be stressed that all the ruthenium-based metathesis catalysts shown are able to initiate the metathesis.[76]

The first well-defined ruthenium-based metathesis catalyst (Figure 1.7, compound **1**) was able to polymerize norbornene in protic media,[77] even in the presence of water and ethanol.[75] Furthermore, this catalyst can be used for living polymerization because chain termination and transfer of the polymerization initiated by the catalyst are slow.[78] Although the initiation behavior and the tolerance of functional groups of the first well-defined ruthenium-based metathesis catalyst were exciting, the activity of this catalyst in the ROMP of low-strained monomers is low. It was found that the activity increases with the basicity of the phosphates, finally leading to the discovery of the first-generation Grubbs catalysts (compound **2**).[79]

The Grubbs catalysts consist of a ruthenium atom surrounded by five ligands. They can be divided into two categories based on the types of ligands: $L_2X_2Ru=CHR$ complexes (where L is a phosphine ligand) discovered first are known as the first-generation Grubbs catalysts (compound **2**), and $(L)(L')X_2Ru=CHR$ complexes (where L is a phosphine ligand and L' is a saturated N-heterocylic carbine or NHC ligand) become as the second-generation Grubbs catalysts (compound **3**).[74]

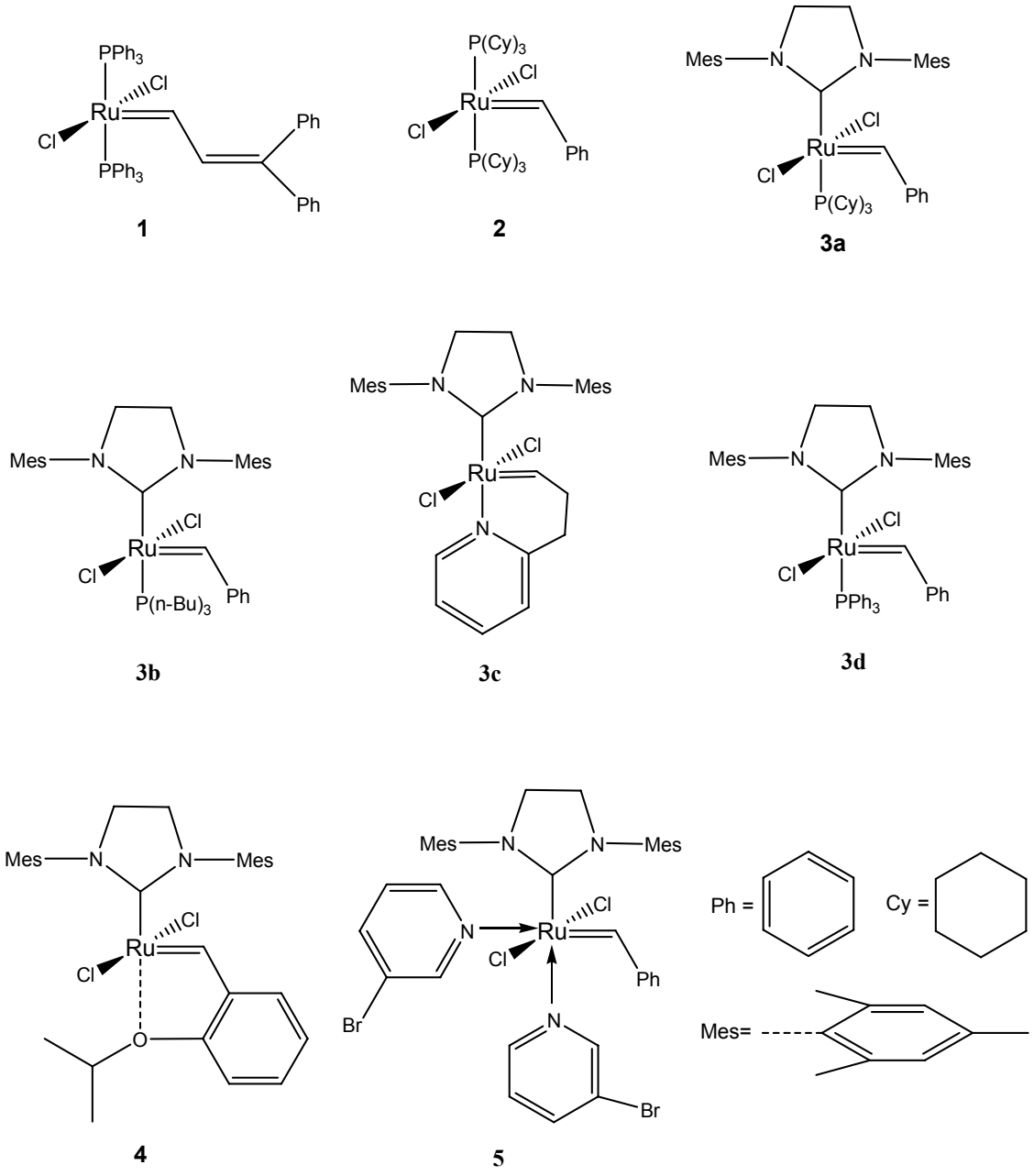

Figure 1.7. Ruthenium-based olefin metathesis catalysts: (1) the first well-defined metathesis-active ruthenium catalyst; (2) the first-generation Grubbs catalyst; (3) the different second-generation Grubbs catalysts (**a-d**); (4) the second-generation Hoveyda-Grubbs catalyst; (5) the third-generation Grubbs catalyst.

The first-generation Grubbs catalysts possess attractive functional group tolerance and can be widely used in metathesis applications, such as ring opening metathesis polymerization,[77] ring closing metathesis,[80,81] ethenolysis,[82,83] cross metathesis,[84] and enyne metathesis.[85] However, the first-generation Grubbs catalysts are not as active as the more sensitive but highly active Schrock catalysts.[74] The substitution of one $P(Cy_3)$ ligand of the first-generation Grubbs catalyst with an N-heterocyclic carbine (NHC) led to the discovery of the second-generation Grubbs catalysts (compound **3a**), which possess excellent metathesis activity and broad functional group tolerance.[76] Furthermore, the second-generation Grubbs (compound **3a**) and Hoveyda-Grubbs catalysts (compound **4**) can still function in some metathesis applications of sterically hindered and electronically deactivated olefins.[74]

Discovered in 1999, the second-generation Grubbs catalysts have rapidly evolved into a large family of catalysts with various properties that are widely used in a broad range of applications, such as fine chemicals, pharmaceuticals, and materials.[74] There is no single second-generation Grubbs catalyst that is optimal for all transformations and applications. In fact, many second-generation Grubbs catalysts have been developed for specific purposes.[74] Slow-initiating phosphine containing (compound **3b**) and phosphine free (compound **3c**) second-generation Grubbs catalysts were developed for the controlled ROMP of strained cyclic olefins, while fast-initiating phosphine containing (compound **3d**) second-generation Grubbs catalysts were designed for low temperature metathesis processes or for the production of polymers with narrow polydispersities.[74]

The third-generation Grubbs catalyst (compound **5**, sometimes referred as a modified second-generation Grubbs catalyst) also contains an N-heterocyclic carbene group, but a phosphine ligand is replaced by two bromo-pyridine groups. This catalyst has improved initiation rates and high activity to a range of monomers. The polydispersity indexes of polymers obtained by this reaction has been improved.[86,87]

As mentioned above, olefin metathesis provides a route to prepare unsaturated molecules that are difficult or even impossible to prepare by any other means. Thus, it has become an important tool in organic synthetic chemistry.[75] Among its important applications, ring closing metathesis is a straightforward and reliable method for the

preparation of various carbocyclic and heterocyclic ring systems of various sizes and complexity.[64]

Cyclic compounds ranging from five-membered rings to macrocycles can be synthesized via ring closing metathesis and numerous reviews about RCM have been published to date.[70,88-94] Majumdar et al. discussed the reaction conditions of RCM in their paper[64]: many factors, such as the catalyst properties, solvent, reaction temperature, concentration of the starting material, reaction time, and properties of final products influence RCM reactions. Slow addition of the catalyst, higher reaction temperatures and low concentration of starting materials favor the ring formation in the synthesis of macrocycles. However, higher reaction temperatures can accelerate the decomposition of the catalyst and, hence, higher catalyst loading is required for the closure of larger rings.[64]

Ring opening metathesis polymerization is one of the important applications of olefin metathesis and it is a very useful technique for the preparation of polyesters with controlled molecular weight.[21] In most reported examples of ROMP, small strained cycles (3-8-membered) have been used and the polymerization is driven by enthalpy.[21] However, ROMP of macrocycles is driven by entropy, as described by the Jacobson-Stockmayer theory for ring-chain equilibria.[95-97] In contrast to acyclic diene metathesis (ADMET) polymerization[15], polymers prepared by this method could achieve appreciably high molecular weights under appropriate conditions.[98-102]

Entropy-driven ring-opening metathesis polymerization (ED-ROMP) appears as an appropriate technique for the preparation of high molecular weight main-chain bile acid-based polymers. Moreover, the large amount of coupling agents normally used for polycondensations can be avoided by using this technique and, thereby, lowering the toxicity of the final material.

1.4 Objectives of this work

The main objective of this work is to design and prepare high molecular weight polymers that contain bile acids incorporated in their main chain. These degradable polymers are developed because of potential use in biomedical applications. The following specific research objectives have been pursued:

(1) Synthesis of macrocyclic monomers based on bile acids by first attaching two flexible chains containing double bonds to cholic acid or lithocholic acid by ester and amide bonds. Ring-closing metathesis of the resulting dienes generates the macrocyclic bile acid-based monomers.

(2) Preparation of main-chain bile acid-based homopolymers via ring-opening metathesis polymerization from the macrocyclic monomers using the second-generation Grubbs catalysts. A kinetic study of polymerization will be executed on cholic acid-based triester cyclic monomer; the thermal, mechanical and degradation properties of these homopolymers will be studied.

(3) Preparation of copolymers with different monomer ratios of cholic acid-based triester cyclic monomer and cyclic ricinoleic acid via ring-opening metathesis polymerization using the second generation catalysts. Study of the thermal, mechanical and degradation properties of these copolymers. The purpose of the copolymerization is to tune the thermal, mechanical and degradation properties of the homopolymer.

The synthesis of macrocyclic monomers, homopolymers and copolymers is presented in Chapter 2, and the results of the synthesis are presented and discussed in the first parts of Chapter 3. The thermal and mechanical properties, and degradation behavior of homopolymers and copolymers are discussed in the following parts of Chapter 3.

1.5 References

(1) Gautrot, J. E.; Zhu, X. X. *J. Biomater. Sci., Polym. Ed.* **2006**, *17*, 1123-1139.

(2) Lee, K. Y.; Mooney, D. J. *Chem. Rev.* **2001**, *101*, 1869-1879.

(3) Temenoff, J. S.; Mikos, A. G. *Biomaterials* **2000**, *21*, 431-440.

(4) Seal, B. L.; Otero, T. C.; Panitch, A. *Mater. Sci. Eng., R* **2001**, *34*, 147-230.

(5) Luo, L. B.; Tam, J.; Maysinger, D.; Eisenberg, A. *Bioconjugate Chem.* **2002**, *13*, 1259-1265.

(6) Hutmacher, D. W. *Biomaterials* **2000**, *21*, 2529-2543.

(7) Allen, T. M.; Cullis, P. R. *Science* **2004**, *303*, 1818-1822.

(8) Langer, R. *Acc. Chem. Res.* **2000**, *33*, 94-101.

(9) Vert, M. *Biomacromolecules* **2005**, *6*, 538-546.

(10) Nair, L. S.; Laurencin, C. T. *Prog. Polym. Sci.* **2007**, *32*, 762-798.

(11) Elisseeff, J.; Anseth, K.; Sims, D.; McIntosh, W.; Randolph, M.; Langer, R. *P. Natl. Acad. Sci. USA* **1999**, *96*, 3104-3107.

(12) Elisseeff, J.; Anseth, K.; Sims, D.; McIntosh, W.; Randolph, M.; Yaremchuk, M.; Langer, R. *Plast. Reconstr. Surg.* **1999**, *104*, 1014-1022.

(13) Constantinidis, I.; Rask, I.; Long, R. C.; Sambanis, A. *Biomaterials* **1999**, *20*, 2019-2027.

(14) Zhang, J. W.; Zhu, X. X. *Sci. China Ser. B* **2009**, *52*, 849-861.

(15) Gautrot, J. E.; Zhu, X. X. *Angew. Chem. Int. Ed.* **2006**, *45*, 6872-6874.

(16) Nair, P. P., Kritchevsky, D., Eds.; *The Bile Acids-Chemistry, Physiology and Metaboli*sm; Plenum, New York, **1973**, Vol. 2.

(17) Li, Y. X.; Dias, J. R. *Chem. Rev.* **1997**, *97*, 283-304.

(18) Barry, J. F.; Davis, A. P.; Perez-Payas, M. N.; Elsegood, M. R. J.; Jackson, R. F. W.; Gennari, C.; Piarulli, U.; Gude, M. *Tetrahedron Lett.* **1999**, *40*, 2849-2852.

(19) Venkatesan, P.; Cheng, Y.; Kahne, D. *J. Am. Chem. Soc.* **1994**, *116*, 6955-6956.

(20) Gouin, S.; Zhu, X. X.; Lehnert, S. *Macromolecules* **2000**, *33*, 5379-5383.

(21) Gautrot, J. E.; Zhu, X. X. *Chem. Commun.* **2008**, 1674-1676.

(22) Zhang, Y. H.; Zhu, X. X. *Macromol. Chem. Phys.* **1996**, *197*, 3473-3482.

(23) Liu, H. Y.; Avoce, D.; Song, Z. J.; Zhu, X. X. *Macromol. Rapid Commun.* **2001**, *22*, 675-680.

(24) Avoce, D.; Liu, H. Y.; Zhu, X. X. *Polymer* **2003**, *44*, 1081-1087.

(25) Benrebouh, A.; Avoce, D.; Zhu, X. X. *Polymer* **2001**, *42*, 4031-4038.

(26) Zhu, X. X.; Avoce, D.; Liu, H. Y.; Benrebouh, A. *Macromol. Symp.* **2004**, 187-191.

(27) Zou, T.; Cheng, S. X.; Zhang, X. Z.; Zhuo, R. X. *J. Biomed. Mater. Res., Part B: Appl. Biomater.* **2007**, *82B*, 400-407.

(28) Zou, T.; Li, S. L.; Cheng, S. X.; Zhang, X. Z.; Zhuo, R. X. *J. Biomed. Mater. Res., Part A* **2007**, *83A*, 696-702.

(29) Zhang, H.; Tong, S. Y.; Zhang, X. Z.; Cheng, S. X.; Zhuo, R. X.; Li, H. *J. Phys. Chem. C* **2007**, *111*, 12681-12685.

(30) Zou, T.; Li, S. L.; Hu, Z. Y.; Cheng, S. X.; Zhuo, R. X. *J. Biomater. Sci., Polym. Ed.* **2007**, *18*, 519-530.

(31) Wan, T.; Liu, Y.; Yu, J. Q.; Chen, S.; Li, F.; Zhang, X. Z.; Cheng, S. X.; Zhuo, R. X. *J. Polym. Sci., Part A: Polym. Chem.* **2006**, *44*, 6688-6696.

(32) Fu, H. L.; Cheng, S. X.; Zhang, X. Z.; Zhuo, R. X. *J. Controlled Release* **2007**, *124*, 181-188.

(33) Fu, H. L.; Yu, L.; Zhang, H.; Zhang, X. Z.; Cheng, S. X.; Zhuo, R. X. *J. Biomed. Mater. Res., Part A* **2007**, *81A*, 186-194.

(34) Fu, H. L.; Zou, T.; Cheng, S. X.; Zhang, X. Z.; Zhuo, R. X. *J. Tissue Eng. Regen. Med.* **2007**, *1*, 368-376.

(35) Piskin, E. *J. Biomater. Sci., Polym. Ed.* **1995**, *6*, 775-795.

(36) Chandra, R.; Rustgi, R. *Prog. Polym. Sci.* **1998**, *23*, 1273-1335.

(37) Bendix, D. *Polym. Degrad. Stab.* **1998**, *59*, 129-135.

(38) Domb, A. J.; Bentolila, A.; Teomin, D. *Acta Polym.* **1998**, *49*, 526-533.

(39) Domb, A. J.; Amselem, S.; Shah, J.; Maniar, M. *Adv. Polym. Sci.* **1993**, *107*, 93-141.

(40) Katti, D. S.; Lakshmi, S.; Langer, R.; Laurencin, C. T. *Adv. Drug Delivery Rev.* **2002**, *54*, 933-961.

(41) Mikos, A. G.; Thorsen, A. J.; Czerwonka, L. A.; Bao, Y.; Langer, R.; Winslow, D. N.; Vacanti, J. P. *Polymer* **1994**, *35*, 1068-1077.

(42) Griffith, L. G. *Acta Mater.* **2000**, *48*, 263-277.

(43) Nichifor, M.; Carpov, A. *Eur. Polym. J.* **1999**, *35*, 2125-2129.

(44) Nichifor, M.; Lopes, A.; Carpov, A.; Melo, E. *Macromolecules* **1999**, *32*, 7078-7085.

(45) Nichifor, M.; Stanciu, M. C.; Zhu, X. X. *React. Funct. Polym.* **2004**, *59*, 141-148.

(46) Zhu, X. X.; Nichifor, M. *Acc. Chem. Res.* **2002**, *35*, 539-546.

(47) Lee, K. Y.; Jo, W. H.; Kwon, I. C.; Kim, Y. H.; Jeong, S. Y. *Macromolecules* **1998**, *31*, 378-383.

(48) Lee, K. Y.; Kim, J. H.; Kwon, I. C.; Jeong, S. Y. *Colloid. Polym. Sci.* **2000**, *278*, 1216-1219.

(49) Lee, K. Y.; Jo, W. H.; Kwon, I. C.; Kim, Y. H.; Jeong, S. Y. *Langmuir* **1998**, *14*, 2329-2332.

(50) Kwon, S.; Park, J. H.; Chung, H.; Kwon, I. C.; Jeong, S. Y.; Kim, I. S. *Langmuir* **2003**, *19*, 10188-10193.

(51) Kim, K.; Kwon, S.; Park, J. H.; Chung, H.; Jeong, S. Y.; Kwon, I. C. *Biomacromolecules* **2005**, *6*, 1154-1158.

(52) Park, J. H.; Kwon, S. G.; Nam, J. O.; Park, R. W.; Chung, H.; Seo, S. B.; Kim, I. S.; Kwon, I. C.; Jeong, S. Y. *J. Controlled Release* **2004**, *95*, 579-588.

(53) Yoo, H. S.; Lee, J. E.; Chung, H.; Kwon, I. C.; Jeong, S. Y. *J. Controlled Release* **2005**, *103*, 235-243.

(54) Diancourt, F.; Braud, C.; Vert, M. *J. Bioact. Compat. Polym.* **1996**, *11*, 203-218.

(55) Pattinson, N.; Collins, D.; Campbell, B. *J. Chromatogr.* **1980**, *187*, 409-412.

(56) Kobayashi, N.; Katayama, H.; Nagata, M.; Goto, J. *Anal. Sci.* **2000**, *16*, 1133-1138.

(57) Ikegawa, S.; Yamamoto, T.; Miyashita, T.; Okihara, R.; Ishmata, S.; Sakai, T.; Chong, R. H.; Maeda, M.; Hofmann, A. F.; Mitamura, K. *Anal. Sci.* **2008**, *24*, 1475-1480.

(58) Ahlheim, M.; Hallensleben, M. L. *Makromol. Chem. Rapid Commun.* **1988**, *9*, 299-302.

(59) Noll, O.; Ritter, H. *Macromol. Rapid Commun.* **1996**, *17*, 553-557.

(60) Zuluaga, F.; Valderruten, N. E.; Wagener, K. B. *Polym. Bull.* **1999**, *42*, 41-46.

(61) Krasko, M. Y.; Ezra, A.; Domb, A. J. *Polym. Adv. Technol.* **2003**, 832-838.

(62) Calderon, N.; Chen, H. Y.; Scott, K. W. *Tetrahedron Lett.* **1967**, *34*, 3327-3329.

(63) Calderon, N. *Acc. Chem. Res.* **1972**, *5*, 127-132.

(64) Majumdar, K. C.; Rahaman, H.; Roy, B. *Curr. Org. Chem.* **2007**, *11*, 1339-1365.

(65) Hérisson, J. L.; Chauvin, Y. *Makromol. Chem.* **1971**, *141*, 161-176.

(66) Casey, C. P.; Burkhardt, T. J. *J. Am. Chem. Soc.* **1974**, *96*, 7808-7809.

(67) Katz, T. J.; McGinnis, J. *J. Am. Chem. Soc.* **1975**, *97*, 1592-1594.

(68) Grubbs, R. H.; Burk, P. L.; Carr, D. D. *J. Am. Chem. Soc.* **1975**, *97*, 3265-3267.

(69) Grubbs, R. H.; Carr, D. D.; Hoppin, C. *J. Am. Chem. Soc.* **1976**, *98*, 3478-3483.

(70) Nicolaou, K. C.; Bulger, P. G.; Sarlah, D. *Angew. Chem. Int. Ed.* **2005**, *44*, 4490-4527.

(71) Chauvin, Y. *Angew. Chem. Int. Ed.* **2006**, *45*, 3740-3747.

(72) Schrock, R. R. *Angew. Chem. Int. Ed.* **2006**, *45*, 3748-3759.

(73) Grubbs, R. H. *Angew. Chem. Int. Ed.* **2006**, *45*, 3760-3765.

(74) Schrodi, Y.; Pederson, R. L. *Aldrichim. Acta* **2007**, *40*, 45-52.

(75) Trnka, T. M.; Grubbs, R. H. *Acc. Chem. Res.* **2001**, *34*, 18-29.

(76) Rybak, A.; Fokou, P. A.; Meier, M. A. R. *Eur. J. Lipid Sci. Technol.* **2008**, *110*, 797-804.

(77) Nguyen, S. T.; Johnson, L. K.; Grubbs, R. H.; Ziller, J. W. *J. Am. Chem. Soc.* **1992**, *114*, 3974-3975.

(78) Wu, Z.; Benedicto, A. D.; Grubbs, R. H. *Macromolecules* **1993**, *26*, 4975-4977.

(79) Schwab, P.; France, M. B.; Ziller, J. W.; Grubbs, R. H. *Angew. Chem. Int. Ed.* **1995**, *34*, 2039-2041.

(80) Fu, G. C.; Nguyen, S. T.; Grubbs, R. H. *J. Am. Chem. Soc.* **1993**, *115*, 9856-9857.

(81) Ferguson, M. L.; O'Leary, D. J.; Grubbs, R. H. *Org. Synth.* **2003**, *80*, 85.

(82) Andrade, R. B.; Plante, O. J.; Melean, L. G.; Seeberger, P. H. *Org. Lett.* **1999**, *1*, 1811-1814.

(83) Burdett, K. A.; Harris, L. D.; Margl, P.; Maughon, B. R.; Mokhtar-Zadeh, T.; Saucier, P. C.; Wasserman, E. P. *Organometallics* **2004**, *23*, 2027-2047.

(84) Blackwell, H. E.; O'Leary, D. J.; Chatterjee, A. K.; Washenfelder, R. A.; Bussmann, D. A.; Grubbs, R. H. *J. Am. Chem. Soc.* **2000**, *122*, 58-71.

(85) Diver, S. T.; Giessert, A. J. *Chem. Rev.* **2004**, *104*, 1317-1382.

(86) Lambeth, R. H.; Moore, J. S. *Macromolecules* **2007**, *40*, 1838-1842.

(87) Carlise, J. R.; Weck, M. *J. Polym. Sci., Part A: Polym. Chem.* **2004**, *42*, 2973-2984.

(88) Deiters, A.; Martin, S. F. *Chem. Rev.* **2004**, *104*, 2199-2238.

(89) Amblard, F.; Nolan, S. P.; Agrofoglio, L. A. *Tetrahedron* **2005**, *61*, 7067-7080.

(90) Armstrong, S. K. *J. Chem. Soc., Perkin Trans. 1* **1998**, 371-388.

(91) Schuster, M.; Blechert, S. *Angew. Chem. Int. Ed.* **1997**, *36*, 2037-2056.

(92) Yet, L. *Chem. Rev.* **2003**, *103*, 4283-4306.

(93) McReynolds, M. D.; Dougherty, J. M.; Hanson, P. R. *Chem. Rev.* **2004**, *104*, 2239-2258.

(94) Grubbs, R. H.; Chang, S. *Tetrahedron* **1998**, *54*, 4413-4450.

(95) Chen, Z. R.; Claverie, J. P.; Grubbs, R. H.; Kornfield, J. A. *Macromolecules* **1995**, *28*, 2147-2154.

(96) Jacobson, H.; Stockmayer, W. H. *J. Chem. Phys.* **1950**, *18*, 1600-1606.

(97) Semlyen, J. A. *Adv. Polym. Sci.* **1976**, *21*, 41-75.

(98) Hodge, P.; Colquhoun, H. M. *Polym. Adv. Technol.* **2005**, 84-94.

(99) Hodge, P.; Kamau, S. D. *Angew. Chem. Int. Ed.* **2003**, *42*, 2412-2414.

(100) Tripathy, A. R.; MacKnight, W. J.; Kukureka, S. N. *Macromolecules* **2004**, *37*, 6793-6800.

(101) Nomura, R.; Ueno, A.; Endo, T. *Macromolecules* **1994**, *27*, 620-621.

(102) Kamau, S. D.; Hodge, P.; Helliwell, M. *Polym. Adv. Technol.* **2003**, *14*, 492-501.

2 Experimental Part

2.1 Materials

Lithocholic acid, cholic acid, ω-undecylenyl alcohol, ω-undecenoyl chloride, triethyl amine, ethylene glycol, 2-aminoethanol, ethylene diamine, castor oil, dicyclohexylcarbodiimide, 4-(dimethylamino)-pyridine and Grubbs' catalysts (first- and second-generations) were purchased from Aldrich. Dichloromethane (DCM), tetrahydrofuran (THF), methanol, chloroform, hexanes and ethyl acetate were purchased from VWR. They were used as received without further purification unless specified in the text. Anhydrous dichloromethane was purified by the use of a solvent purification system from Glass Contour. Silica gel 230-400 mesh for chromatography was purchased from Qingdao Meicao Co., China. Tetrahydrofuran for GPC was filtered through 0.2 μm Millipore nylon filters. Methyl ester of lithocholic acid was prepared using the conditions previously established in the literature.[1]

2.2 Synthesis of macrocyclic monomers

The macrocyclic monomers were synthesized via three steps as shown in Figures 2.1 and 2.2. Briefly, a diene was synthesized by attaching two long alkane chains with a carbon – carbon double bonds at the end to the group of the (litho)cholic acid core. Then macrocyclic monomers were synthesized via ring closure metathesis in a highly diluted anhydrous diene solution in DCM under argon atmosphere. The reaction was carried out under reflux and catalyzed by first-generation Grubbs' catalyst with a catalytic loading of 5%.

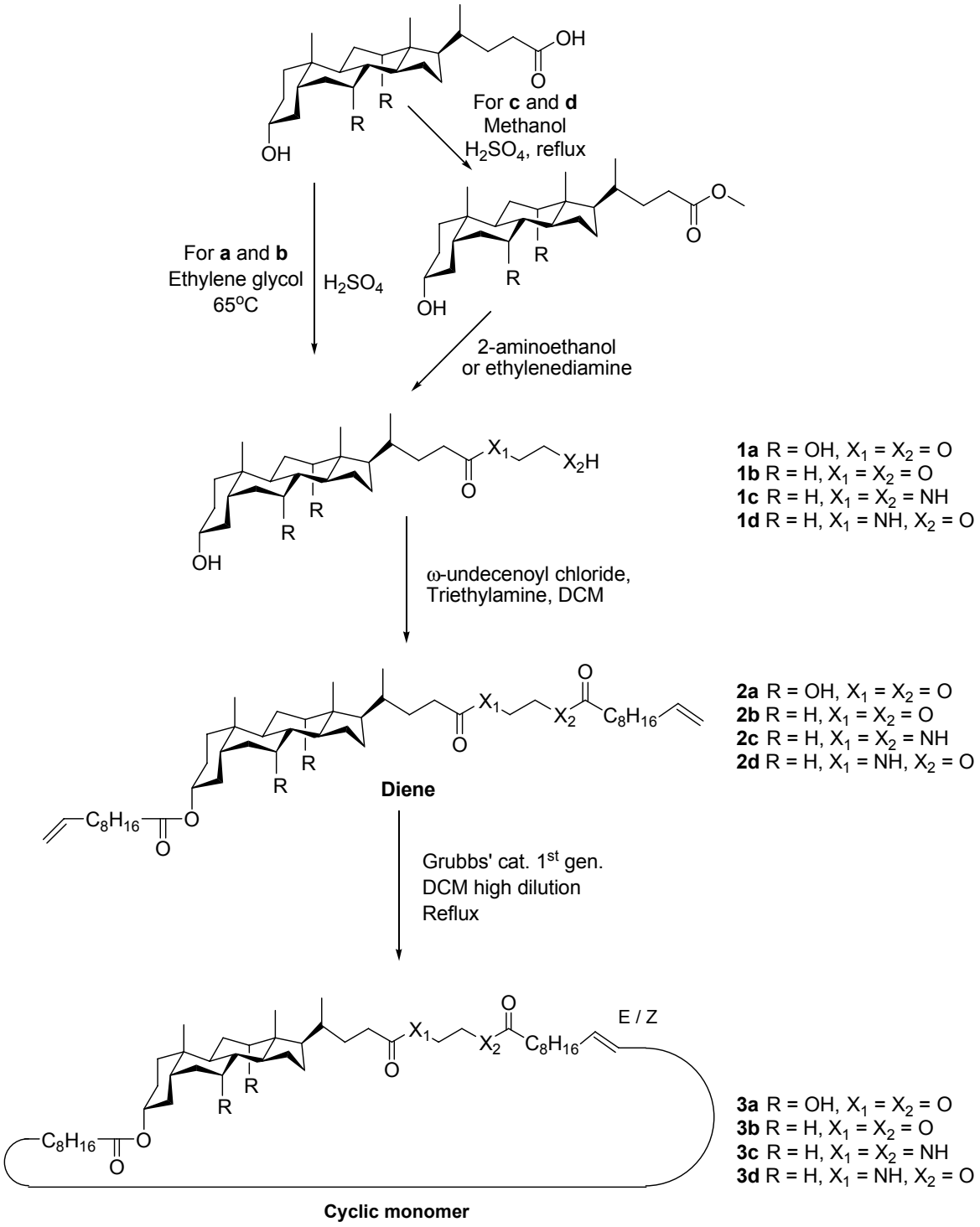

Figure 2.1. Synthesis of bile acid-based cyclic monomers **3a-d**.

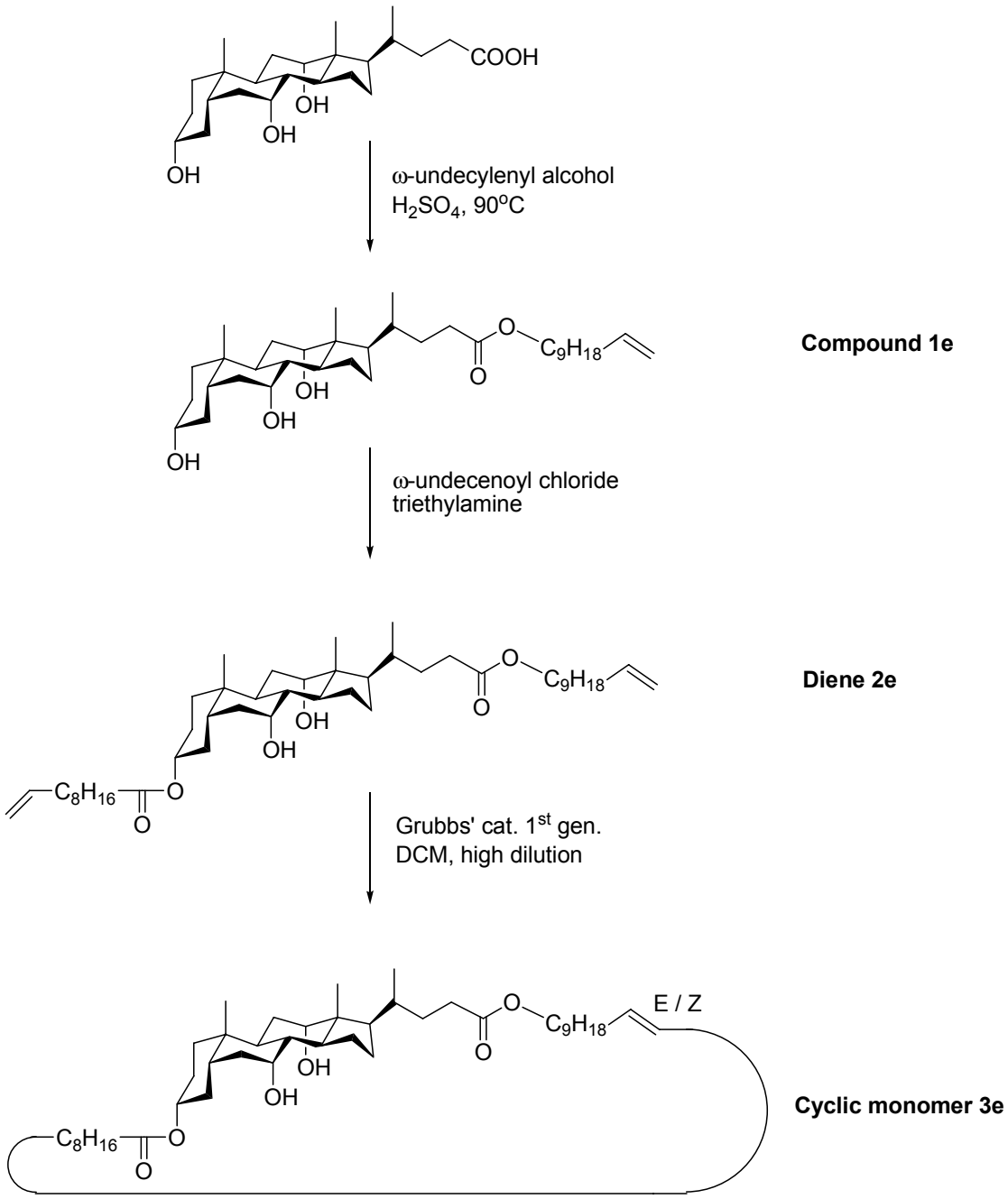

Figure 2.2. Synthesis of bile acid-based cyclic monomer **3e**.

Compound 1a. This compound was synthesized using a procedure established previously.[2] Cholic acid (10 g, 24.5 mmol), ethylene glycol (100 mL) and concentrated hydrochloric acid (1 mL) were placed in a one-neck flask (250 mL) with stirring. The resulting solution was brought to 80°C for 2 h and then poured into cool water (120 mL) to precipitate the solid product. The product was filtered and washed with aqueous sodium carbonate and water. The desired compound was obtained by recrystallization from ethyl acetate (9.4 g, 85%). IR (NaCl, cm^{-1}) 3316, 2935, 2869, 2850, 1735, 1691, 1462, 1414, 1371, 1315, 1247, 1112, 1076, 1046, 1016, 980, and 912; ^{1}H NMR ($CDCl_3$, ppm) δ 4.23 (t, 2H, $C\underline{H}_2CH_2OH$), 4.00 (s, 12 α-CH), 3.84 (m, 3H, 7 α-CH, $CH_2C\underline{H}_2OH$), 3.47 (m, 1H, 3α-CH), 1.00 (d, 3H, 21-CH_3), 0.91 (s, 3H, 19-CH_3), 0.70 (s, 3H, 18-CH_3);^{13}C NMR ($CDCl_3$, ppm) δ 12.86, 17.77, 22.89,23.67,27.98, 28.56, 30.72, 31.26, 31.37, 35.07, 35.20, 35.71, 35.75, 39.89, 41.90, 42.02, 46.82, 46.99, 61.26, 66.39, 68.86, 72.26, 73.50 and 175.34 (25 observed, 26 required).

Compound 1b. This compound was synthesized following a similar procedure as for compound **1a**. Lithocholic acid (10 g), ethylene glycol (100 mL) and concentrated hydrochloric acid (0.1 mL) were placed in a one-neck flask (250 mL) with stirring. The resulting solution was brought to 80°C for 2 h and then poured into cool water (120 mL) to precipitate a solid. The product was filtered and washed with sodium carbonate aqueous solution and water. The desired compound was obtained by recrystallization from ethyl acetate (9.8 g, 88%). IR (NaCl, cm^{-1}) 3243, 2926, 2865, 2848, 1730, 1445, 1374, 1331, 1240, 1169, 1081, 1069, 1040, 1019, 995, 947, 892, 876, 829, 677, 605 and 515; ^{1}H NMR ($CDCl_3$, ppm) δ 4.21 (m, 2H, $COC\underline{H}_2CH_2OH$), 3.82 (m, 2H, $CH_2C\underline{H}_2OH$), 3.63 (m, 1H, 3α-CH), 0.93 (d, 3H, 21-CH_3), 0.92 (s, 3H, 19-CH_3), 0.65 (s, 3H, 18-CH_3); ^{13}C NMR ($CDCl_3$, ppm) δ 12.46, 18.70, 21.23, 23.80, 24.62, 26.84, 27.61, 28.63, 30.90, 31.35, 31.56, 34.98, 35.76, 36.25, 36.80, 40.58, 40.84, 42.50, 43.15, 56.35, 56.90, 61.61, 66.34, 72.25 and 175.12 (25 observed, 26 required).

Compound 1c. This compound was prepared following a procedure established previously.[3] Methyl ester of lithocholic acid (10 g, 25.6 mmol) was dissolved in dry ethylenediamine (90 mL) and refluxed (116°C) for 5 h. The reaction solution was then cooled down and ice-water (70 mL) was added into the reaction media. The resulting

mixture was then stirred at room temperature for 2 h and placed into a refrigerator for 20 h. The white precipitate was filtered, washed thoroughly with water and then dried in a vacuum oven for 20 h (9.6 g, 90%). IR (NaCl, cm^{-1}) 3266, 2927, 2863, 1648, 1556, 1446, 1374, 1265, 1193, 1068, 1047, 945 and 607; ^{1}H NMR ($CDCl_3$, ppm) δ 5.98 (s, 1H, CONH), 3.64 (m, 1H, 3α-CH), 3.33 (m, 2H, $CONHCH_2CH_2$), 2.85 (m, 2H, $NHCH_2CH_2NH_2$), 0.95 (s, 3H, 19-CH_3), 0.93 (s, 3H, 21-CH_3), 0.66 (s, 3H, 18-CH_3); ^{13}C NMR ($CDCl_3$, ppm) δ 12.47, 18.82, 21.24, 23.80, 24.63, 26.84, 27.62, 28.67, 30.97, 32.25, 34.09, 34.99, 35.77, 35.94, 36.27, 36.88, 40.61, 40.85, 41.85, 42.33, 42.51, 43.16, 56.43, 56.92, 72.24 and 174.32 (26 observed, 26 required).

Compound 1d. The methyl ester of lithocholic acid (10 g, 25.6 mmol) was dissolved in 2-aminoethanol (100 mL) with stirring. The resulting mixture was brought to 100°C for 4 h. The reaction solution was then cooled down to room temperature, poured into cold water (500 mL), and placed into a refrigerator for 20 h. The white precipitate was filtered, washed thoroughly with water and then dried in a vacuum oven for 20 h (9.6 g, 89%). IR (NaCl, cm^{-1}) 3301, 2930, 2866, 1647, 1554, 1440, 1370, 1358, 1290, 1184, 1112, 1066, 1049, 1032, 1014, 945, 703, 607 and 497; ^{1}H NMR ($CDCl_3$, ppm) δ 5.89 (s, 1H, CONH), 3.76 (t, 2H, CH_2CH_2OH), 3.65 (m, 1H, 3α-CH), 3.46 (m, 2H, $CONHCH_2$), 0.95 (s, 3H, 21-CH_3), 0.94 (s, 3H, 19-CH_3), 0.67 (s, 3H, 18-CH_3); ^{13}C NMR (CD_3OD, ppm) δ 11.56, 17.93, 20.99, 23.01, 24.32, 26.70, 27.40, 28.29, 30.22, 32.27, 33.11, 34.71, 35.52, 35.90, 36.19, 36.26, 40.56, 40.90, 41.96, 42.55, 42.94, 56.46, 56.94, 60.67, 71.43 and 176.10 (26 observed, 26 required).

Compound 1e. This compound was synthesized following a procedure established previously.[4] Cholic acid (10 g, 24.5 mmol), ω-undecylenyl alcohol (30 mL) and concentrated sulfuric acid (0.05 mL) were placed in a round-bottom flask (100 mL). The resulting mixture was heated up to 90°C and stirred at this temperature for 5 h. After the reaction solution cooled down to room temperature, it was mixed with ethyl acetate (250 mL) and extracted with water (3 × 200 mL). It was then dried with magnesium sulfate, filtered and concentrated. Chromatography (silica gel, hexanes/ethyl acetate 80/20) yielded a white solid (12.8 g, 93%). IR (NaCl, cm^{-1}) 3726, 3375, 3975, 3926, 2855, 2113, 1989, 1735, 1640, 1464, 1375, 1309, 1251, 1172, 1078, 1044, 998, 980, 950, 912; ^{1}H

NMR ($CDCl_3$, ppm) δ 5.82 (1H; m; C<u>H</u>=C), 5.03 - 4.93 (2H; m; C<u>H_2</u>=C), 4.06 (2H, t, COOC<u>H_2</u>CH_2), 3.98 (s, 12 α-CH), 3.86 (s, 1H, 7 α-CH), 3.46 (m, 1H, 3α-CH), 1.00 (d, 3H, 21-CH_3), 0.90 (s, 3H, 19-CH_3), 0.69 (s, 3H, 18-CH_3); ^{13}C NMR ($CDCl_3$, ppm) δ 12.81, 17.66, 22.83, 23.65, 26.30, 26.53, 27.96, 28.51, 29.03, 29.26, 29.46, 29.61, 29.77, 29.83, 30.70, 31.38, 31.75, 34.15, 35.18, 35.74, 39.67, 39.85, 41.81, 41.95, 46.72, 47.29, 64.73, 68.72, 72.18, 73.40, 114.54, 139.36 and 174.83 (33 observed, 35 required).

<u>Diene 2a.</u> Compound **1a** (12.00 g, 26.51 mmol), freshly distilled triethylamine (8.8 mL, 64.1 mmol) and anhydrous DCM (200 mL) were placed in a flame-dried round bottom flask (three-neck, 500 mL) equipped with a pressure equalizing dropping funnel under an argon atmosphere. The mixture was cooled down to 0^{o}C in an ice-water bath and freshly distilled ω-undecenoyl chloride (11.80 g, 58.3 mmol) in anhydrous DCM (30 mL) was added via dropping funnel over 2 h. During the addition, compound **1a** dissolved slowly and the reaction solution became transparent. With more ω-undecenoyl chloride added into the reaction system, a white precipitate (triethylammonium chloride) appeared. After the addition finished, the reaction solution was stirred for 20 h at room temperature. Before stopping the reaction, thin layer chromatography (TLC) analysis (hexanes/ethyl acetate 60/40) confirmed the presence of the desired diene and then the reaction solution was poured into an aqueous hydrochloric acid solution (0.1 M, 500 mL). The DCM phase was then extracted with water (3 × 200 mL). The resulting milky DCM phase was moved into a 500 mL conical flask and dried by anhydrous magnesium sulphate (50 g). The mixture was stirred overnight. The magnesium sulphate was filtered and the solvent was evaporated. Chromatography (silica gel, hexanes/ethyl acetate 70/30) yielded a colourless solid. The resulting compound was dried in vacuum for 20 h (13.12 g, 63%); T_m (DSC) 88ºC; IR (NaCl, cm^{-1}) 3492, 3076, 2969, 2928, 2856, 1738, 1641, 1464, 1447, 1418, 1379, 1360, 1243, 1171, 1096, 1073, 1040, 994 and 911; ^{1}H NMR ($CDCl_3$, ppm) δ 5.80 (2H; m; C<u>H</u>=C), 5.02 - 4.89 (4H; m; C<u>H_2</u>=C), 4.57 (1H; m; H-3), 4.26 (4H; s; C<u>H_2</u>OCO), 3.98 (1H; m; H-12), 3.85 (1H; m; H-7), 2.44 - 1.00 (56H; mm), 0.98 (3H; d, J = 6.2 Hz; 21-C<u>H_3</u>), 0.90 (3H; s; 19-C<u>H_3</u>) and 0.69 (3H; s; 18-C<u>H_3</u>); ^{13}C NMR ($CDCl_3$, ppm) δ 12.99, 17.76, 22.97, 23.57, 25.30, 25.48, 27.14, 27.16, 27.86, 28.83, 29.32, 29.50, 29.53, 29.57, 29.64, 29.72, 29.73, 31.19, 31.48, 34.21, 34.23, 34.56, 34.83, 35.12, 35.23,

35.32, 35.54, 35.67, 39.99, 41.63, 42.50, 46.98, 47.62, 62.44, 62.51, 68.68, 73.32, 74.42, 114.55, 114.60, 139.59, 139.66, 173.97, 174.04 and 174.39 (45 observed, 48 required); MS (MALDI-TOF) : calc for $C_{48}H_{80}O_8Na^+$ 807.6, found 807.4; elemental analysis: calc: C, 73.4%, H, 10.3%; found: C, 73.5%, H, 9.0%.

Diene 2b. This compound was prepared following a similar procedure as for diene **2a**, from compound **1b** (12.00 g, 28.53 mmol), anhydrous DCM (100 mL), triethylamine (freshly distilled, 13.7 mL, 99.1 mmol) and freshly distilled ω-undecenoyl chloride (14.50 g, 71.5 mmol). Chromatography (silica gel, hexanes/ethyl acetate 90/10) and recrystallization from hexanes produced white crystals (16.46 g, 77%). Mp 57 - 58°C; IR (NaCl, cm^{-1}) 2928, 2855, 1739, 1641, 1451, 1380, 1242, 1163, 1117, 1097, 1065, 993, 909 and 724; ^{1}H NMR ($CDCl_3$, ppm) δ 5.78 (2H; m; C$\underline{H}$=C), 4.96 (4H; m; C$\underline{H_2}$=C), 4.73 (1H; m; H-3), 4.27 (4H; s; C$\underline{H_2}$OCO), 2.39 - 0.96 (60H; mm), 0.92 (3H; s; 21-C$\underline{H_3}$), 0.90 (3H; s; 19-C$\underline{H_3}$) and 0.64 (3H; s; 18-C$\underline{H_3}$); ^{13}C NMR ($CDCl_3$, ppm) δ 12.02, 18.24, 20.81, 23.32, 24.16, 24.86, 25.05, 26.31, 26.67, 27.01, 28.17, 28.87, 29.03, 29.05, 29.07, 29.17, 29.19, 29.26, 30.90, 31.09, 32.28, 33.76, 34.11, 34.58, 34.75, 35.03, 35.33, 35.77, 40.12, 40.38, 41.88, 42.72, 55.99, 56.46, 61.98, 61.99, 74.03, 114.11, 114.14, 139.09, 139.13, 173.37, 173.53 and 173.97 (44 observed, 48 required); MS (electrospray) : calc for $C_{48}H_{80}O_6Na^+$ 775.5853, found 775.5825; elemental analysis: calc: C, 76.5%, H, 10.7%; found: C, 76.8%, H, 11.0%.

Diene 2c. This compound was prepared following a similar procedure as for diene **2a**, from compound **1c** (12.00 g, 28.66 mmol), anhydrous DCM (300 mL), triethylamine (freshly distilled, 12.3 mL, 88.8 mmol) and freshly distilled ω-undecenoyl chloride (17.36 g, 85.6 mmol). Chromatography (silica gel, ethyl acetate/methanol 95/5) yielded the desired product as a colourless oil (17.34 g, 81%). IR (NaCl, cm^{-1}) 3295, 3213, 3080, 2973, 2927, 2855, 1736, 1639, 1555, 1466, 1449, 1422, 1380, 1243, 1174, 1118, 992 and 909; ^{1}H NMR ($CDCl_3$, ppm) δ 6.45 (2H; s; N$\underline{H}$), 5.79 (2H; m; C$\underline{H}$=C), 5.01 - 4.87 (4H; m; C$\underline{H_2}$=C), 4.71 (1H; m; H-3), 3.35 (4H; t, J = 2.3 Hz; C$\underline{H_2}$NHCO), 2.28 - 0.95 (60H; mm), 0.91 (3H; s; 19-C$\underline{H_3}$), 0.90 (3H; s, 21-C$\underline{H_3}$) and 0.62 (3H; s; 18-C$\underline{H_3}$); ^{13}C NMR ($CDCl_3$, ppm) δ 12.37, 18.71, 21.15, 23.65, 24.51, 25.38, 26.11, 27.00, 27.34, 28.58, 29.19, 29.22, 29.35, 29.40, 29.44, 29.50, 29.59, 29.67, 29.70, 29.71, 32.17, 32.61, 33.83,

34.09, 34.10, 34.90, 35.07, 35.36, 35.89, 36.10, 36.93, 40.22, 40.28, 40.47, 40.72, 42.21, 43.04, 56.39, 56.78, 74.38, 114.47, 114.51, 139.35, 139.42, 173.74, 174.93 and 175.37 (47 observed, 48 required); MS (MALDI-TOF) : calc for $C_{48}H_{82}O_4N_2Na^+$ 773.6, found 773.5; elemental analysis: calc: C, 76.7%, H, 11.0%, N, 3.7%; found: C, 76.8%, H, 11.5%, N, 3.7%.

Diene 2d. This compound was prepared following a similar procedure as for diene **2a**, from compound **1d** (12.00 g, 28.60 mmol), anhydrous DCM (250 mL), triethylamine (freshly distilled, 12 mL, 86.0 mmol) and freshly distilled ω-undecenoyl chloride (17.3 g, 85.3 mmol). Chromatography (silica gel, hexanes/ethyl acetate 40/60) yielded the desired product as a colourless oil (21.68 g, 85%). IR (NaCl, cm^{-1}) 3296, 3076, 2928, 2855, 1736, 1679, 1648, 1545, 1465, 1452, 1419, 1380, 1357, 1328, 1240, 1173, 1118, 992 and 909; ^1H NMR ($CDCl_3$, ppm) δ 5.81 (2H; m; C<u>H</u>=C), 5.72 (1H; t, J = 5.1 Hz; N<u>H</u>), 5.03 - 4.88 (4H; m; C<u>H</u>$_2$=C), 4.72 (1H; m; H-3), 4.17 (2H; t, J = 5.3 Hz; C<u>H</u>$_2$OCO), 3.51 (2H; q, J = 5.4 Hz; CO NH C<u>H</u>$_2$), 2.37 - 0.81 (66H; mm) and 0.64 (3H; s; 18-C<u>H</u>$_3$); ^{13}C NMR ($CDCl_3$, ppm) δ 12.50, 18.82, 21.28, 23.78, 24.63, 25.36, 25.52, 26.77, 27.15, 27.47, 28.70, 29.33, 29.49, 29.51, 29.54, 29.58, 29.64, 29.67, 29.73, 29.75, 32.16, 32.75, 34.05, 34.22, 34.23, 34.63, 35.05, 35.23, 35.50, 35.95, 36.24, 39.32, 40.61, 40.86, 42.36, 43.20, 56.52, 56.94, 63.57, 74.52, 114.59, 114.64, 139.57, 139.63, 173.89, 174.11 and 174.45 (47 observed, 48 required); MS (MALDI-TOF) : calc for $C_{48}H_{81}O_5NNa^+$ 774.6, found 774.5; elemental analysis: calc: C, 76.6%, H, 10.9%, N, 1.9%; found: C, 76.4%, H, 10.5%, N, 1.9%.

Diene 2e. This compound was prepared following a similar procedure as for diene **2a**, from compound **1e** (12.00 g, 21.43 mmol), anhydrous DCM (250 mL), triethylamine (freshly distilled, 4.2 mL, 30.0 mmol) and freshly distilled ω-undecenoyl chloride (5.20 g, 25.7 mmol). Chromatography (silica gel, hexanes/ethyl acetate 80/20) yielded the desired product as a white solid (14.10 g, 91%). IR (NaCl, cm^{-1}) 3511, 2920, 2852, 1724, 1639, 1464, 1416, 1364, 1345, 1312, 1273, 1246, 1198, 1171, 1128, 1093, 1073, 1039, 1024, 992, 948, 910; ^1H NMR ($CDCl_3$, ppm) δ 5.82 (2H; m; C<u>H</u>=C), 5.03 - 4.94 (4H; m; C<u>H</u>$_2$=C), 4.60 (m, 1H, 3α-CH), 4.07 (t, 2H, COOC<u>H</u>$_2$CH$_2$), 4.01 (s, 12 α-CH), 3.88 (s, 1H, 7 α-CH), 1.01 (d, 3H, 21-CH_3), 0.93 (s, 3H, 19-CH_3), 0.72 (s, 3H, 18-CH_3); ^{13}C

NMR ($CDCl_3$, ppm) δ 12.92, 17.76, 22.87, 23.61, 25.48, 26.35, 26.98, 27.18, 27.91, 28.65, 29.06, 29.30, 29.32, 29.48, 29.52, 29.58, 29.65, 29.71, 29.81, 29.88, 31.28, 31.68, 34.21, 34.96, 35.11, 35.24, 35.35, 35.57, 35.64, 39.84, 41.64, 42.37, 46.95, 47.63, 64.87, 68.74, 73.46, 74.45, 114.55, 139.56, 173.85 and 174.83 (42 obs, 46 req).

Cyclic monomer 3a. Diene **2a** (3.00 g, 3.82 mmol) was dissolved in DCM (1.5 L) in a 3-neck flame-dried round bottom flask (2 L) attached to a condenser. The resulting solution was heated up to reflux and degassed by bubbling with argon for 30 minutes while stirring. Then a solution of 157 mg benzylidene-bis(tricyclohexylphosphine) dichlororuthenium (first-generation Grubbs catalyst) (1.91×10^{-4} mol) in 20 mL argon-degassed DCM was added via a syringe (50 mL). The reaction continued with stirring for 5 h under reflux with the protection of argon. Thin layer chromatography (TLC) analysis revealed the desired cyclic monomer in the reaction system. Finally, ethyl vinyl ether (2 mL, excess) was added in order to quench the catalyst and the reaction solution was stirred for 1 h further at room temperature. Column chromatography (silica gel, hexanes/ethyl acetate 70/30) produced a white solid (2.46 g, 85%); T_m (DSC) 119ºC; IR (NaCl, cm^{-1}) 3452, 3385, 2974, 2925, 2854, 1738, 1462, 1377, 1301, 1253, 1173, 1075, 1039 and 966; ^1H NMR ($CDCl_3$, ppm) δ 5.44 - 5.29 (2H; mm; C<u>H</u>=), 4.59 (1H; m; H-3), 4.35 - 4.18 (4H; m; C<u>H</u>$_2$OCO), 3.97 (1H; m; H-12), 3.85 (1H; m; H-7), 2.42 - 1.03 (56H; mm), 1.00 (3H; d, J = 10.2 Hz; 21-C<u>H</u>$_3$), 0.90 (3H; s; 19-C<u>H</u>$_3$) and 0.70 (3H; s; 18-C<u>H</u>$_3$); ^{13}C NMR ($CDCl_3$, ppm) δ 12.96, 17.78, 23.00, 23.53, 25.31, 25.55, 27.08, 27.32, 27.79, 29.00, 29.12, 29.14, 29.19, 29.43, 29.56, 29.59, 29.71, 29.77, 30.07, 30.85, 31.25, 32.91, 33.05, 34.65, 34.82, 35.04, 35.22, 35.27, 35.44, 35.62, 39.98, 41.60, 42.71, 46.78, 46.90, 62.59, 62.55, 68.58, 73.22, 74.32, 130.75, 130.84, 174.02, 174.10 and 174.51 (45 observed, 46 required); MS (MALDI-TOF) : calc for $C_{46}H_{76}O_8Na^+$ 779.5, found 779.4; elemental analysis: calc: C, 73.0%, H, 10.1%; found: C, 72.8%, H, 9.2%.

Cyclic monomer 3b. This compound was prepared following a similar procedure as for cyclic monomer **3a**, from diene **2b** (3.00 g, 3.98 mmol), benzylidene-bis(tricyclohexylphosphine) dichlororuthenium (first-generation Grubbs' catalyst) (164 mg, 1.99×10^{-4} mol) and DCM (1.5 L). Chromatography (silica gel, hexanes/ethyl acetate 90/10) yielded a white solid (2.31 g, 80%). T_m (DSC) 95ºC; IR (NaCl, cm^{-1}) 2927, 2855, 1738, 1450, 1378, 1245, 1162, 1096, 1061, 1018 and 966; ^1H

NMR ($CDCl_3$, ppm) δ 5.37 (2H; mm; C<u>H</u>=), 4.74 (1H; m; H-3), 4.28 (4H; m; C<u>H</u>$_2$OCO), 2.42 - 0.97 (60H; mm), 0.93 (3H; s; 21-C<u>H</u>$_3$), 0.92 (3H; s; 19-C<u>H</u>$_3$) and 0.65 (3H; s; 18-C<u>H</u>$_3$); ^{13}C NMR ($CDCl_3$, ppm) δ 12.38, 18.59, 21.17, 23.67, 24.51, 25.22, 25.41, 26.66, 27.03, 27.36, 28.51, 29.22, 29.37, 29.42, 29.46, 29.54, 29.58, 29.65, 29.96, 31.25, 31.47, 32.64, 32.93, 34.11, 34.46, 34.91, 34.93, 35.10, 35.15, 35.38, 35.68, 36.13, 40.48, 40.74, 42.24, 43.07, 56.38, 56.81, 62.32, 62.52, 74.39, 130.64, 130.68, 173.73, 173.90 and 174.33 (46 observed, 46 required); MS (MALDI-TOF) : calc for $C_{46}H_{76}O_6Na^+$ 747.55, found 747.50; elemental analysis: calc: C, 76.2%, H, 10.6%; found: C, 75.8%, H, 10.9%.

<u>Cyclic monomer 3c.</u> This compound was prepared following a similar procedure as for cyclic monomer **3a**, from diene **2c** (3.00 g, 3.99 mmol), benzylidene-bis (tricyclohexylphosphine) dichlororuthenium (first-generation Grubbs' catalyst) (164 mg, 1.99×10^{-4} mol) and DCM (1.5 L). Chromatography (silica gel, ethyl acetate/methanol 95/5) yielded the desired compound as a white solid (2.36 g, 82%). T_m (DSC) 134ºC; IR (NaCl, cm^{-1}) 3299, 3220, 3080, 2971, 2927, 2854, 1731, 1670, 1649, 1546, 1464, 1449, 1378, 1334, 1246, 1176, 1020 and 966; ^{1}H NMR ($CDCl_3$, ppm) δ 6.34 (2H; s; N<u>H</u>), 5.43 - 5.29 (2H; mm; C<u>H</u>=), 4.74 (1H; m; H-3), 3.48 - 3.29 (4H; m; C<u>H</u>$_2$NHCO), 2.31 - 0.97 (60H; mm), 0.92 (3H; s; 19-C<u>H</u>$_3$), 0.91 (3H; d, J = 6.4 Hz; 21-C<u>H</u>$_3$) and 0.64 (3H; s; 18-C<u>H</u>$_3$); ^{13}C NMR ($CDCl_3$, ppm) δ 12.45, 18.81, 21.29, 23.75, 24.61, 25.55, 26.14, 26.74, 27.08, 27.42, 28.76, 28.99, 29.00, 29.30, 29.60, 29.70, 29.72, 29.75, 29.76, 29.82, 30.05, 32.35, 32.69, 32.85, 33.03, 33.89, 34.99, 35.33, 35.45, 36.11, 36.19, 37.15, 40.62, 40.76, 40.88, 42.27, 43.17, 56.30, 56.99, 74.41, 130.65, 130.81, 173.95, 175.20 and 175.66 (45 obs, 46 req); MS (MALDI-TOF) : calc for $C_{46}H_{78}O_4N_2Na^+$ 745.6, found 745.5; elemental analysis: calc: C, 76.4%, H, 10.9%, N, 3.9%; found: C, 75.4%, H, 11.2%, N, 3.7%.

<u>Cyclic monomer 3d.</u> This compound was prepared following a similar procedure as for cyclic monomer **3a**, from diene **3d** (3.00 g, 3.99 mmol), benzylidene-bis (tricyclohexylphosphine) dichlororuthenium (first-generation Grubbs' catalyst) (164 mg, 1.99×10^{-4} mol) and DCM (1.5 L). Chromatography (silica gel, hexanes/ethyl acetate 50/50) yielded a white solid (2.40 g, 83%). T_m (DSC) 13ºC; IR (NaCl, cm^{-1}) 3300, 3075, 2927, 2855, 1735, 1675, 1649, 1546, 1460, 1450, 1380, 1241, 1174, 1121 and 966; ^{1}H

NMR ($CDCl_3$, ppm) δ 5.77 (1H; t, J = 5.1 Hz; N<u>H</u>), 5.43 - 5.29 (2H; mm; C<u>H</u>=), 4.74 (1H; m; H-3), 4.18 (2H; t, J = 4.9 Hz; C<u>H</u>$_2$OCO), 3.52 (2H; m; C<u>H</u>$_2$NHCO), 2.36 - 0.97 (60H; mm), 0.93 (3H; d, J = 5.9 Hz; 21-C<u>H</u>$_3$), 0.92 (3H; s; 19-C<u>H</u>$_3$) and 0.64 (3H; s; 18-C<u>H</u>$_3$); ^{13}C NMR ($CDCl_3$, ppm) δ 12.44, 18.84, 21.28, 23.75, 24.60, 25.35, 25.55, 26.75, 27.09, 27.41, 28.68, 29.00, 29.05, 29.35, 29.52, 29.55, 29.57, 29.69, 29.72, 29.82, 30.02, 32.27, 32.69, 32.86, 33.00, 33.54, 34.66, 34.99, 35.33, 35.45, 35.73, 36.18, 39.47, 40.64, 40.89, 42.27, 43.16, 56.04, 57.04, 63.54, 74.41, 130.69, 130.79, 173.90, 174.16 and 174.53 (46 observed, 46 required); MS (MALDI-TOF) : calc for $C_{46}H_{77}O_5NNa^+$ 746.6, found 746.4; elemental analysis: calc: C, 76.3%, H, 10.7%, N, 1.9%; found: C, 76.0%, H, 9.9%, N, 1.9%.

<u>Cyclic monomer 3e.</u> This compound was prepared following a similar procedure as for cyclic monomer **3a**, from diene **2e** (3.00 g, 4.13 mmol), benzylidene-bis (tricyclohexylphosphine) dichlororuthenium (first-generation Grubbs' catalyst) (170 mg, 2.07×10^{-4} mol) and DCM (1.5 L). Chromatography (silica gel, hexanes/ethyl acetate 80/20) yielded a white solid (2.34 g, 81%). IR (NaCl, cm^{-1}) 3332, 2922, 2853, 2113, 1727, 1462, 1377, 1253, 1186, 1123, 1075, 1036, 1020, 1004, 965 and 912; ^{1}H NMR ($CDCl_3$, ppm) δ 5.43 (2H; mm; C<u>H</u>=), 4.60 (m, 1H, 3α-C<u>H</u>), 4.16 - 4.03 (m, 2H, COOC<u>H</u>$_2$CH$_2$), 4.00 (s, 12 α-CH), 3.87 (s, 1H, 7 α-CH), 1.03 (d, 3H, 21-CH_3), 0.92 (s, 3H, 19-CH_3), 0.73 (s, 3H, 18-CH_3); ^{13}C NMR ($CDCl_3$, ppm) δ 12.92, 17.77, 23.00, 23.48, 25.65, 26.78, 27.01, 27.41, 27.84, 29.00, 29.18, 29.30, 29.33, 29.43, 29.63, 29.73, 29.85, 29.89, 30.01, 30.76, 31.33, 33.08, 33.20, 34.77, 34.96, 35.19, 35.24, 35.53, 35.67, 39.92, 41.56, 42.91, 46.42, 46.81, 64.89, 68.54, 73.24, 74.34, 130.69, 130.74, 173.98 and 174.95 (42 obs, 44 req); MS (electrospray) 721.53834, $C_{44}H_{74}O_6Na^+$ requires 721.53776; elemental analysis: calc: C, 75.60%, H, 10.67%; found: C, 75.93%, H, 10.93%.

2.3 Kinetic study of ring-opening metathesis polymerization

The kinetic study of ring-opening metathesis polymerization by second-generation Grubbs' catalyst was conducted. To a concentrated solution (1.3 M) of cyclic monomer **3a** in anhydrous DCM (2 mL), a catalytic amount (1% eq.) of second-generation Grubbs' catalyst was added. A small amount of reaction medium (40

μL) was taken out via a syringe at specific time intervals and quenched by ethyl vinyl ether immediately. The molecular weight of the polymer in the resulting solution was measured by GPC, and a plot of molecular weight vs. time was constructed.

2.4 The preparation of bile acid-based polymers 1-5

The polymers were prepared via entropy-driven ring-opening metathesis polymerization of the cyclic bile acid monomers as shown in Figure 2.3. To a concentrated solution of cyclic monomer (1.3 mol/L) in anhydrous DCM, a catalytic amount (0.067 eq.) of second-generation Grubbs catalyst was added. The resulting solution was vigorously stirred and then ethyl vinyl ether was added to quench the catalyst. The desired polymer was obtained by precipitation in a hexanes/methanol (2:1) mixture.

Polymers 1a-f. Polymer **1a** was prepared via entropy driven ring-opening metathesis polymerization of cyclic monomer **3a**. Cyclic monomer **3a** (2.50 g, 3.3 mmol) and anhydrous DCM (degassed with argon for one hour, 2.1 mL) were placed in a flame-dried round-bottomed flask (1-neck, 50 mL) under argon. A solution of [1,3-bis-(2,4,6-trimethylphenyl)-2-imidazolidinylidene) dichloro(phenylmethylene)-(tricy clehexylphos-phine)ruthenium] (second-generation Grubbs catalyst) in DCM (19 mg, 2.2 $\times$ 10^{-5} mol in 400 μL degassed anhydrous DCM), amounting to 0.67 mol% with respect to the monomer, was added via a syringe. The mixture was left to react at room temperature for 20 minutes. The vigorously stirred solution rapidly became very viscous and finally stirring stopped. Ethyl vinyl ether (1 mL) was added and left to diffuse for 1 h in order to quench the catalyst and DCM (40 mL) was added. The resulting viscous solution was precipitated in a hexanes/methanol (2/1, v/v) mixture (1 L). The colourless gum that precipitated was filtered, quickly dried in vacuum, dissolved in DCM (40 mL) and precipitated in a hexanes/methanol (2/1, v/v) mixture (1 L) again. Filtration and drying in vacuum for 20 h yielded a colourless gum (2.3 g, 92 %). TGA: T_{dec}: 349^{o}C; IR (NaCl, cm^{-1}) 4508, 2926, 2855, 1732, 1464, 1418, 1380, 1251, 1172, 1096, 1074, 969 and 914; ^{1}H NMR ($CDCl_3$, ppm) δ 5.43 - 5.27 (2H; mm; C<u>H</u>=C<u>H</u>), 4.57 (1H; m; H-3), 4.26 (4H; s; C<u>H</u>$_2$OCO), 3.98 (1H; m; H-12), 3.85 (1H; m; H-7), 2.45 - 0.80 (62H; mm) and 0.69 (3H; s; 18-C<u>H</u>$_3$); ^{13}C NMR ($CDCl_3$, ppm) δ 12.97, 14.55, 17.77, 22.93, 23.09, 23.62,

25.31, 25.50, 27.06, 27.18, 27.64, 27.91, 28.75, 29.54, 29.62, 29.68, 29.70, 29.76, 30.05, 31.18, 31.51, 31.53, 32.02, 33.03, 34.56, 34.58, 35.14, 35.25, 35.26, 35.64, 39.92, 41.66, 42.44, 46.99, 47.66, 62.44, 62.52, 68.73, 74.47, 130.73, 130.76, 130.78, 130.81, 173.98, 174.07 and 174.44 (46 observed, 46 required); elemental analysis: calc for $(C_{46}H_{76}O_8)_n$: C, 73.0%, H, 10.1%; found: C, 72.7%, H, 10.6%.

Polymers **1b-f** were prepared following a similar procedure as for polymer **1a** from cyclic monomer **3a** using different catalyst loadings and reaction times (shown in Table 2.1). Their IR and NMR spectra are the same as those for polymer **1a**.

Table 2.1. Catalytic loading of second-generation Grubbs catalyst and quenching time of polymers **1a-f**.

Homopolymer	Catalytic loading (%)	Quenching time
1a	0.67	20 min
1b	0.67	20 h
1c	1	3 h
1d	1	20 h
1e	2	20 h
1f	1	1 min

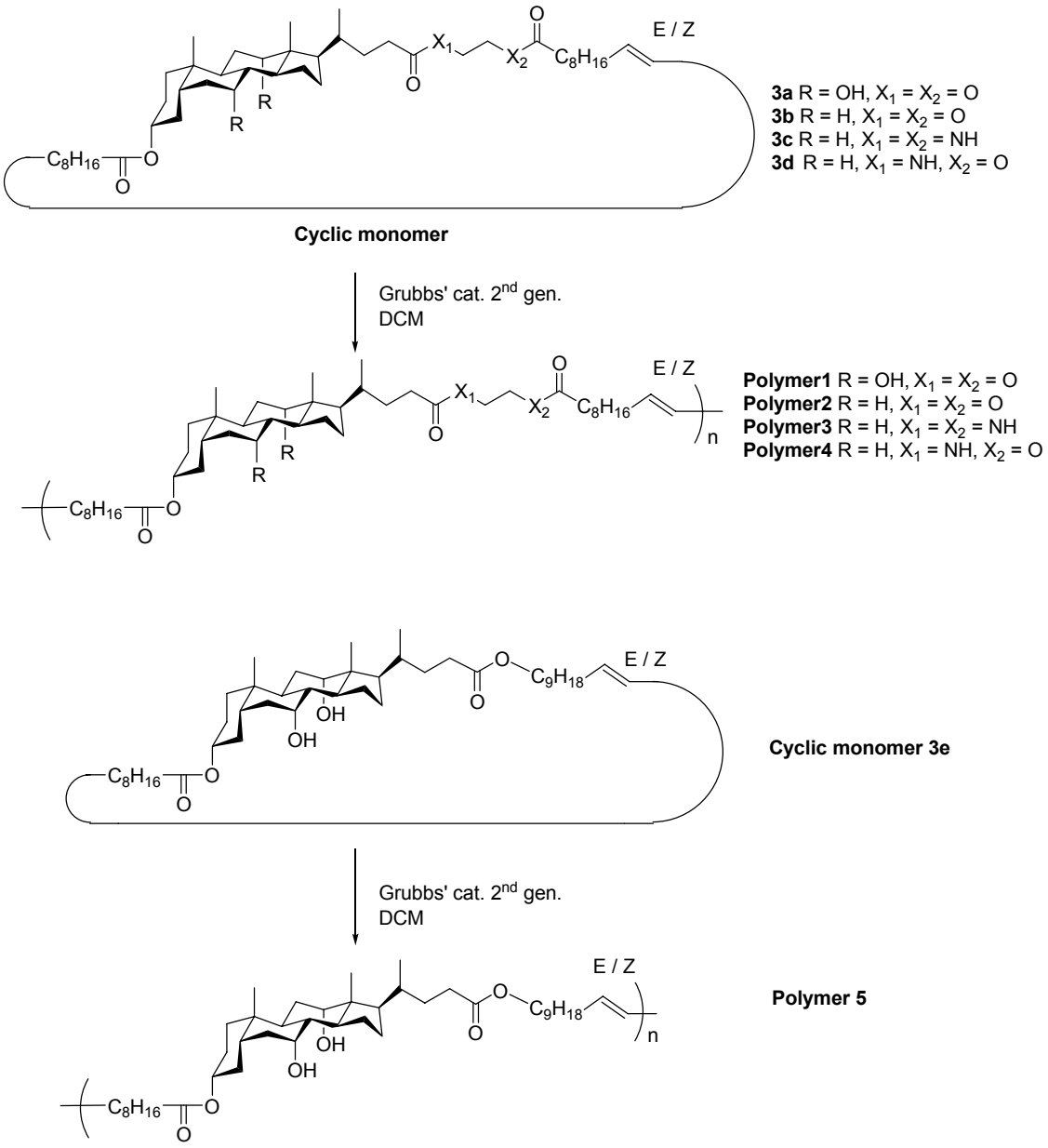

Figure 2.3. Preparation of polymers **1-5** via ring-opening metathesis polymerization.

Polymer 2. This polymer was prepared following a similar procedure as for polymer **1**, from cyclic monomer **3b** (2.50 g, 3.5 mmol), anhydrous DCM (degassed with argon for one hour, 2.1 mL) and a solution of [1,3-bis-(2,4,6-trimethylphenyl)-2-imidazo-

lidinylidene)dichloro(phenylmethylene)-(tricyclohexylphosphine)ruthenium] (second-generation Grubbs catalyst) in DCM (20 mg, 2.3×10^{-5} mol in 400 μL degassed anhydrous DCM), amounting to 0.67 mol% with respect to the monomer. This produced a colourless gum (2.38 g, 95 %). TGA: T_{dec}: 348°C; IR (NaCl, cm^{-1}) 2927, 2854, 1739, 1453, 1380, 1243, 1163, 1122, 1097, 1065, 967, 930 and 737; ^{1}H NMR ($CDCl_3$, ppm) δ 5.35 (2H; m; C<u>H</u>=), 4.72 (1H; m; H-3), 4.26 (4H; s; C<u>H</u>$_2$OCO), 2.41 - 0.96 (60H; mm), 0.92 (3H; s; 21-C<u>H</u>$_3$), 0.90 (3H; s; 19-C<u>H</u>$_3$) and 0.64(3H; s; 18-C<u>H</u>$_3$); ^{13}C NMR ($CDCl_3$, ppm) δ 12.03, 18.25, 20.82, 23.33, 24.18, 24.78, 24.87, 25.06, 26.32, 26.69, 27.02, 27.20, 28.18, 29.12, 29.24, 29.32, 29.63, 30.90, 31.14, 32.30, 32.59, 34.11, 34.59, 34.75, 35.05, 35.35, 35.79, 40.13, 40.39, 41.90, 42.73, 56.05, 56.46, 62.00, 74.04, 130.30, 173.39, 173.55 and 173.97 (39 observed, 46 required); elemental analysis: calc for $(C_{46}H_{76}O_6)_n$: C, 76.2%, H, 10.6%; found: C, 75.5%, H, 11.5%.

<u>Polymer 3.</u> This polymer was prepared following a similar procedure as for polymer **1**, from cyclic monomer **3c** (2.50 g, 3.5 mmol), anhydrous DCM (degassed with argon for one hour, 2.1 mL) and a solution of [1,3-bis-(2,4,6-trimethylphenyl) 2-imidazolidinylidene)dichloro(phenylmethylene)-(tricyclohexylphosphine)ruthenium] (second-generation Grubbs catalyst) in anhydrous DCM (20 mg, 2.3×10^{-5} mol in 400 μL degassed anhydrous DCM), amounting to 0.67 mol% with respect to the monomer. This yielded a colourless gum (2.3 g, 92 %). TGA: T_{dec}: 350°C; IR (NaCl, cm^{-1}) 3290, 3216, 3083, 2926, 2854, 2696, 1732, 1644, 1560, 1550, 1465, 1449, 1379, 1359, 1245, 1177, 1120, 967 and 912; ^{1}H NMR ($CDCl_3$, ppm) δ 6.68 (2H; s; N<u>H</u>), 5.43-5.28 (2H; mm; C<u>H</u>=), 4.72 (1H; m; H-3), 3.36 (4H; s; C<u>H</u>$_2$NHCO), 2.33-0.81 (66H; mm) and 0.63 (3H; s; 18-C<u>H</u>$_3$); ^{13}C NMR ($CDCl_3$, ppm) δ 12.52, 18.85, 21.28, 23.79, 24.64, 25.53, 26.24, 26.29, 26.79, 27.14, 27.48, 28.71, 29.41, 29.49, 29.53, 29.57, 29.62, 29.67, 29.72, 29.76, 29.80, 29.86, 30.02, 30.05, 30.09, 32.27, 32.75, 33.03, 35.04, 35.23, 35.50, 36.24, 37.11, 40.60, 40.86, 42.34, 43.19, 56.51, 56.92, 74.52, 130.74, 130.77, 130.84, 173.92, 175.11 and 175.51 (46 observed, 46 required); elemental analysis: calc for $(C_{46}H_{78}O_4N_2)_n$: C, 76.4%, H, 10.9%, N, 3.9%; found: C, 74.9%, H, 10.0%, N, 3.8%.

<u>Polymer 4.</u> This polymer was prepared following a similar procedure as for polymer **1**, from cyclic monomer **3d** (2.50 g, 3.5 mmol), anhydrous DCM (degassed with

argon for one hour, 2.1 mL) and a solution of [1,3-bis-(2,4,6-trimethylphenyl)-2-imidazolidinylidene)dichloro(phenylmethylene)-(tricyclohexylphosphine)ruthenium] (second-generation Grubbs catalyst) in anhydrous DCM (20 mg, 2.3×10^{-5} mol in 400 μL degassed anhydrous DCM), amounting to 0.67 mol% with respect to the monomer. This yielded a colourless gum (2.35 g, 93 %). TGA: T_{dec}: 350°C; IR (NaCl, cm^{-1}) 3433, 3366, 3300, 3222, 3075, 2927, 2854, 1733, 1679, 1651, 1547, 1464, 1454, 1422, 1380, 1239, 1175, 1120, 990 and 967; ^{1}H NMR ($CDCl_3$, ppm) δ 5.81 (1H; m; N<u>H</u>), 5.42-5.29 (2H; mm; C<u>H</u>=), 4.72 (1H; m; H-3), 4.15 (2H; t, J = 5.3 Hz; C<u>H</u>$_2$OCO), 3.51 (2H; q, J = 5.5 Hz; C<u>H</u>$_2$NHCO), 2.34-0.81 (66H; mm) and 0.63 (3H; s; 18-C<u>H</u>$_3$); ^{13}C NMR ($CDCl_3$, ppm) δ 12.49, 18.82, 21.28, 23.78, 24.63, 25.36, 25.52, 25.71, 26.77, 27.14, 27.47, 27.64, 28.69, 29.54, 29.57, 29.68, 29.70, 29.76, 29.78, 30.06, 32.14, 32.75, 34.05, 34.62, 35.04, 35.21, 35.50, 35.96, 36.24, 39.26, 40.60, 40.85, 42.35, 43.19, 56.55, 56.92, 63.54, 74.52, 130.72, 130.75, 130.76, 130.80, 173.88, 174.11 and 174.42 (45 observed, 46 required); elemental analysis: calc for $(C_{46}H_{77}O_5N)_n$: C, 76.3%, H, 10.7%, N, 1.9%; found: C, 75.8%, H, 11.2%, N, 1.9%.

<u>Polymer 5.</u> This polymer was prepared following a similar procedure as for polymer **1**, from cyclic monomer **3e** (2.50 g, 3.6 mmol), anhydrous DCM (degassed with argon for one hour, 2.1 mL) and a solution of [1,3-bis-(2,4,6-trimethylphenyl) 2-imidazolidinylidene)dichloro(phenylmethylene)-(tricyclohexylphosphine)ruthenium] (second-generation Grubbs catalyst) in DCM (21 mg, 2.4×10^{-5} mol in 400 μL degassed anhydrous DCM, amounting to 0.67 mol% with respect to the monomer). This produced a colourless gum (2.35 g, 94 %). TGA: T_{dec}: 363 °C; IR (NaCl, cm^{-1}) 3439, 2921, 2852, 1730, 1464, 1378, 1249, 1172, 1093, 1072, 1038, 967, 912 and 722; ^{1}H NMR ($CDCl_3$, ppm) δ 5.40 (2H; mm; C<u>H</u>=), 4.60 (m, 1H, 3α-CH), 4.07 (t, 2H, COOC<u>H</u>$_2$CH$_2$), 4.01 (s, 12 α-CH), 3.87 (s, 1H, 7 α-CH), 1.01 (d, 3H, 21-CH_3), 0.93 (s, 3H, 19-CH_3), 0.72 (s, 3H, 18-CH_3); ^{13}C NMR ($CDCl_3$, ppm) δ 12.97, 17.79, 22.94, 23.62, 25.50, 26.36, 27.06, 27.18, 27.63, 27.90, 28.73, 29.08, 29.53, 29.62, 29.69, 29.75, 29.82, 29.85, 29.90, 29.92, 30.04, 31.33, 31.75, 33.02, 34.91, 35.13, 35.26, 35.35, 35.62, 39.92, 41.65, 42.42, 46.98, 47.69, 64.91, 68.73, 73.41, 73.44, 74.45, 130.74, 130.76, 173.91 and 174.83 (43 observed,

44 required); elemental analysis: calc for $(C_{46}H_{76}O_6)_n$: C, 75.60%, H, 10.67%; found: C, 75.81%, H, 10.92%.

2.5 Synthesis of copolyesters based on cholic acid and ricinoleic acid

Ricinoleic acid methyl ester. Castor oil (10.00 g, 10.7 mmol), methanol (50 mL) and potassium hydroxide (0.22 g, 3.9 mmol) were placed in a one-neck round-bottom flask (100 mL) equipped with a condenser. The resulting solution was stirred and heated to reflux for 4 h using an oil bath and then condensed to 20 mL by evaporation. The remaining mixture was dissolved in 200 mL DCM, extracted with water (3 × 250 mL), dried with magnesium sulfate, filtered and then the solvent was evaporated. Column chromatography (silica gel, hexanes/ethyl acetate 95/5) resulted in a colourless oil (8.81 g, 88%); ^{1}H NMR ($CDCl_3$, ppm) δ 5.63 - 5.37 (2H; m; C9, C10, -C<u>H</u>=C<u>H</u>-), 3.69 (4H; m; C12, C<u>H</u>-OH; -OC<u>H</u>$_3$), 2.32 (2H; m; C2, -C<u>H</u>$_2$-), 2.23 (2H; m; C11, -C<u>H</u>$_2$-), 2.06 (2H; m; C8, -C<u>H</u>$_2$-), 1.62 (2H; m; C3, -C<u>H</u>$_2$-), 1.46 (2H; m; C13, -C<u>H</u>$_2$-), 1.31 (16H; m; C4-7,C14-17, -C<u>H</u>$_2$-), 0.89 (3H; m; C18, -C<u>H</u>$_3$).

Ricinoleic acid. Methyl ester of ricinoleic acid (10.00 g, 32.1 mmol) was placed in a three-neck flask (500 mL) fitted with a pressure equalizing dropping funnel and stirred while potassium hydroxide methanol-water solution (6 M, 200 mL, methanol : water = 1:1, v/v) was added into the flask quickly. The resulting mixture solidified quickly and became a wax. Three hours later, the reaction system was cooled down to 0^{o}C in an ice bath. Concentrated hydrochloride acid (12.1 M, 100 mL) was added over 3 h via a dropping funnel. The solid was dissolved gradually and the resulting solution separated into water and oil phases. DCM (200 mL) was added into the flask and the DCM phase was extracted with water (3 × 250 mL), dried with magnesium sulfate, filtered and the solvent was evaporated. The desired compound is a colorless viscous liquid (8.79 g, 92%); ^{1}H NMR ($CDCl_3$, ppm) δ 5.58-5.35 (2H; m; C9, C10, -C<u>H</u>=C<u>H</u>-), 3.64 (1H; m; C12, C<u>H</u>-OH), 2.35 (2H; m; C2, -C<u>H</u>$_2$-), 2.23 (2H; m; C11, -C<u>H</u>$_2$-), 2.07 (2H; m; C8, -C<u>H</u>$_2$-), 1.64 (2H; m; C3, -C<u>H</u>$_2$-), 1.48 (2H; m; C13, -C<u>H</u>$_2$-), 1.33 (16H; m; C4-7,C14-17, -C<u>H</u>$_2$-), 0.90 (3H; m; C18, -C<u>H</u>$_3$).

Ricinoleic acid monolactone. This compound was prepared following the same procedure as published in the literature[5] as shown in Figure 2.4. Ethanol-free dry $CHCl_3$ (500 mL $CHCl_3$ extracted with 50 mL concentrated sulfuric acid, then extracted with 200 mL water three times, dried by calcium chloride, filtered and then distilled) (900 mL), DCC (13.7 g, 66.4 mmol), DMAP (12.2 g, 99.5 mmol) and DMAP·HCl (10.5 g, 66.2 mmol) were placed into a three-neck, round-bottom flask (2 L) equipped with a magnetic stirrer, condenser and dropping funnel with an argon inlet (through a septum cap). The resulting mixture was heated up to reflux under argon protection and a solution of ricinoleic acid (10.00 g, 33.5 mmol in 100 mL ethanol-free dry $CHCl_3$) was added via a dropping funnel during 5 h. The reaction system was then cooled down to room temperature. The reaction continued for 10 h under argon protection. Methanol (40 mL) and acetic acid (7.5 mL) were then added, and stirring was continued for 30 minutes. Meanwhile, no DCC was detected by TLC (hexanes/ethyl acetate 90/10), indicating the reaction was completed. The reaction mixture was concentrated to 200 mL and diluted with diethyl ether (800 mL). The resulting solution was filtered and the solvent was evaporated. The remaining viscous mixture was dissolved in minimum hexane and column chromatography (silica gel, hexanes/DCM 50/50) yielded a colourless liquid (3.2 g, 46%); ^{1}H NMR ($CDCl_3$, ppm) δ 5.54-5.34 (2H; m; C9, C10, -C<u>H</u>=C<u>H</u>-), 5.02-4.92 (J=6Hz, 1H; m; C12, C<u>H</u>-OH), 2.50 (1H; m; C11, C<u>H</u>$_a$), 2.30 (3H; m; C2, -C<u>H</u>$_2$-; C11, C<u>H</u>$_b$), 2.12 (2H; m; C8, -C<u>H</u>$_2$-), 1.77-1.64 (3H; m; C3, -C<u>H</u>$_2$-; C13, C<u>H</u>$_a$), 1.64-1.16 (17H; m; C13, C<u>H</u>$_b$; C4-7,C14-17, -C<u>H</u>$_2$-), 0.90 (3H; m; C18, -C<u>H</u>$_3$). ^{13}C NMR ($CDCl_3$, ppm) δ 13.94, 22.47, 23.36, 24.48, 25.60, 25.64, 26.02, 27.26, 29.00, 29.40, 31.64,31.74, 33.73, 35.06, 73.67, 124.74, 132.29 and 174.14 (18 obs, 18 req); MS (electrospray) : calc for $C_{18}H_{32}O_2Na^+$ 303.22945, found 303.22837.

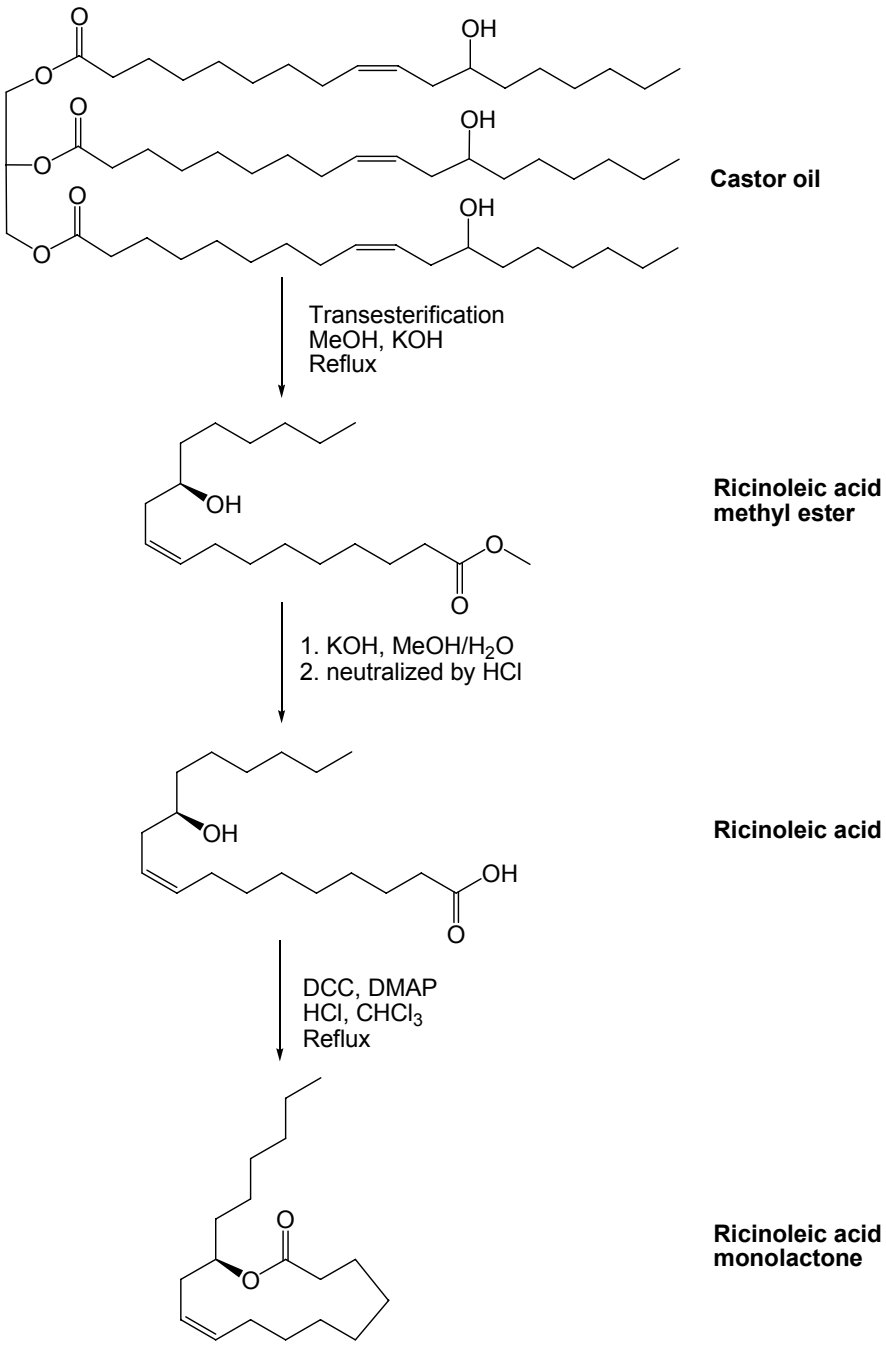

Figure 2.4. Synthesis of monolactone of ricinoleic acid.

Copolymers 6a-f. Copolymer **6a** was prepared following a procedure established previously[6] (shown in Figure 2.5) based on cyclic monomer **3a** and ricinoleic acid

monolactone in the desired proportions (shown in Table 2.2). Cyclic monomer **3a** (2.00 g, 2.55 mmol), ricinoleic acid monolactone (126 mg, 0.45 mmol) and anhydrous DCM (1.9 mL) were placed in a round-bottom flask (10 mL). A solution of second-generation Grubbs catalyst in anhydrous DCM (19 mg, 2.2×10^{-5} mol in 400 μL degassed anhydrous DCM, amounting to 0.67 mol% with respect to the total monomer quantity) was injected via a syringe. The resulting solution became viscous quickly and formed a gel. Ethyl vinyl ether (1 mL) was added into the reaction system to quench the catalyst after 20 h, and left to diffuse for 2 h. DCM (40 mL) was added and the resulting viscous solution was precipitated in a hexanes/methanol (2/1, v/v) mixture (1 L). The colourless gum that precipitated was filtered, quickly dried in vacuum, dissolved in DCM (40 mL) and precipitated in a hexanes/methanol (2/1, v/v) mixture (1 L) again. Filtration and drying in vacuum for 20 h yielded a colourless gum (1.7 g, 85%). TGA: T_{dec}: 357°C; IR (NaCl, cm^{-1}) 3441, 2922, 2852, 1729, 1456, 1378, 1242, 1159, 1094, 1072, 1038, 967, 913 and 724; ^{1}H NMR ($CDCl_3$, ppm) δ 5.46-5.32 (2.51H, mm, C<u>H</u>=, CA + RA), 4.88 (0.28H, m, C<u>H</u>OCO, RA), 4.60 (1H, m, H-3, CA), 4.29, (4H, s, CH_2OCO, CA), 4.01 (1H, s, H-12, CA), 3.88 (1H, s, H-7, CA), 2.50-0.83 (68.5H, mm, CA + RA), 0.72 (3H, s, 18 –CH_3, CA); ^{13}C NMR ($CDCl_3$, ppm) δ 12.97, 14.51, 17.76, 22.94, 23.00, 23.60, 25.30, 25.49, 27.06, 27.16, 27.62, 27.90, 28.75, 29.39, 29.53, 29.60, 29.67, 29.75, 29.87, 30.03, 30.15, 31.17, 31.50, 32.16, 33.01, 34.54, 34.89, 35.13, 35.23, 35.34, 35.63, 39.91, 41.64, 42.42, 46.97, 47.65, 62.42, 62.50, 68.69, 73.36, 74.43, 130.70, 130.73, 130.75, 130.79, 173.90, 173.94, 174.02 and 174.41.

Copolymers **6b-f** were prepared following a similar procedure as for copolymer **6a** from cyclic monomer **3a** and ricinoleic acid monolactone in the desired proportions (shown in Table 2.2). Their spectroscopic data (IR, ^{1}H and ^{13}C NMR) are similar to those of copolymer **6a**, with differences in peak area ratios.

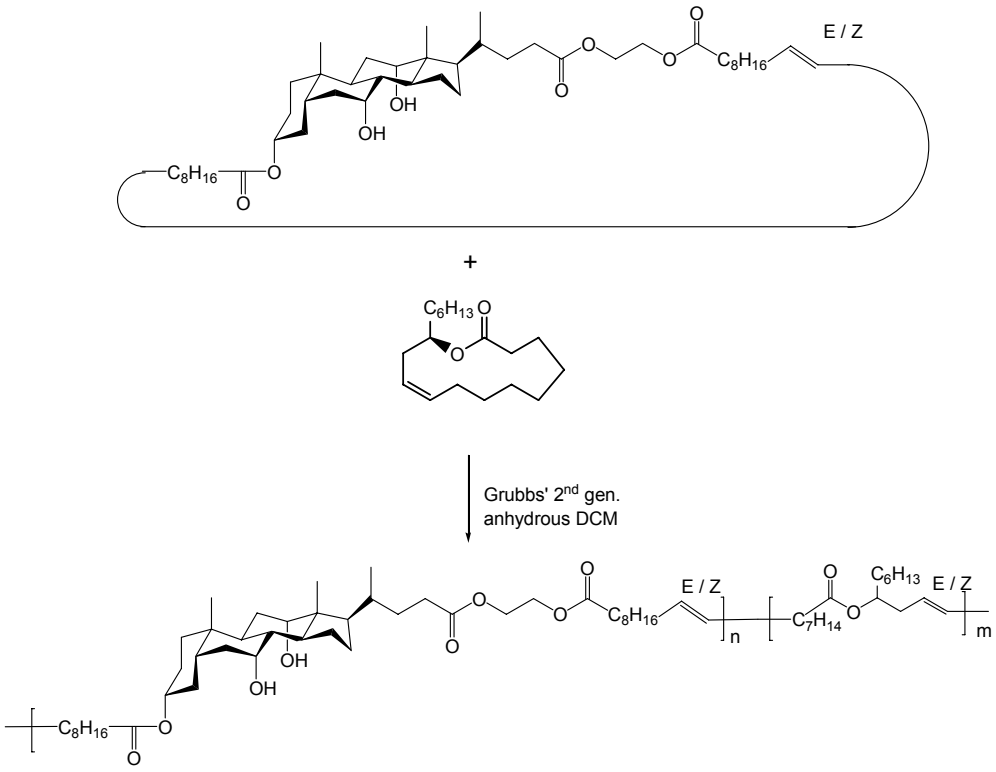

Figure 2.5. Synthesis of copolymers **6a-f**.

Table 2.2. Designed molar ratios of cyclic monomer **3a** and ricinoleic acid monolactone for copolymers **6a-f**.

Copolymer	Cyclic monomer **3a** (mol %)	Ricinoleic acid monolactone (mol %)
6a	85	15
6b	70	30
6c	55	45
6d	40	60
6e	25	75
6f	10	90

2.6 Characterization

Thermogravimetric analyses (TGA) of polymers were recorded on a Hi-Res TGA 2950 thermogravimetric analyzer from TA Instruments. A heating rate of 10°C/min from room temperature to a final temperature of 700°C was used for all samples. T_{dec} was defined as the onset of decomposition temperature.

Differential scanning calorimetry (DSC) experiments were performed on a DSC Q1000 from TA Instruments. The heating and cooling rates were 10 ºC/min, and T_g was defined as the inflection point temperature of the transition of the second run.

^{1}H and ^{13}C NMR spectra were recorded at room temperature on a Bruker AV400 spectrometer operating at 400.13 MHz for proton and 100.61 MHz for carbon-13. The samples were dissolved in deuterated chloroform (or as indicated in the text) and measured.

IR spectra were recorded on an Excalibur HE series FTS 3100 instrument from Digilab. All samples were dissolved in DCM and then coated onto NaCl crystal pallets.

Size exclusion chromatography (SEC) was performed on a Breeze system from Waters equipped with a 1525 HPLC pump, a 717 Plus autosampler, a 2410 refractive index refractometer detector and a heater. Three Styragel Waters columns (HR3, HR4 and HR6, all three 7.8 × 300 mm) were used in series. The eluent (THF) flow rate was 1 mL/min. The temperature of the columns was set at 33 ºC. Calibration was performed by the use of the polystyrene kit SM-105 (10 points) from Shodex.

Mechanical analysis was done on a DMA 2980 from TA Instruments. Polymer films for mechanical tests were prepared by evaporating the polymer solution in DCM in a PTFE mould (6.5 × 6.5 × 1 cm) covered with a Petri dish under atmospheric pressure for 24 h. The Petri dish helped to slow the evaporation and reduced the formation of air bubbles. Films were then further dried under vacuum for 24 h. Small rectangular samples (3.5 mm × 3.0 cm × 0.2 mm) were cut from these films with a knife and used for the mechanical tests. The dimensions of the samples were measured by the use of an electronic digital calliper with a precision of 0.01 mm.

Stress-strain experiments were carried out with a preload force of 0.02 N and a force ramp of 0.5 N/min. Young's modulus is defined as the slope of the stress-strain curves between the starting point of the deformation and the point of 10% strain. For multifrequency experiments, a preload force of 0.02 N, an amplitude of 10 μm, a temperature sweeping rate of 1 ^{o}C/min, and a frequency of 1 Hz were used. T_g is defined as the extrapolated onset of the change in the storage modulus from the hard glassy state to the soft rubbery state of the material.

Shape memory experiments were carried out with the controlled force mode. In a typical experiment, the sample was equilibrated for 5 min at a temperature 10^{o}C higher than the T_g of the polymer determined from multifrequency experiment, and then was stretched at 1 N/min to at least 200%. The temperature was reduced to 10^{o}C lower than the T_g and kept constant for 5 min. The force was then released and the sample was allowed to relax for 5 min. The sample was then heated to 10^{o}C higher than the T_g at 10^{o}C/min, and allowed to relax for 5 min at this temperature.

In a typical cold drawing experiment, the sample was held at 10^{o}C lower than the T_g for 5 min, and then stretched at 1 N/min to at least 150%. The force was released and the sample allowed to relax at this temperature for 5 min. The temperature was finally increased to 10^{o}C higher than the T_g at 10^{o}C/min, and the sample was allowed to relax at this temperature for 5 min.

Polarizing optical microscopy was done on a Zeiss Axioshop 40Pol microscope coupled with a Linkam Instruments THMS600 hot stage and a TMS94 temperature controller.

X-ray diffractograms were obtained at room temperature with a Bruker D8 Discover system equipped with a Bruker Hi-Star two-dimensional detector and CuKα radiation source.

Light scattering experiments for determining the molecular weight of polymer **3** were carried out on a static light scattering Daen EOS coupled with a Optilab Rex differential refractive index detector, both from Wyatt Technology Corporation. The isocratic pump is a Waters 600E, and the manual injector is a Rheodyne 7126 with 1 mL

loop. The control of the instrument and analysis of data were carried out using the Astra 5.3.4.13 software of Wyatt Technology Corporation. Eight samples of polymer **3** of different concentrations in $CHCl_3$ were prepared and injected automatically into the LS instrument to obtain a standard curve for calculating the specific refractive index (dn/dc). The rms radius and absolute molecular weight can be obtained by injection of another sample of polymer **3**.

2.7 Degradation studies

Glass slides (1.25 × 1.25 cm, 24 slides) were washed by dipping into a sodium carbonate solution (0.1 M, 100 mL) for 20 h, rinsing thoroughly with Millipore water, then drying in vacuum for 20 h and weighting on a balance with a precision of 0.01 mg. The polymer (250 mg) was dissolved completely in DCM (10 mL), coated onto the glass slides with about 10 mg per slide, dried at room temperature for 20 h and in vacuum for 20 h, and then weighed on a balance with a precision of 0.01 mg. The polymer-coated glass slides were put into a small vial (20 mL). Phosphate buffer solution (10 mL, pH = 7.4) was added into the vials, and the vials were placed into an incubator (Precision Scientific Reciprocating Shaker Bath model 25) at 37 ^{o}C. The buffer solution was changed every two weeks, and samples (4 samples at a time) were withdrawn at regular time intervals (4 weeks), weighed and analyzed by SEC.

2.8 Preparation of liquid crystalline film

Polymer **3** was dissolved in refluxing THF. The solution was then cooled down to room temperature to precipitate polymer **3** from the solution. The precipitate was dried at 40^{o}C under vacuum for 20 h. For comparison, the sample was also dissolved in chloroform, precipitated and treated following the same procedure. Among all the polymers **1-5** tested, only polymer **3** obtained from THF showed the presence of a LC phase.

2.9 References

(1) Ono, Y.; Kawase, A.; Watanabe, H.; Shiraishi, A.; Takeda, S.; Higuchi, Y.; Sato, K.; Yamauchi, T.; Mikami, T.; Kato, M.; Tsugawa, N.; Okano, T.; Kubodera, N. *Bioorg. Med. Chem.* **1998**, *6*, 2517-2523.

(2) Hu, X. Z.; Zhang, Z.; Zhang, X.; Li, Z. Y.; Zhu, X. X. *Steroids* **2005**, *70*, 531-537.

(3) Avoce, D.; Liu, H. Y.; Zhu, X. X. *Polymer* **2003**, *44*, 1081-1087.

(4) Gautrot, J. E.; Zhu, X. X. *Angew. Chem. Int. Ed.* **2006**, *45*, 6872-6874.

(5) Slivniak, R.; Domb, A. J. *Biomacromolecules* **2005**, *6*, 1679-1688.

(6) Gautrot, J. E.; Zhu, X. X. *Chem. Commun.* **2008**, *14*, 1674-1676.

3 Results and Discussion

3.1 Synthesis of macrocyclic monomers

In the synthesis of macrocyclic bile acids via ring-closure metathesis (RCM), cyclic monomers **3a-d** (38-membered rings) and **3e** (35-membered rings) were prepared (Figure 3.1). There are three main differences between these cyclic monomers. First, different bile acid cores are used (cholic acid core for cyclic monomers **3a** and **3e**, lithocholic acid core for cyclic monomers **3b-d**). Cholic acid has two extra hydroxyl groups at positions 7 and 12 compared to lithocholic acid. Consequently, cyclic monomers with a cholic acid core are more hydrophilic than those with a lithocholic acid core. Second, the types of linkages between bile acid core and long alkane chain are different. Some of the linkages are ester bonds and some are amide bonds. Generally, amide groups are more stable and more hydrophilic than ester groups. Third, the number of linkages is different. Cyclic monomers **3a-d** possess three linkages and cyclic monomer **3e** has only two. These differences make polymers prepared from cyclic monomers **3a-e** different and interesting.

The macrocyclic monomers were obtained in high yields (80 – 85 %) from the corresponding dienes as shown in Figures 2.1 and 2.2. Cyclic monomer **3b** and diene **2c** were prepared as previously reported.[1,2] Therefore, the synthesis of these two compounds is not discussed here.

3.1.1 Synthesis of cholic acid-based cyclic triester monomer 3a

Cyclic monomer **3a** can be synthesized in three steps as shown in Figure 2.1. In the first step, compound **1a** was prepared using the conditions established previously.[3] The ^{1}H NMR spectra of cholic acid and compound **1a** are shown in Figure 3.2. This step was executed successfully with a yield of 90%.

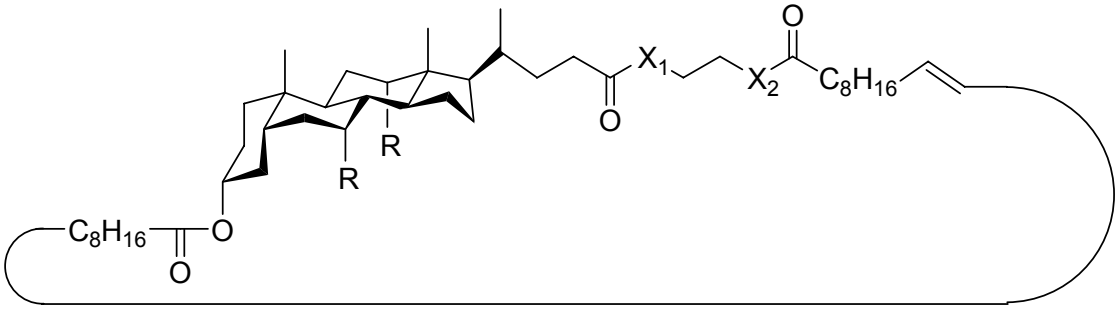

Cyclic monomer

3a R = OH, $X_1 = X_2 = O$
3b R = H, $X_1 = X_2 = O$
3c R = H, $X_1 = X_2 = NH$
3d R = H, $X_1 = NH$, $X_2 = O$

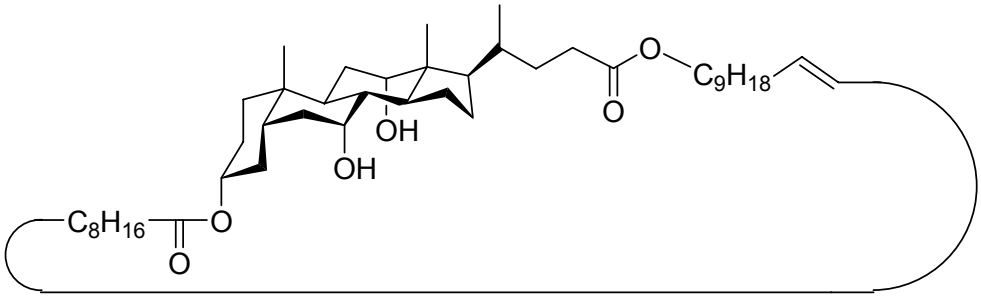

Cyclic monomer 3e

Figure 3.1. The structure of cyclic monomers **3a-e**.

In the second step, two flexible chains, each with a double bond at the end, were attached to the cholic acid core through ester bonds. From the ^{1}H NMR spectra shown in Figures 3.2 and 3.3, three obvious differences in the spectra of compound **1a** and diene **2a** can be observed. First, the peak of 3α–H shifted from 3.50 to 4.60 ppm because the hydroxyl group was transformed to an ester and one flexible chain was successfully attached to the cholic acid core. Second, the peaks of the methylene groups at 4.23 and 3.85 ppm of compound **1a** merged into a singlet at 4.29 ppm for diene **2a.** This indicates that the hydrogen atoms of these two methylene groups are chemically equivalent, and

that the flexible chain was attached to the cholic acid core on the other side. Third, the multiplets at 5.82 and 4.96 ppm are the signals of the hydrogen of the double bonds.

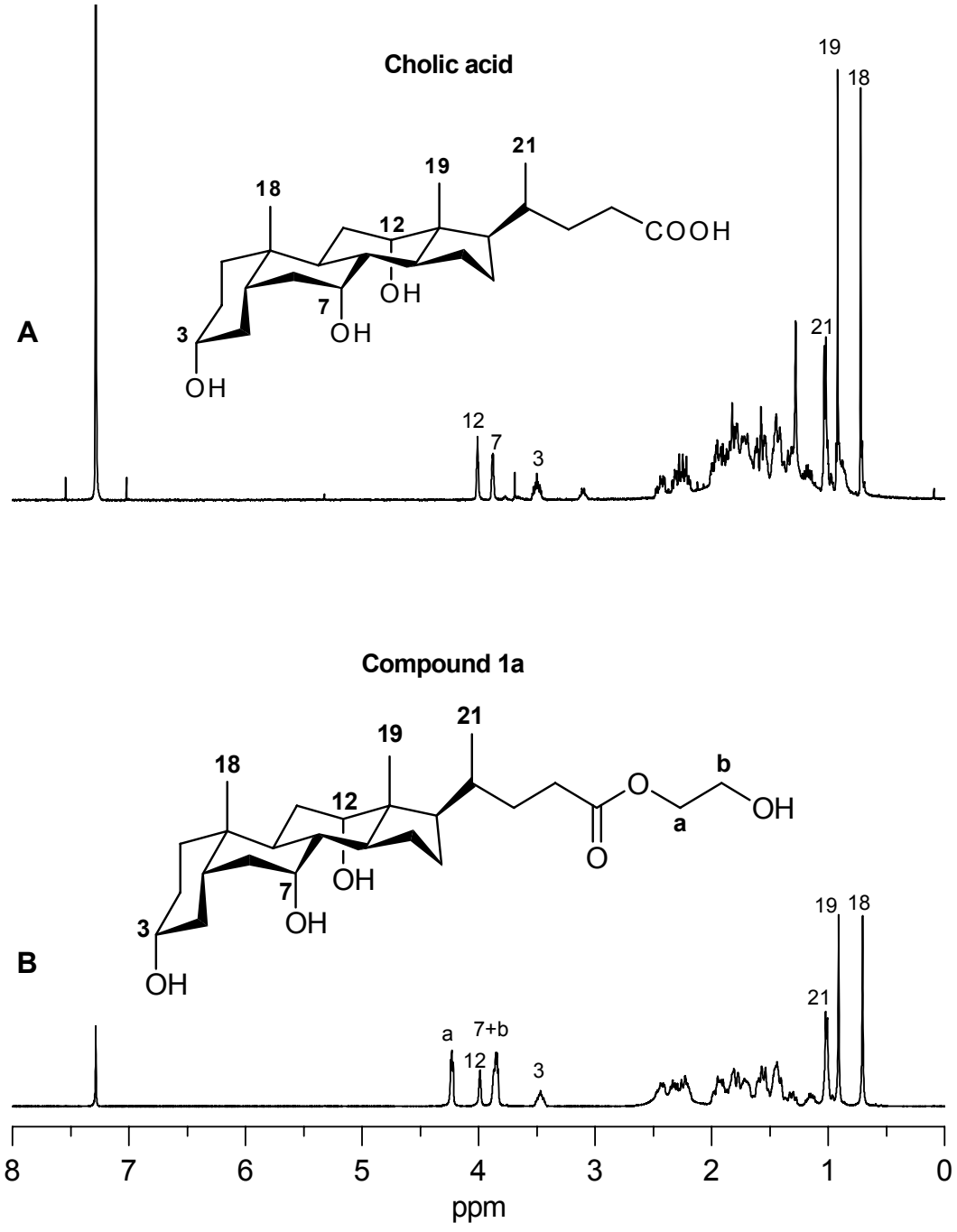

Figure 3.2. ^{1}H NMR spectra of (A) cholic acid and (B) compound **1a** in $CDCl_3$.

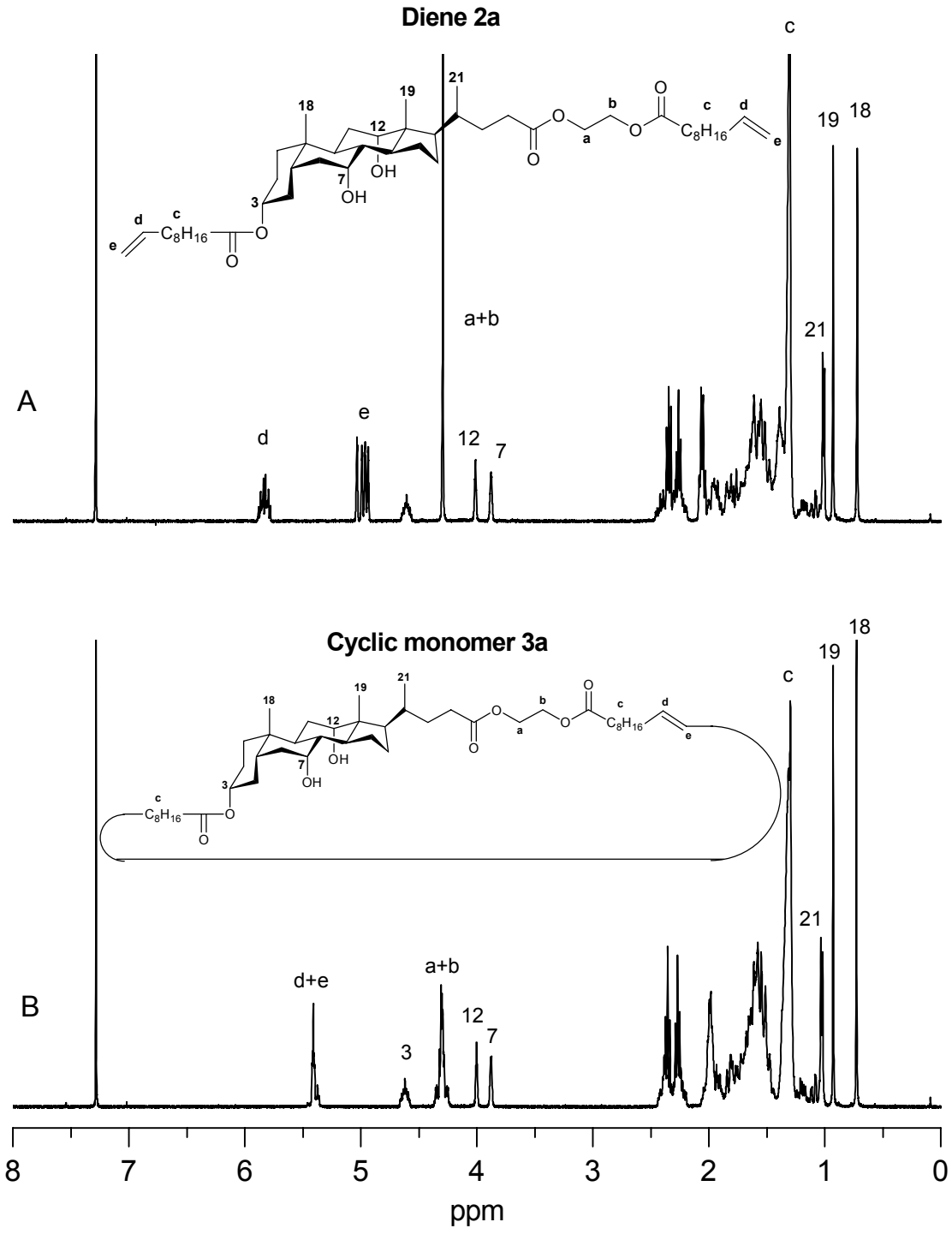

Figure 3.3. ^{1}H NMR spectra of (A) diene **2a** and (B) cyclic monomer **3a** in $CDCl_3$.

The synthetic procedure initially used to make cyclic monomer **3a** was based on a procedure developed earlier.[4] Here, the concentration of the starting diene material **2a** was 13 mM, a catalyst corresponding to 5 mol% of the cyclic monomer was used, and the reaction was completed in 24 h at room temperature. There were, however, some problems encountered with this procedure. For one, as indicated by TLC (shown in A and B of Figure 3.4), the starting material remained in quite a large proportion even 24 h after the reaction started. Moreover, the reaction system formed a series of oligomers, such as dimers, trimers, tetramers, etc., which made the purification of the desired cyclic monomers more difficult and reduced the yield.

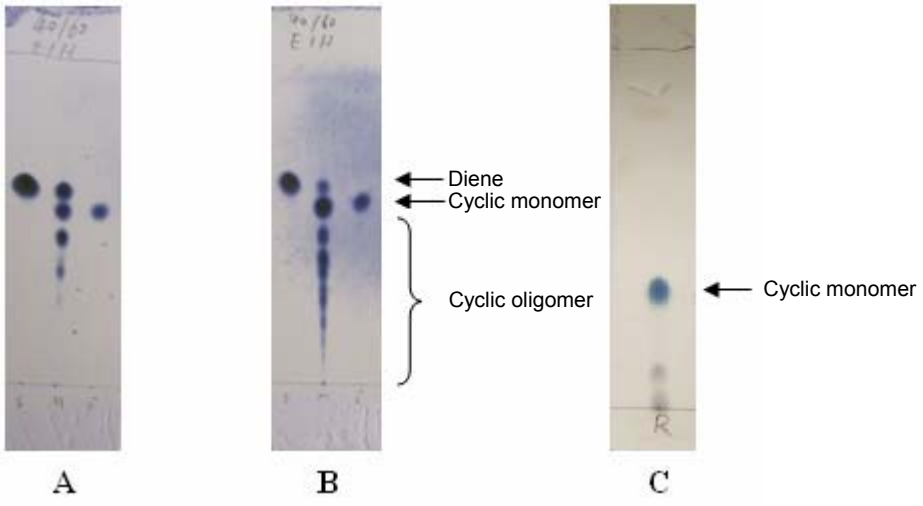

Figure 3.4. TLC plates of the synthesis of cyclic monomer **3a**, (A) 4 h and (B) 24 h after the reaction started at room temperature with 13 mM of diene, (C) 5 h after the reaction started at 40^{o}C (reflux) with 3 mM of diene.

To overcome these problems, another method was used to synthesize the cyclic monomer.[5] It consists of using a lower concentration of starting material (3 mM) and the reaction was completed in DCM under reflux (shown in Figure 3.4 C). In comparison with the method used earlier, this method resulted in a significantly improved yield of

cyclic monomer **3a** (from 53 to 90%) and easier separation of the cyclic monomer from the reaction mixture because the amount of cyclic oligomers was greatly decreased.

Comparison of the ^{1}H NMR spectrum of diene **2a** and cyclic monomer **3a** reveals two main differences (Figure 3.3). First, the multiplets at 5.82 and 4.96 ppm of the protons of the two double bonds at the end of the long alkene chains were merged into one multiplet after the formation of the cycle because the protons on the double bond of cyclic monomer **3a** became chemically equivalent. Second, the single peak of the protons on carbons *a* and *b* of diene **2a** became a multiplet because the formation of the macrocycle is slightly hampered by the rotation of carbons a and b, and the relaxation times of the protons on these carbons became longer compared to the NMR time scale. Combined with the results of MALDI-TOF and elemental analysis (Chapter 2), the results of ^{1}H NMR spectroscopy further confirmed the formation of the macrocycle.

3.1.2 Synthesis of lithocholic acid-based cyclic ester-amide-amide monomer 3c

The cyclic monomer **3c** was prepared from diene **2c**.[2] The ^{1}H NMR spectra of diene **2c** and cyclic monomer **3c** are shown in Figure 3.5.

Conversion of diene **2c** to cyclic monomer **3c** results in the same changes in the ^{1}H NMR spectra that were observed when diene **2a** was converted to cyclic monomer **3a**. The combined results of MALDI-TOF, elemental analysis (Chapter 2) and ^{1}H NMR spectroscopy confirmed the formation of cyclic monomer **3c**.

The differences in the structures of cyclic monomers **3a** and **3c** are clearly observed in the ^{1}H NMR spectra. The peaks at 3.97 and 3.85 ppm in the ^{1}H NMR spectrum of cyclic monomer **3a** are not present in the ^{1}H NMR spectrum of cyclic monomer **3c** because the core is a lithocholic acid, which has, in contrast with those of cyclic monomer **3a**, no hydroxyl group at positions 7 and 12. In addition, there is an extra peak at 6.34 ppm in the ^{1}H NMR spectrum of the cyclic monomer **3c** attributed to the proton on the amide group.

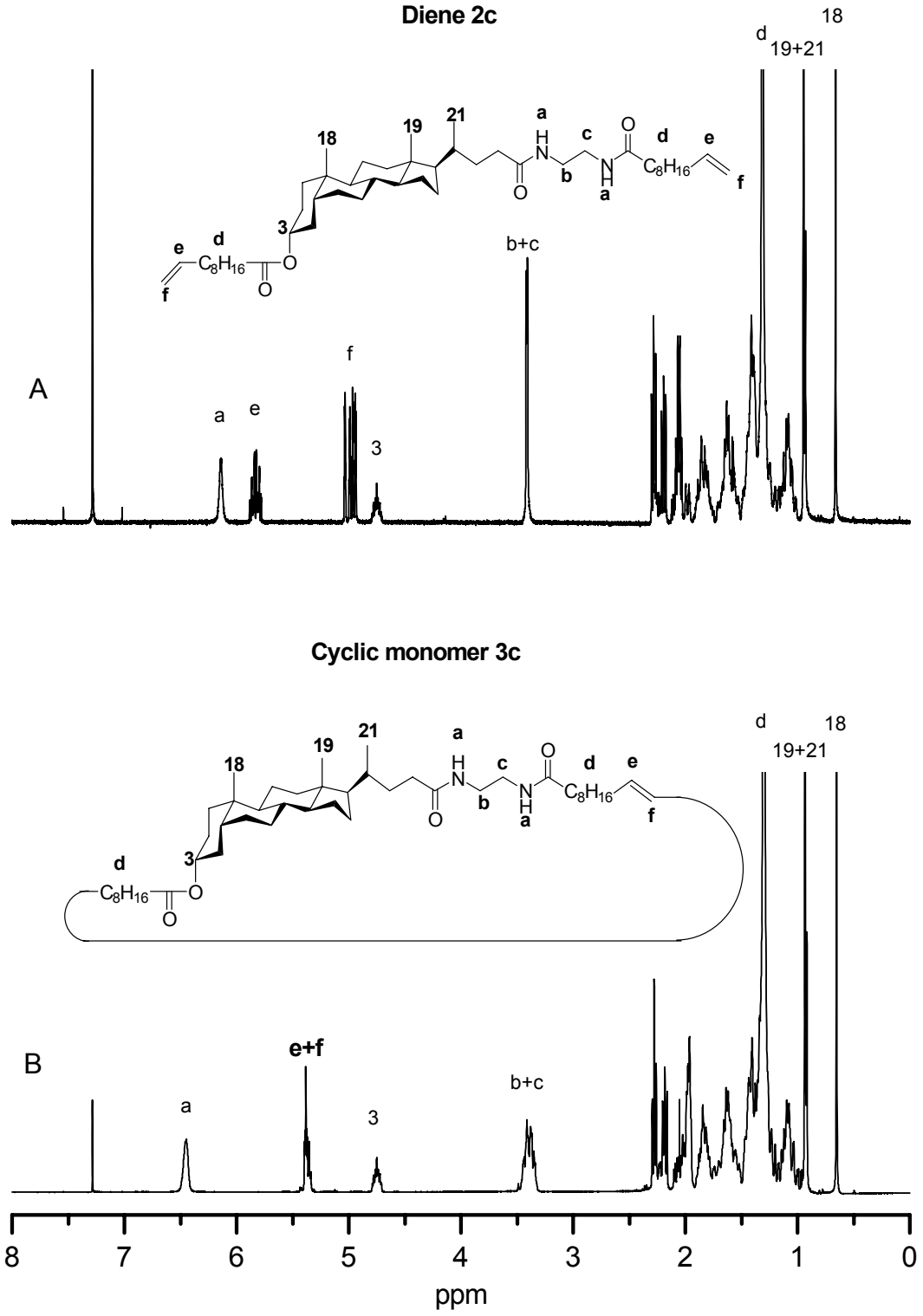

Figure 3.5. ^{1}H NMR spectra of (A) diene **2c** and (B) cyclic monomer **3c** in $CDCl_3$.

3.1.3 Synthesis of lithocholic acid-based cyclic ester-amide-ester monomer 3d

The synthesis of cyclic monomer **3d** was completed in 3 steps, as shown in Figure 2.1. The ^{1}H NMR spectra of methyl ester of lithocholic acid, compound **1d**, diene **2d** and cyclic monomer **3d**, are shown in Figures 3.6 and 3.7.

The sharp singlet at 3.67 ppm in the ^{1}H NMR spectrum of the methyl ester of lithocholic acid is a typical peak for methyl ester. After refluxing with 2-aminoethanol, the ester bond was transformed to an amide group. As a result, the sharp singlet at 3.67 ppm disappeared and the peaks of two methylene groups at 3.76 and 3.46 ppm were observed in the ^{1}H NMR spectrum of compound **1d**. In the ^{1}H NMR spectrum of diene **2d,** the peak shifts of 3α-H (from 3.65 to 4.75 ppm) and protons on carbon *c* (from 3.76 to 4.19 ppm) are similar to those observed for diene **2a**. In the ^{1}H NMR spectrum of cyclic monomer **3d**, the peaks of the protons on the two carbon-carbon double bonds were merged into one peak, which is also what was observed for cyclic monomer **3a**. For cyclic monomer **3d**, the protons on carbon *b* (next to an amide group) and carbon *c* (next to an ester group) are not equivalent; they show distinct peaks in the ^{1}H NMR spectra of diene **2d** and cyclic monomer **3d**.

3.1.4 Synthesis of cholic acid-based diester cyclic monomer 3e

The synthesis of the cholic acid-based diester cyclic monomer is different from the synthesis of cyclic monomers **2a-d** in which the two long alkane chains were attached to the core in separate reactions (as shown in Figure 2.2). In the first step, the cholic acid was reacted with ω-undecylenyl alcohol and a long alkane chain was attached to the cholic acid core through an ester bond. In the ^{1}H NMR spectrum of compound **1e** (shown in Figure 3.8), two multiplet-peaks at 5.83 and 4.96 ppm were caused by the proton on the carbon-carbon double bonds at the end of the alkane chain. In the second step, another long alkane chain was attached to the cholic acid core through an ester bond at position 3 of cholic acid. In the ^{1}H NMR spectrum of diene **2e** (shown in Figure 3.9), the peak of 3α-H shifted from 3.46 to 4.60 ppm when compound **1e** was transformed to diene **2e**. Meanwhile, the relevant integration of peaks *c* and *d* of diene **2e** is two times of that for compound **1e**. The difference between diene **2e** and cyclic monomer **3e** followed the same tendency as the differences for diene **2a** and cyclic monomer **3a**.

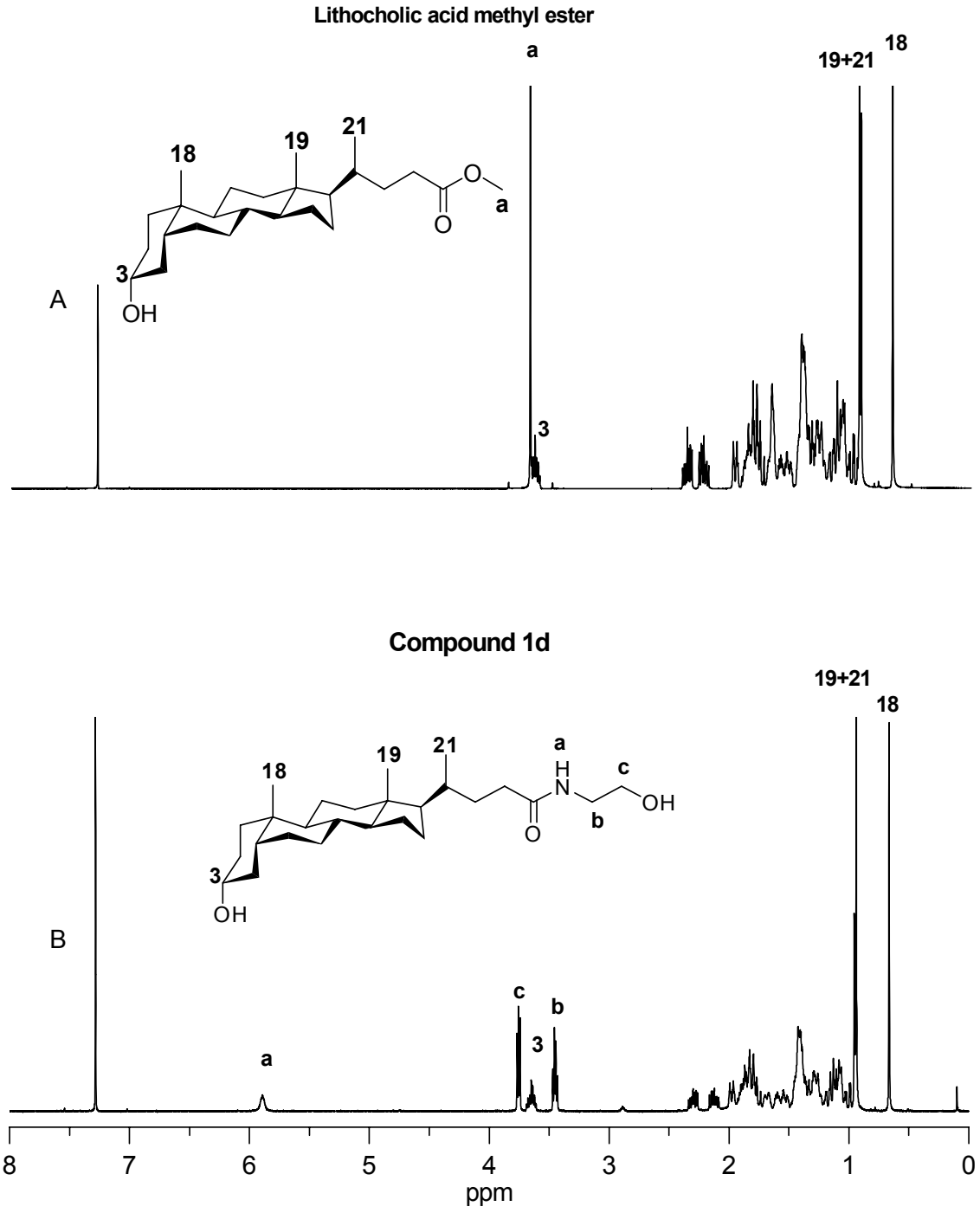

Figure 3.6. ^{1}H NMR spectra of (A) lithocholic acid methyl ester and (B) compound **1d** in $CDCl_3$.

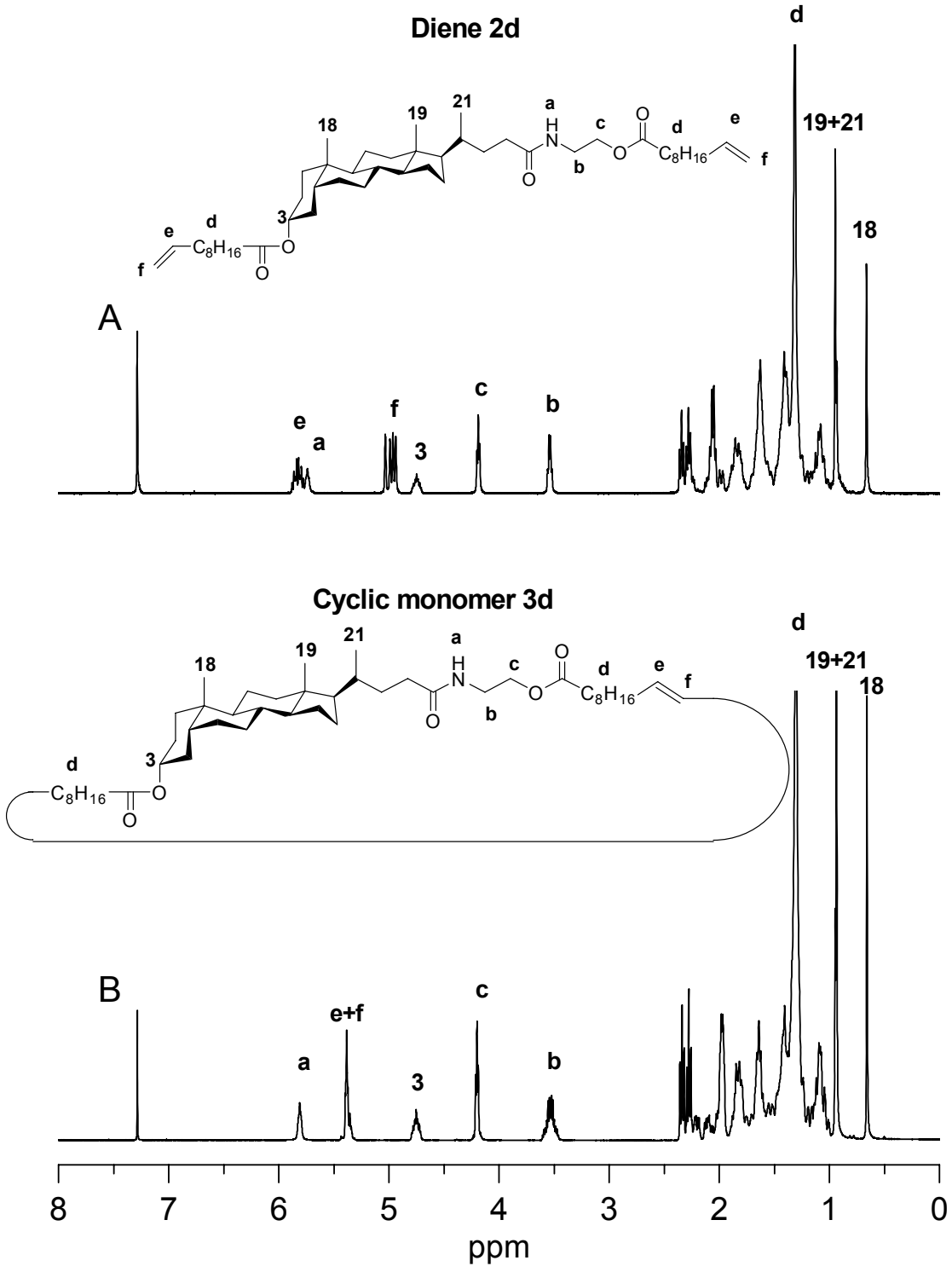

Figure 3.7. ^{1}H NMR spectra of (A) diene **2d** and (B) cyclic monomer **3d** in $CDCl_3$.

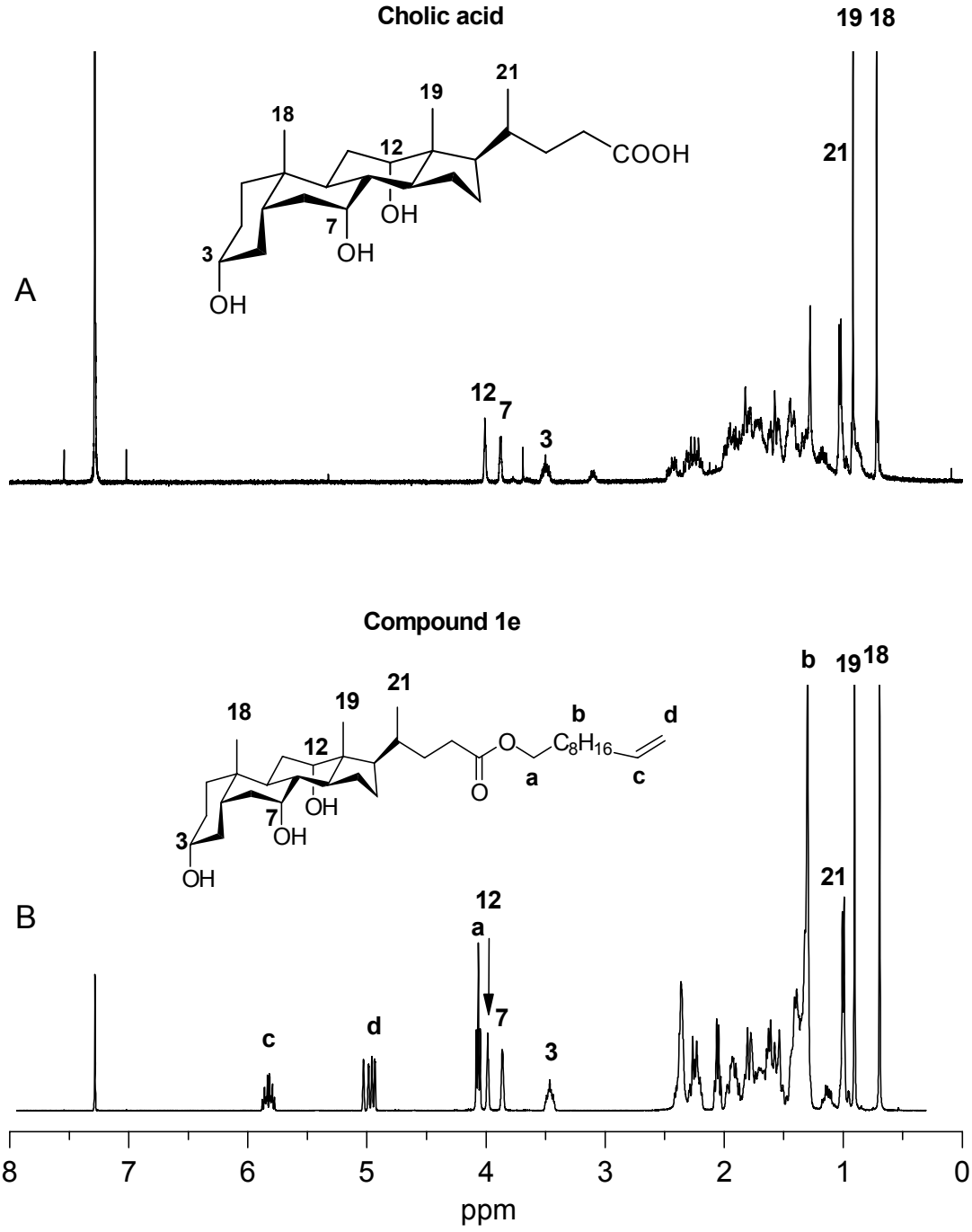

Figure 3.8. ^{1}H NMR spectra of (A) cholic acid and (B) compound **1e** in $CDCl_3$.

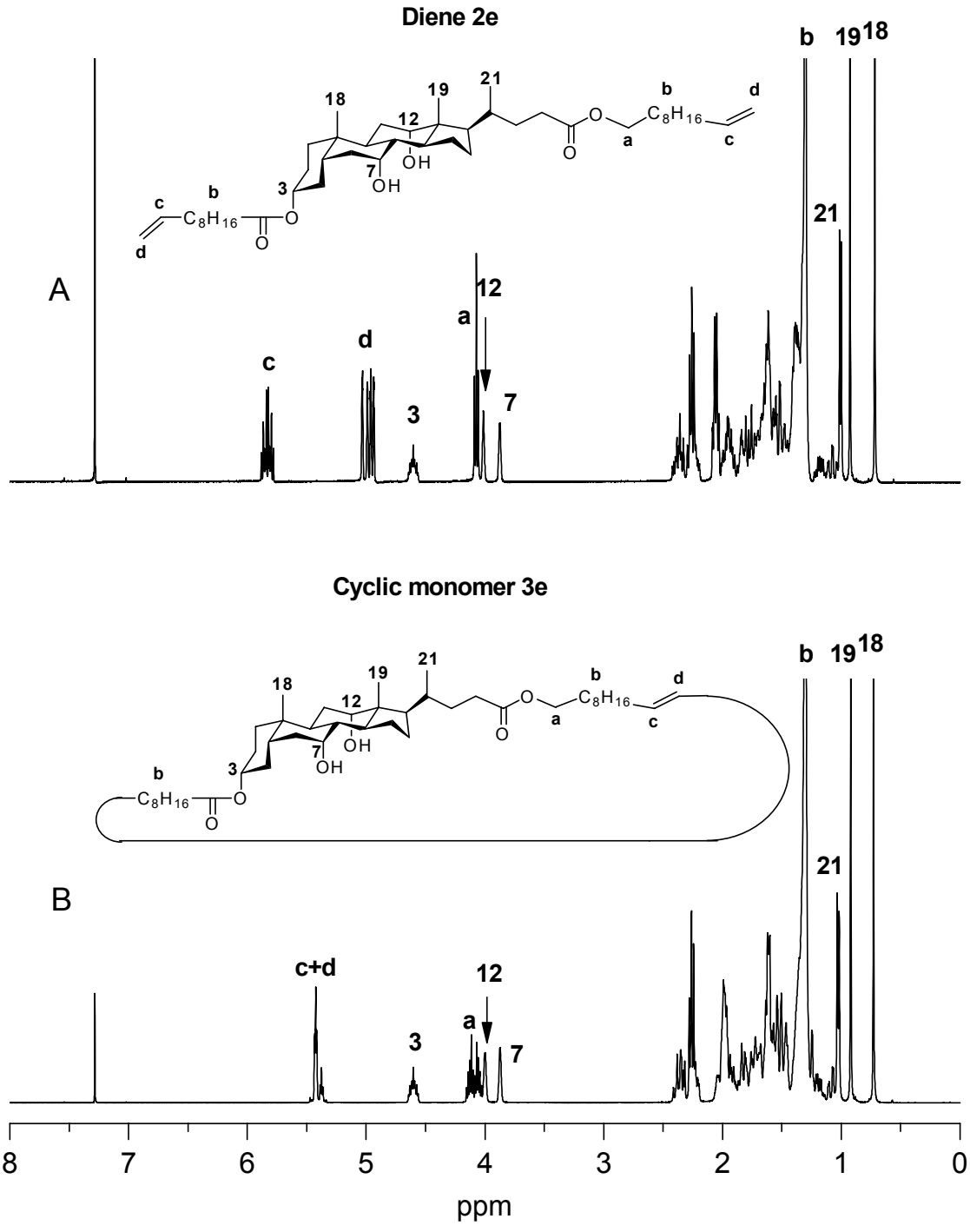

Figure 3.9. ^{1}H NMR spectra of (A) diene **2e** and (B) cyclic monomer **3e** in $CDCl_3$.

3.2 Kinetic study of ED-ROMP via second-generation Grubbs catalyst

The purpose of the kinetic study was to provide a guideline of the polymerization process to terminate the reaction at an optimal time. The kinetic study was conducted in a concentrated solution (1.3 M) of cyclic monomer **3a** in anhydrous DCM (2 mL) with a catalytic amount (1% eq.) of the second-generation Grubbs catalyst. A small amount of reaction medium (40 μL) was taken out via a syringe at specific time intervals and then quenched immediately by ethyl vinyl ether. The molecular weight of the polymer in the resulting solution was monitored by GPC as shown in Figure 3.10. The cyclic monomer **3a** was almost consumed completely 31 minutes after the polymerization started.

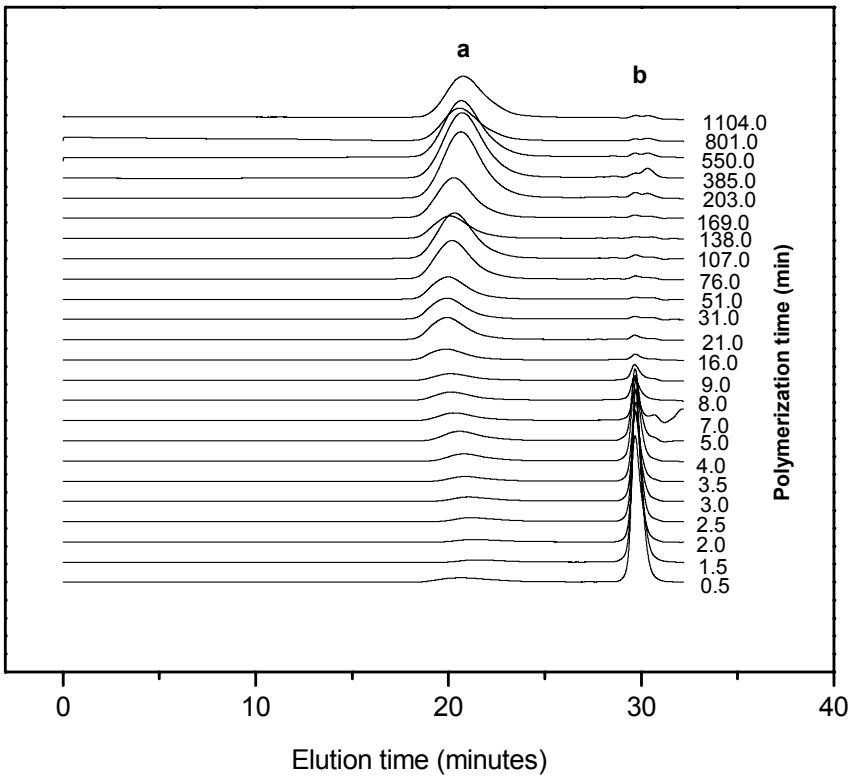

Figure 3.10. GPC traces of samples quenched at different polymerization times. THF was used as eluent. (a) indicates the peak of the polymer **1** while (b) indicates the peak of the cyclic monomer **3a**.

The graph of M_n versus reaction time of ring-opening metathesis polymerization of cyclic monomer **3a**, shown in Figure 3.11, exhibits a maximum with its summit at 15 minutes and a plateau at 6-7 h after the beginning of the polymerization. This can be explained by the well-known equilibrium between the cyclic oligmers and the polymers.[6-9] At the beginning of the polymerization, the ROMP is predominant, gradually establishing an equilibrium of polymerization and cyclo-depolymerization, leading to a lower M_n at a higher conversion rate.

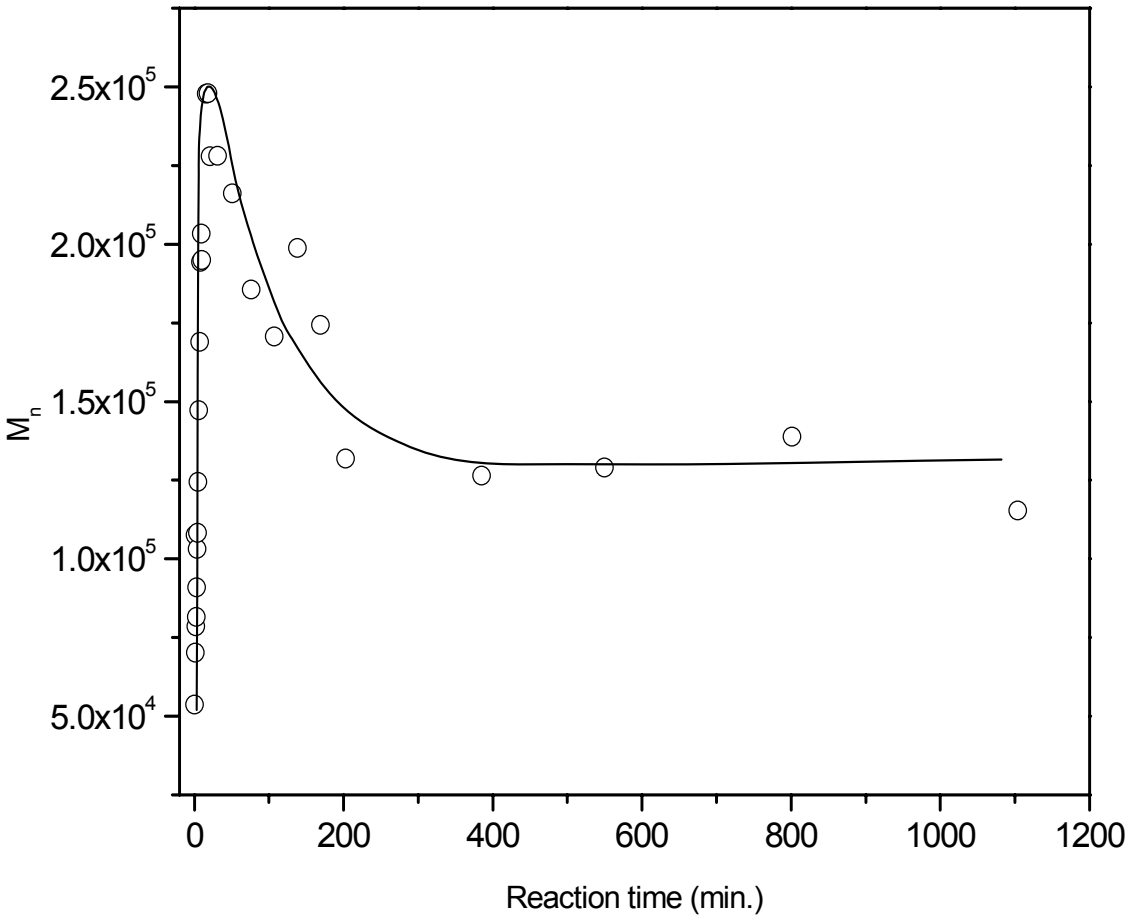

Figure 3.11. M_n as a function of polymerization time of cyclic monomer **3a** via ROMP with an initial monomer concentration of 1.28 M and 1 mol% loading of second-generation Grubbs catalyst in anhydrous DCM. The plain curve serves as a visual guide.

3.3 Preparation of bile acid-based homopolymers via ED-ROMP

The polymers prepared via ED-ROMP exhibit similar ^{1}H NMR spectra as those of the corresponding cyclic monomers. For example, the ^{1}H NMR spectra of cyclic monomer **3a** and polymer **1** are shown in Figure 3.12. Except the peak **a + b**, the peaks of cyclic monomer **3a** and polymer **1** are mostly the same. In the ^{1}H NMR spectrum of cyclic monomer **3a**, this peak is a multiplet, but it becomes a singlet in the ^{1}H NMR spectrum of polymer **1**. This is because the carbons **a** and **b** cannot rotate freely in cyclic monomer **3a** as they can in polymer **1** and the relaxation times of the protons on these carbons became shorter than the NMR time scale.

Polymers **1a - f** with molecular weight varied from 6.3 to 52.1 × 10^4 were prepared using different amounts of catalyst and various quenching times (Table 3.1).

Table 3.1. Physical properties of polymers **1a-f** prepared using different amounts of second-generation Grubbs catalyst and polymerization times.

Homopolymers	Catalytic loading (mol %)	Polymerization time	M_n ($\times 10^3$)[a]	PDI	T_g (^{o}C)[b]
1a	0.67	20 min.	521	1.60	49.4 ± 0.4
1b	0.67	20 h	394	1.52	49.0 ± 0.5
1c	1	3 h	231	1.71	48.0 ± 0.3
1d	1	20 h	148	1.63	48.8 ± 0.6
1e	2	20 h	111	1.65	46.6 ± 0.4
1f	1	1 min.	63	1.71	45.0 ± 0.5

Note:

[a] M_n was determined by GPC using THF as the eluent and polystyrene as the standards.

[b] T_g measured by DSC with a heating rate of 10^{o}C/min. The standard deviation is calculated from the T_g values by selecting different start and end points of the DSC curves.

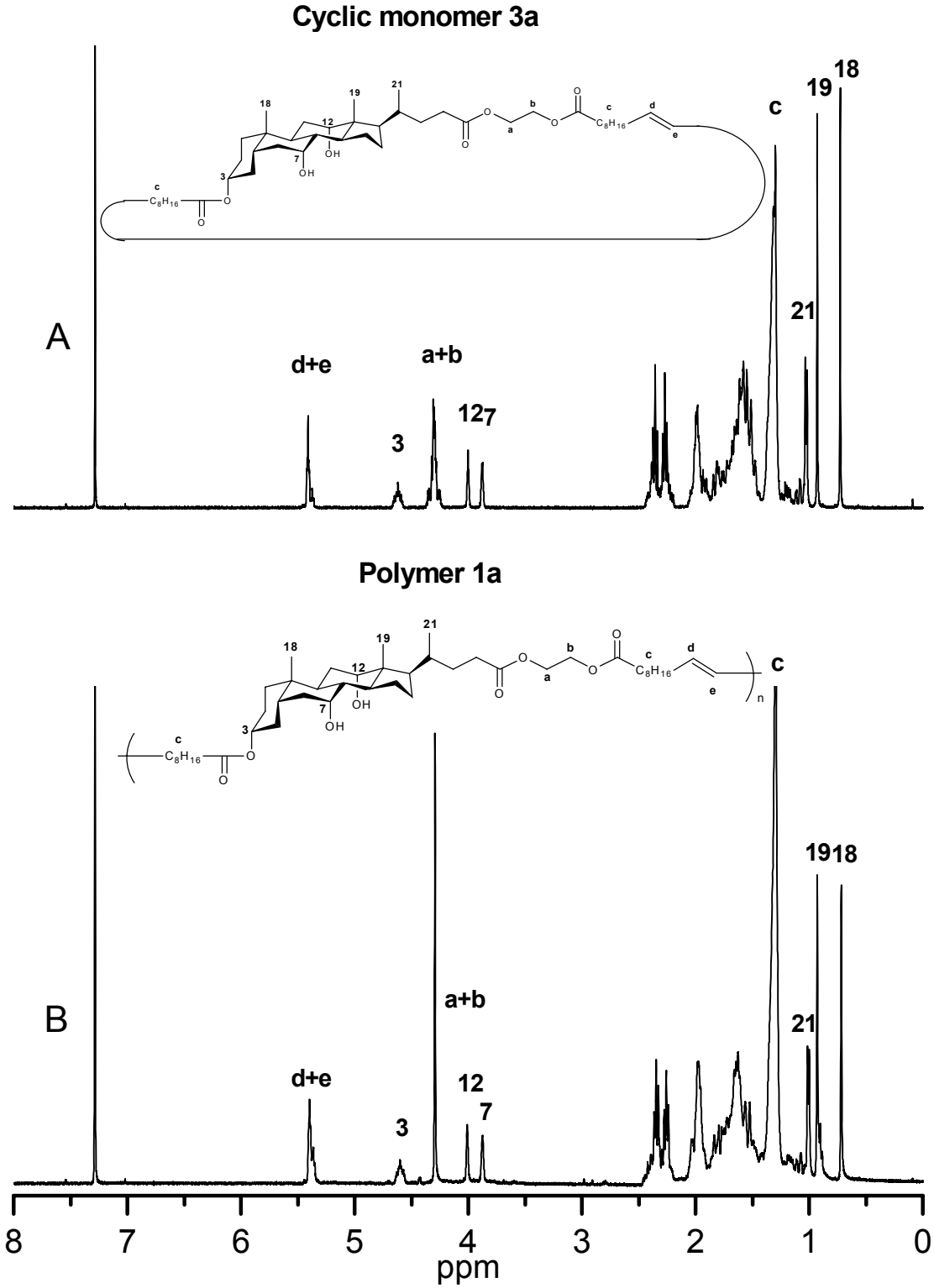

Figure 3.12. ^{1}H NMR spectra of (A) cyclic monomer **3a** and (B) polymer **1a** in $CDCl_3$.

The molecular weights of polymers **1c** and **1d** are higher than those obtained from the curves of the kinetic study (Figure 3.11), even if the reaction conditions were the same in the preparation of polymers **1c** and **1d**. However, the samples for the kinetic study were injected into GPC directly without being precipitated in methanol/hexanes, a process that may eliminate some chains having low molecular weights.

3.4 Synthesis of copolyesters based on cholic acid and ricinoleic acid

A series of copolyesters based on cyclic monomer **3a** and ricinoleic acid monolactone were prepared via ED-ROMP using second-generation Grubbs catalyst. The mechanical and thermal properties of these copolyesters vary significantly, rendering the polymers potentially useful for a variety of applications.

3.4.1 Preparation of purified ricinoleic acid

Ricinoleic acid is an unsaturated fatty acid naturally existing in the mature castor plant seeds. About 90% of triglycerides in the castor oil are formed from ricinoleic acid. Meanwhile, some other unsaturated fatty acids (5-15%), such as oleic acid and linoleic acid, also exist in the triglycerides of castor oil.[10] Thus, hydrolysis and purification of castor oil are necessary to obtain purified ricinoleic acid (Figure 2.4).

In the first step (Figure 2.4), the methyl ester of ricinoleic acid was formed by transesterification of castor oil. The methyl ester is easier to separate by column chromatography than ricinoleic acid itself because of its lower polarity. In the second step, the purified methyl ester of ricinoleic acid was hydrolyzed by potassium hydroxide and then neutralized by concentrated hydrochloric acid. The ^{1}H NMR spectra of methyl ester of ricinoleic acid and ricinoleic acid are shown in Figure 3.13. These two spectra are similar, except for the methyl ester peak in Figure 3.13 A. The ^{1}H NMR spectrum of the ricinoleic acid (Figure 3.13 B) is exactly the same as that reported in the literature.[11]

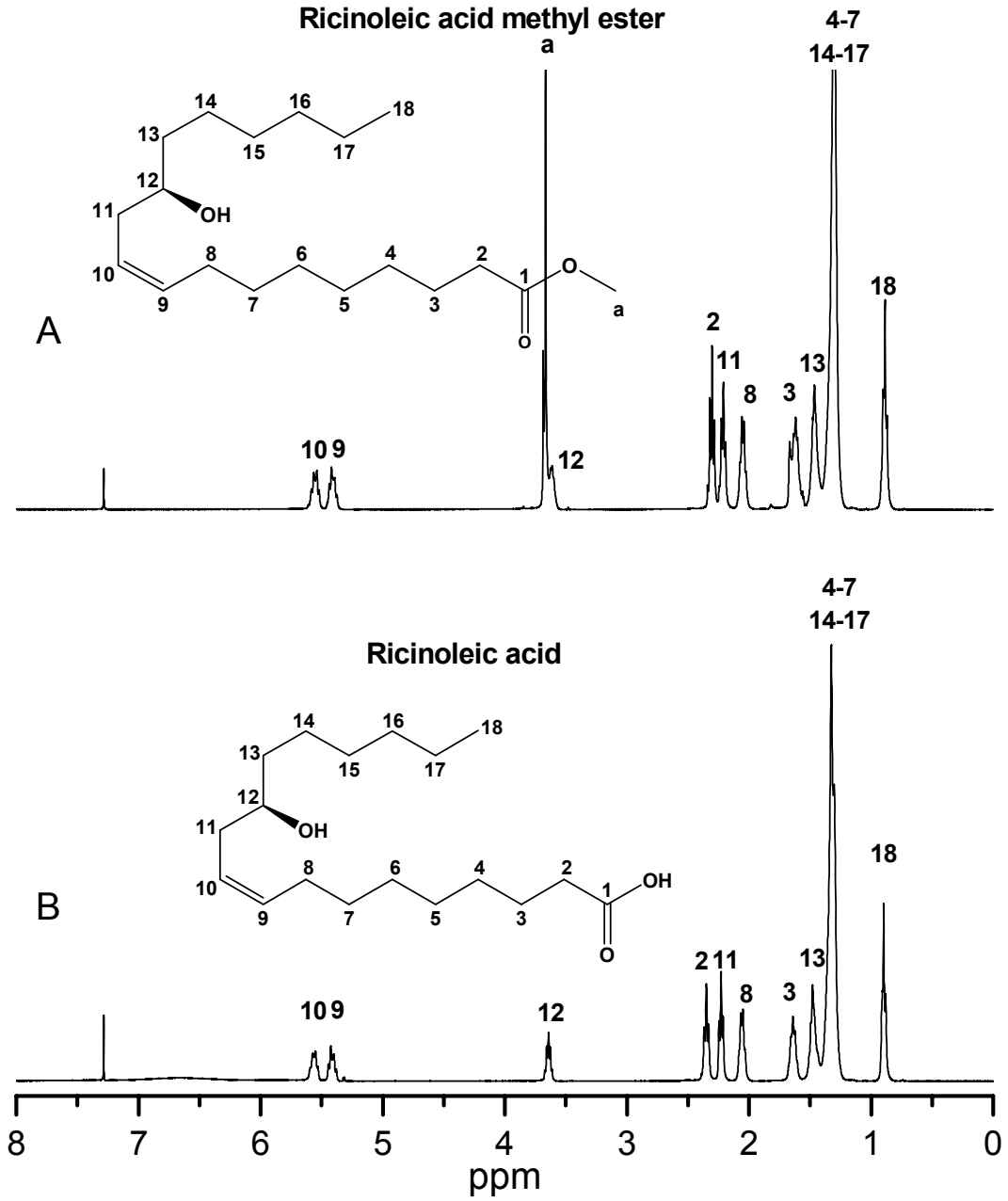

Figure 3.13. The ^{1}H NMR spectra of (A) methyl ester of ricinoleic acid and (B) ricinoleic acid in $CDCl_3$.

3.4.2 Synthesis of monolactone of ricinoleic acid

The synthesis of the monolactone of ricinoleic acid was performed as described by Slivniak and Domb.[11] However, the ^{1}H NMR spectrum (as shown in Figure 3.14) obtained for ricinoleic acid monolactone was somewhat different.[11] The differences of ^{1}H

NMR spectra of ricinoleic acid monolactone between the literature and this study are highlighted in Table 3.2 by bold characters.

Table 3.2. Differences of peak assignments for the ^{1}H NMR spectrum of ricinoleic acid monolactone in this study and in the literature.

^{1}H NMR in literature[11]			^{1}H NMR in this study		
Peak (ppm)	Integration	Assignments (protons)	Peak (ppm)	Integration	New assignments (protons)
5.35 – 5.48	2H	C9, C10	5.34 -5.52	2H	C9, C10
4.93 -4.96	1H	C12	4.97	1H	C12
2.28	**2H**	**C2**	**2.50**	**1H**	**C11 (1H)**
2.23	**2H**	**C11**	**2.30**	**3H**	**C11 (1H), C2 (2H)**
2.09	2H	C8	2.10	2H	C8
1.59	**2H**	**C3**	**1.69**	**3H**	**C13 (1H), C3 (2H)**
1.52	**2H**	**C13**			
1.29	**16H**	**C4-7, C14-17**	**1.15 – 1.62**	**17H**	**C13 (1H), C4-7, C14-17**
0.87	3H	C18	0.90	3H	C18

* Bold letters highlight the differences in the new assignments of proton signals

In the ^{13}C NMR spectrum of the ricinoleic acid monolactone (Figure 3.14), 18 peaks are observed, which exactly match the number of carbons in the molecule. Two peaks at 125 and 132 ppm are assigned to the vinyl carbons (C9 and C10). One carbonyl group (C1) is observed at 174 ppm. The peak at 73.7 ppm is the signal of C12.

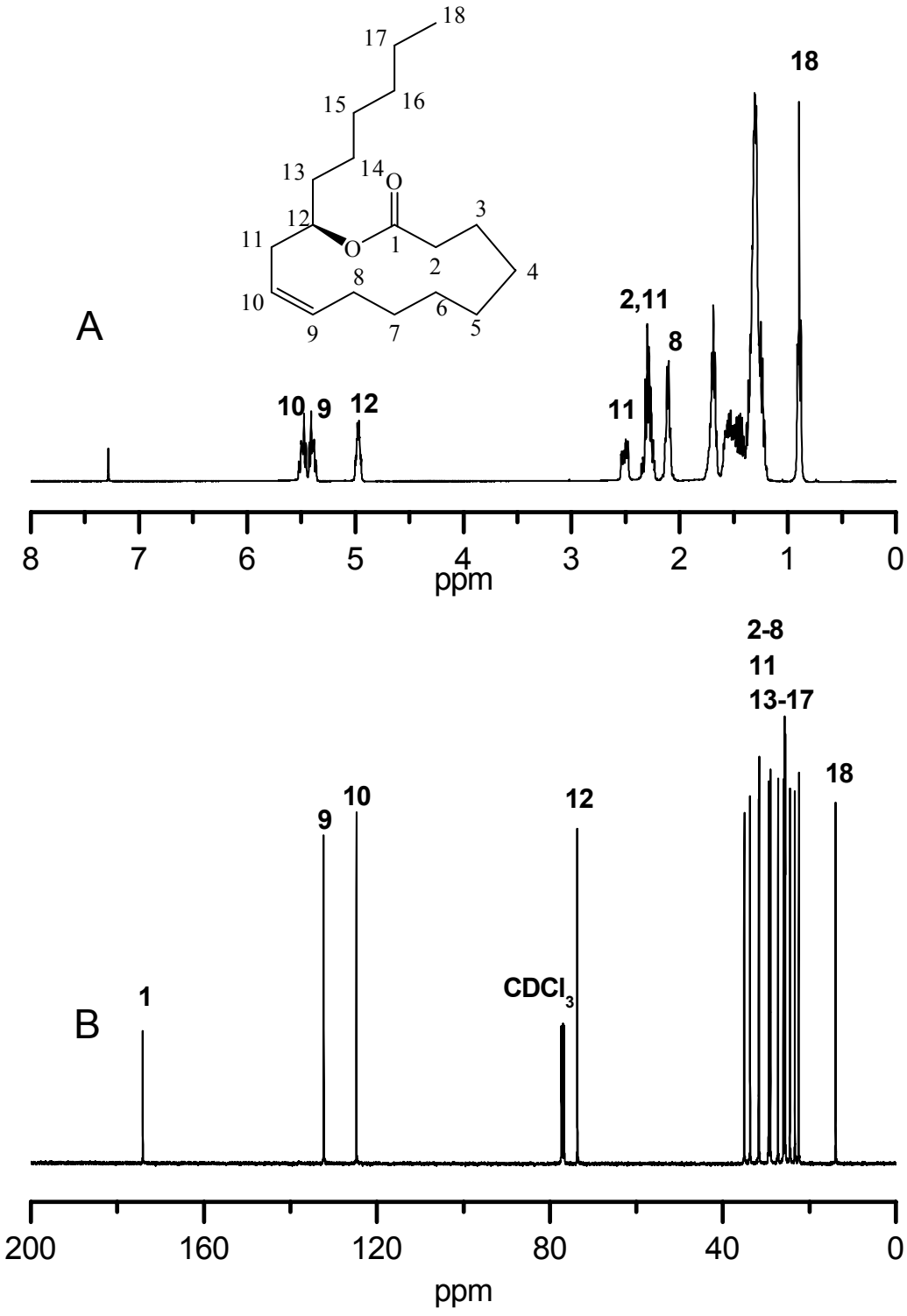

Figure 3.14. (A) ^{1}H NMR and (B) ^{13}C spectra of the monolactone of ricinoleic acid in $CDCl_3$.

The structure of ricinoleic acid monolactone was also confirmed by ^{1}H-^{1}H COSY, ^{1}H-^{13}C HMQC and mass spectrometry. The ^{1}H-^{1}H COSY spectrum of ricinoleic acid monolactone is shown in Figure 3.15, which also gives the ^{1}H proton spectrum of ricinoleic acid monolactone along both axes. The spectrum shows clearly the presence of two multiplets from the signals of the protons on the carbon-carbon double bonds: peak **a** (1H, C10), peak **b** (1H, C9), and peak **c** (1H) from the signal of the proton on C12. Peak **a** has a cross-correlation with peaks **e** (3H) and **d** (1H); Peak **c** has a cross-correlation with peaks **e** and **d**, and peak **e** has a cross-correlation with peak **d.** It is evident that both peaks **e** and **d** contain the signal from the protons of C11. The rotation of C11 is restricted due to the ester bond of C12 and carbon-carbon double bond, so that the signal of the protons from C11 is divided into two peaks due to a slow exchange (on the NMR time scale).

^{13}C-^{1}H HMQC spectrum (shown in Figure 3.16) also verifies this conclusion because peaks **d** and **e** have a cross-correlation with the same carbon. Moreover, peak **e** contains two kinds of protons, one kind from C11, and the other from the methylene group on C2. The HMQC spectrum also shows that peak **e** has two kinds of cross-correlation with two different carbons. Meanwhile, peak **f** is the signal of protons from C8 because it has a cross-correlation with peak **b**. Peak **g** contains the signals of two different protons from C3 and C13. Peak **h** contains the signals of two different protons from C7 and C13. Peak **i** is the signal of the protons from the methylene group and peak **j** is the signal of the protons of C18. Based on the results of ^{1}H-^{1}H COSY, ^{1}H-^{13}C HMQC, a new assignment of the ^{1}H NMR is obtained and shown in Table 3.2.

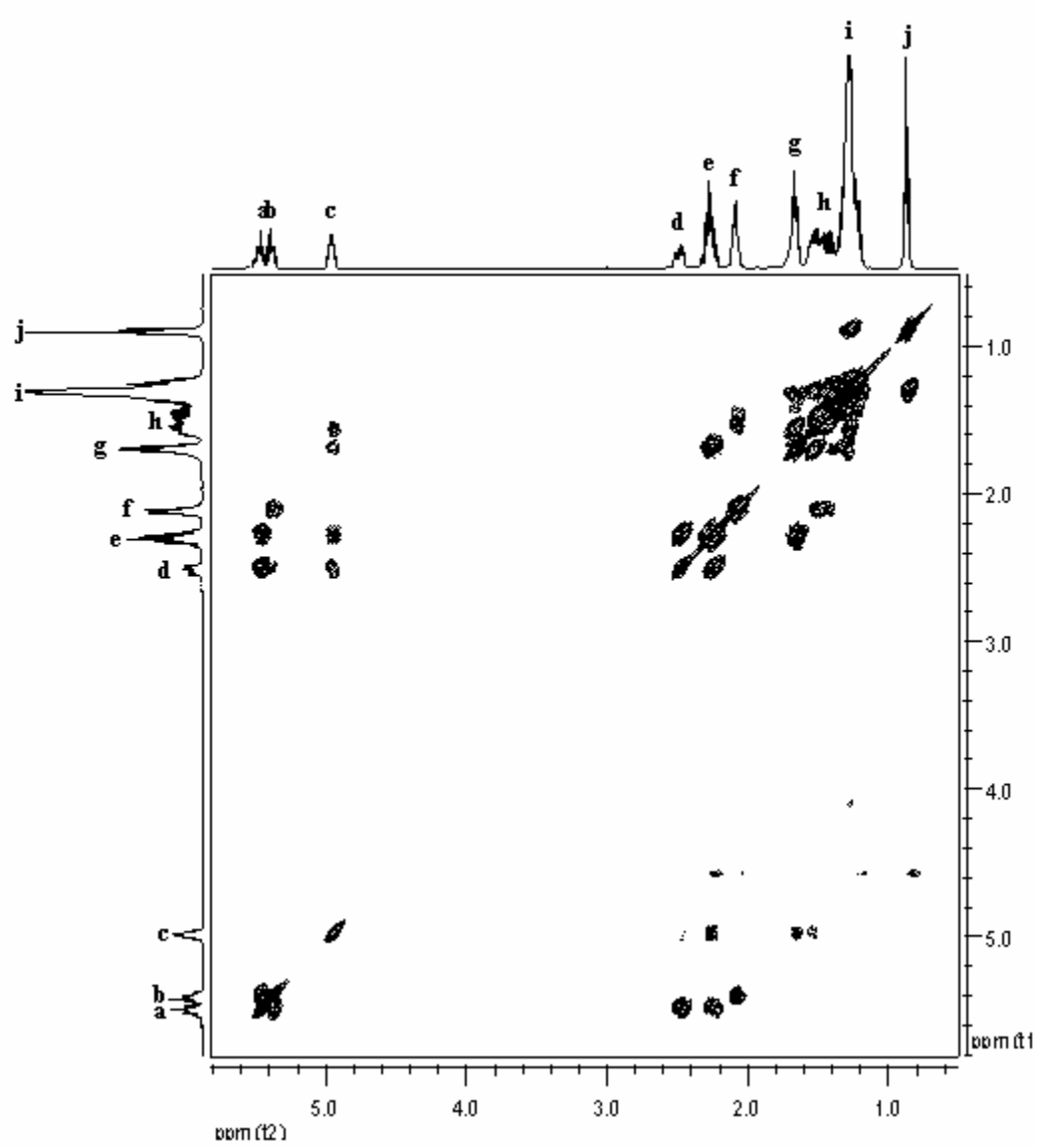

Figure 3.15. The ^{1}H-^{1}H COSY spectrum of ricinoleic acid monolactone in $CDCl_3$.

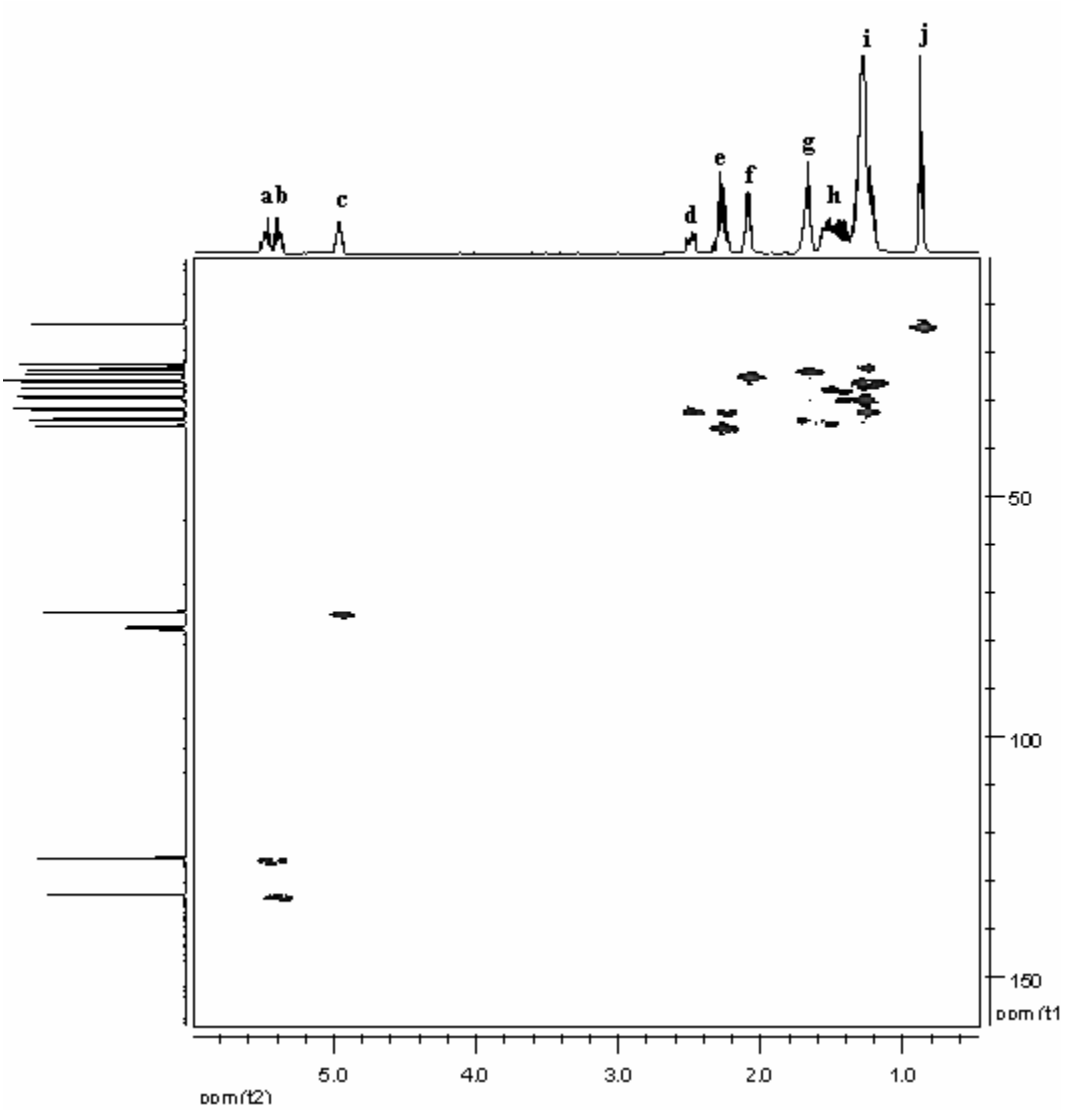

Figure 3.16. The ^{13}C-^{1}H HMQC spectrum of ricinoleic acid monolactone in $CDCl_3$.

The mass spectrum also confirms that the prepared compound matches the mass of the monolactone of ricinoleic acid. A peak at 281.25 amu, which is the $[M+H]^+$ peak (required 281.25 amu) is observed, and another peak at 303.23 amu, which is the $[M+Na]^+$ peak (required 303.23 amu), is also observed

3.4.3 Preparation of copolyesters based on cholic acid and ricinoleic acid

A series of copolymers **6a-f** were prepared from ricinoleic acid monolactone and cyclic monomer **3a** (shown in Table 2.2). The ^{1}H NMR spectra of ricinoleic acid monolactone, cyclic monomer **3a** and copolymer **6d** are shown in Figure 3.17. In the ^{1}H NMR spectrum of copolymer **6d**, peak *1* is the signal of the protons on the carbon-carbon double bonds in the repeat units of both ricinoleic acid monolactone and cyclic monomer **3a**. Peak *2* is the signal of the proton on C12 of ricinoleic acid monolactone. Peaks *3*, *4*, *5*, and *6* are the proton signals of the repeat unit of the cyclic monomer **3a**, assigned to 3α-H, protons **a** + **b**, 7α-H and 12α-H, respectively. The molar percentage of the ricinoleic acid monolactone in the copolymers can be calculated from the integration of peaks *1* and *2*.

The ^{1}H NMR spectra of copolymers **6a-f** are shown in Figure 3.18. With increasing molar percentage of ricinoleic acid monolactone (RCA), peak *2* became more obvious and peaks *3*, *4*, *5* and *6* became almost invisible. However, peak *1* remained stable because both ricinoleic acid monolactone and the cyclic monomer contain carbon-carbon double bonds. Thus, the changes of molar percentage of ricinoleic acid monolactone did not affect this peak too much. The actual molar percentage of ricinoleic acid monolactone in the copolymers can be calculated based on the integration of ^{1}H NMR signals (shown in Table 3.3). The properties of copolymers **6a-f** are discussed in the following section.

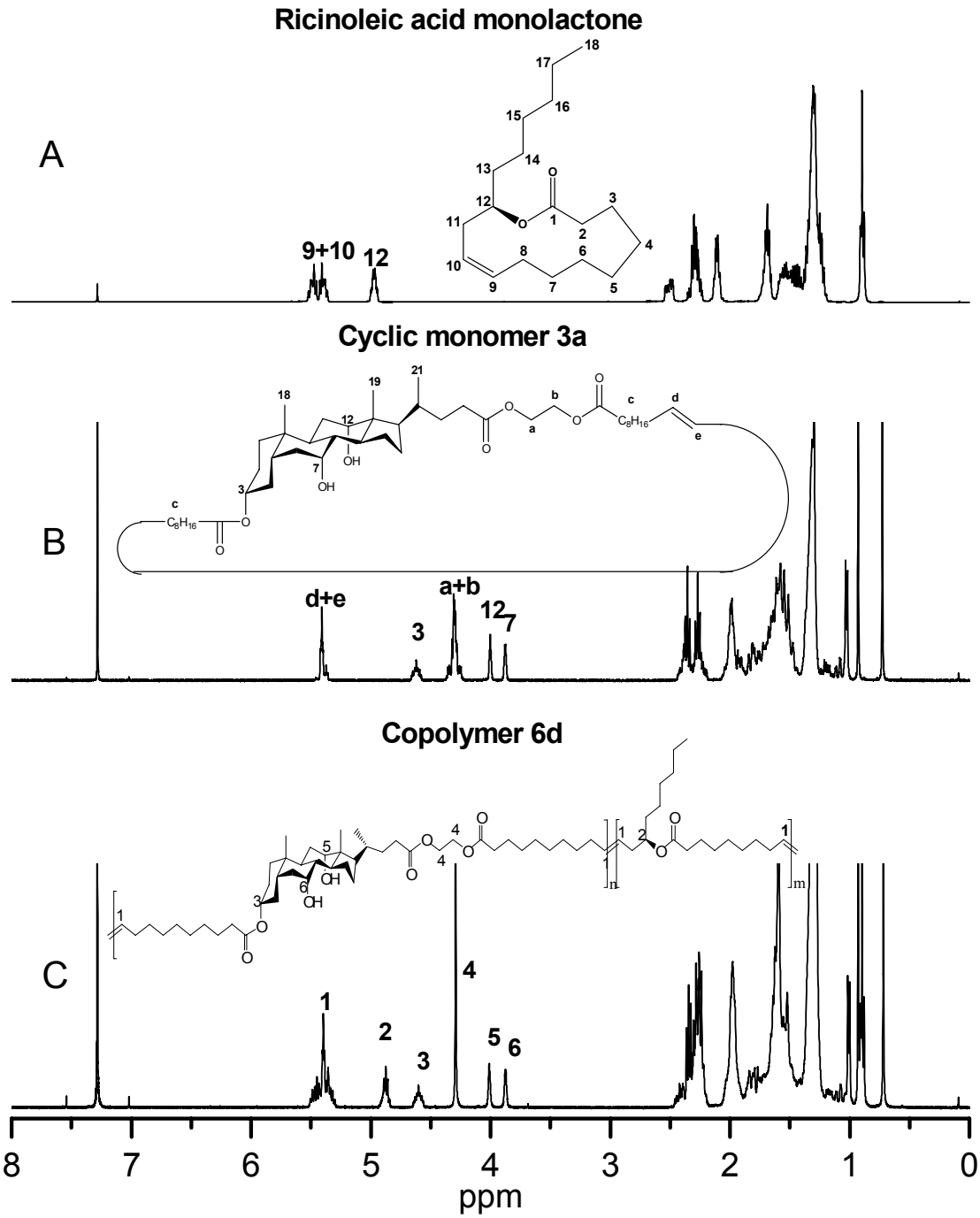

Figure 3.17. The ^{1}H NMR spectra of (A) ricinoleic acid monolactone, (B) cyclic monomer **3a** and (C) copolymer **6d** ($M_n = 1.1 \times 10^5$) in $CDCl_3$.

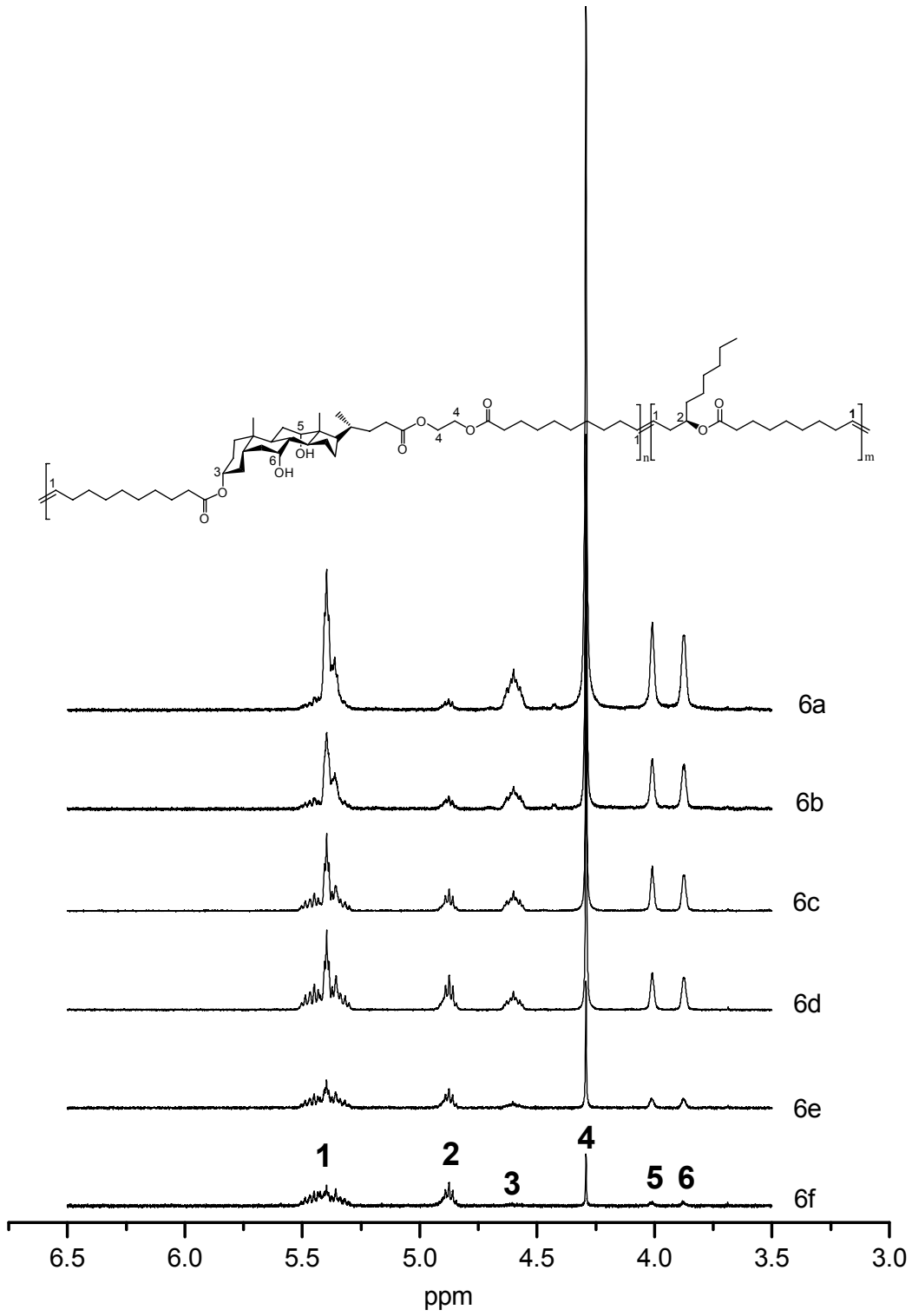

Figure 3.18. The ^{1}H NMR spectra (from 6.5 to 3.5 ppm) of copolymers **6a-f** in $CDCl_3$.

Table 3.3. Molar ratio of RCA in copolymers **6a-f** calculated from ^{1}H NMR spectra.

Copolymer	Mol% of RCA in polymer	Mol% of RCA in feed	M_n ($\times 10^3$)[a]	PDI	T_g (^oC)[b]	E at 25^{o}C[c] (MPa)
6a	24	15	305	1.59	49.4 ± 0.4	101 ± 2
6b	37	30	207	1.85	21.1 ± 0.5	5 ± 1
6c	44	45	139	1.64	-1.8 ± 0.9	2.5 ± 0.5
6d	57	60	107	1.72	-19.6 ± 0.9	1.3 ± 0.5
6e	77	75	90	1.69	-42 ± 2	NA
6f	86	90	70	1.65	NA	NA

Note:

[a] M_n was determined by GPC using THF as the eluent and polystyrene as the standards.

[b] T_g measured by DSC with a heating rate of 10^{o}C/min. The standard deviation is calculated from the T_g values by selecting different start and end points of the DSC curves.

[c] E is Young's modulus measured by DMA at 25^{o}C. The standard deviation is calculated from three measurements.

3.5 Thermal and mechanical properties of polymers

The thermal and mechanical properties of homopolymers **1-5** and copolymers **6a-f** were characterized by TGA, DSC, and DMA. Polymers **1-5** display a glass transition temperature varying from 6.2 to 84.0 ^{o}C (Table 3.4) without any evidence of melting before decomposition. The films prepared from polymers **1-5** are transparent, which also suggests that these materials are amorphous.

At the glass transition temperature (T_g), the materials change from a 'glassy' (rigid) to a 'rubbery' (soft) state. Many factors affect the glass transition temperature of polymers, such as the structure of the main chain, the polarity or flexibility of the side

chain, copolymerization, and molecular weight. Table 3.1 lists the glass transition temperatures of polymer **1** with different molecular weights. When the molecular weight increases from 6.3 to 52 × 10^4, the glass transition temperature changes from 45 to 49.4^{o}C, and reach a stable value at about 49.5^{o}C (Figure 3.19).

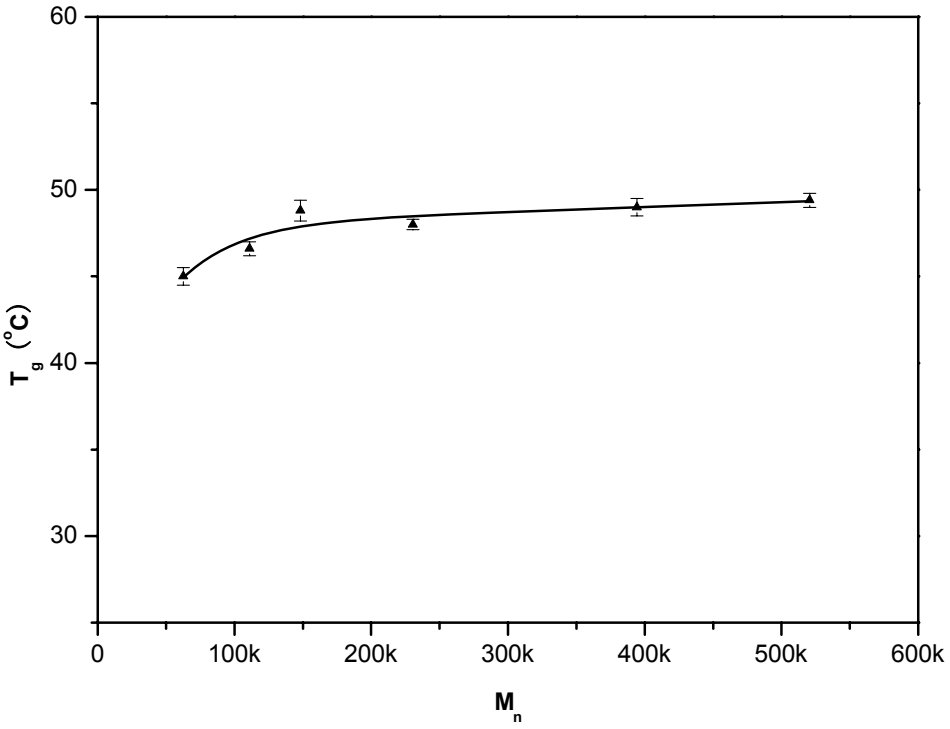

Figure 3.19. T_g of polymers **1a-f** as a function of molecular weight.

Table 3.4 shows the glass transition temperatures of polymers **1-5**. First, it can be seen that the different types of functionality affect the T_g'. Polymers **2**, **3** and **4** have the same core (lithocholic acid), but different functional groups in their structure. In their repeat units, polymer **2** has three ester bonds, polymer **3** has two amide bonds and one ester bond, and polymer **4** has one amide bond and two ester bonds. Normally, the ester bond is more flexible than the amide bond. Thus, it is not surprising that polymer **3** has the highest T_g' and polymer **2** has the lowest T_g' (polymer **3** > polymer **4** > polymer **2**) because they have similar molecular weights. Second, different cores also affect T_g'. Polymers **1** and **2** have the same functionality (three ester bonds) except that they possess

a different core: polymer **1** has cholic acid and polymer **2** has lithocholic acid. Polymer **1** has a higher T_g' than polymer **2** and this is due to the presence of the extra hydroxyl groups on the cholic acid core, which may facilitate the interactions in polymer **1**. Third, the number of ester bonds in the repeat unit also affects the T_g'. Polymers **1** and **5** possess the same cholic acid core, but polymer **1** has three ester bonds in the repeat unit while polymer **5** has two. Polymer **5** has fewer ester bonds and thus a higher T_g' than polymer **1**.

Table 3.4. Molecular weight and T_g of polymers **1-5**.

Polymers	M_w ($\times 10^3$)[a]	PDI	T_g' (^oC)[b]	T_g" (^oC)[c]	E (MPa)[d]	
					T_g"-10^{o}C	T_g"+10^{o}C
1c	395	1.71	48.0 ± 0.4	45.3 ± 0.6	301	4.6
2	468	1.95	6.2 ± 0.5	NA	NA	NA
3	198[e]	NA[e]	83 ± 1	67 ± 2	179	29.0
4	354	1.71	48.1 ± 0.6	46.4 ± 0.9	139	4.1
5	410	1.43	67 ± 1	54 ± 2	197	17

[a] Weight-average molecular weight measured by GPC by using polystyrene as the standard.

[b] T_g' measured by DSC with a heating rate 10^{o}C/min. The standard deviation is calculated from the T_g' values by selecting different start and end points of the DSC curves.

[c] T_g" measured by DMA at a frequency of 1 Hz. The standard deviation of T_g" is calculated from the T_g" values obtained by selecting of the DMA data of storage modulus plotted as a function of temperature (Figure 3.21).

[d] Young's modulus (E) measured by DMA.

[e] Could not be measured by GPC as the refractive index of the polymer is close to that of the solvent; M_w measured by light scattering.

Table 3.3 shows the glass transition temperatures of copolymers **6a-f**. With the increasing molar percentage of ricinoleic acid (RCA), the T_g decreases linearly as shown in Figure 3.20. Copolymerization with RCA is the main factor contributing to a drop in T_g because the contribution from the variation of molecular weight (from 6.3×10^4 to 5.2×10^5) should be within 5^oC (Table 3.1).

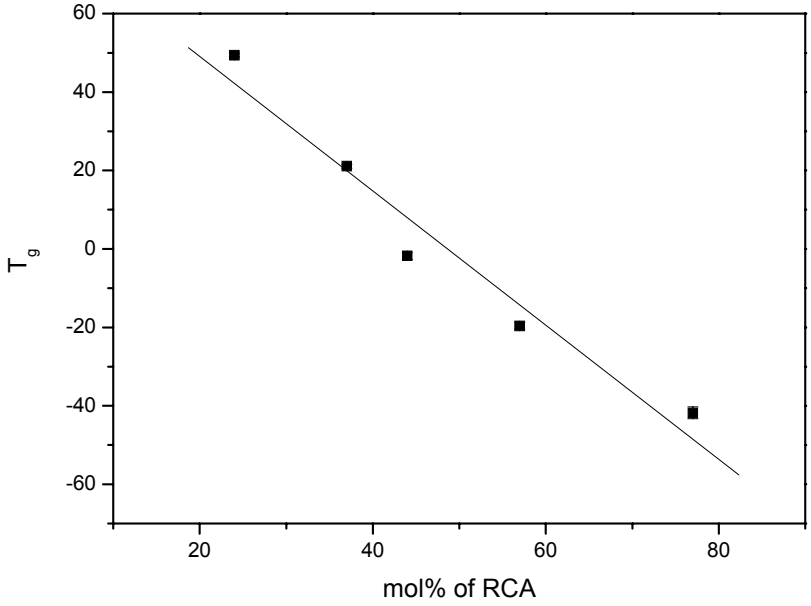

Figure 3.20. T_g of copolymers **6a-e** as a function of molar content of ricinoleic acid (RCA) in the copolymers.

The mechanical properties of homopolymers (**1c** and **3-5**) and copolymers **6a-f** were studied with dynamic mechanical analysis (DMA). These materials are elastomers with tunable mechanical properties and shape memory properties.

Typical spectra of multifrequency experiments at 1 Hz and stress-strain curve at $T_g'' - 10^oC$ and $T_g'' + 10^oC$ are shown in Figure 3.21.

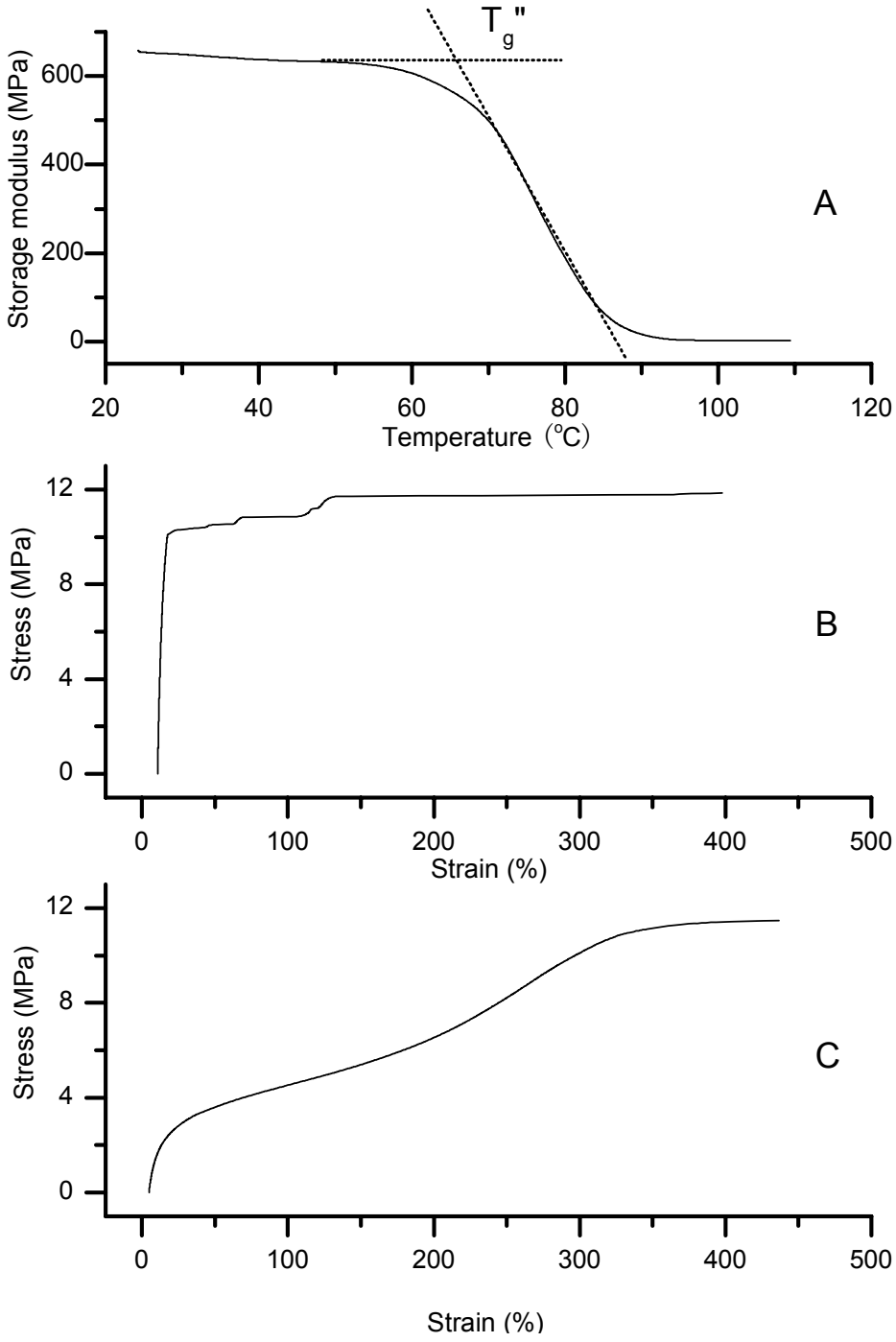

Figure 3.21. DMA results obtained for a film of polymer **3**: (A) Evolution of the storage modulus as a function of temperature; (B) Stress-strain curve at T_g" - 10°C; (C) Stress-strain curve at T_g" + 10°C.

Main-chain bile acid-based polymers **1c** and **3-5** display T_g"'s (measured by DMA) ranging from 45 to 67°C (Table 3.4). Below these temperatures, they are hard materials with E values ranging from 139 to 301 MPa. Above T_g", they are rubber-like materials with E values ranging from 4 to 29 MPa. The T_g"'s measured by DMA are clearly influenced by the polymer structures.

Polymers **1c** and **3-5** have been found to have shape memory properties in both warm and cold drawing modes with high strain recovery and strain fixity. The range from 10°C below T_g" to 10°C above T_g" has been used in the literature.[2] This area is well-defined to study the glass transition of the materials as it covers the sharp transition and adjacent range of temperatures. In the warm drawing mode (Figure 3.22 A), the sample film is stretched to at least 200% of strain at 10°C above its T_g" (curve 1), the film is then cooled down to 10°C below T_g" (curve 2) and the force is released (curve 3). The strain of the film has a small decrease because of the relaxation, which is characterized by the strain fixity R_f (Eq. 1). Finally, the temperature is raised to 10°C above its T_g" and the film recovers its permanent shape (curve 4). This process is characterized by the strain recovery R_r (Eq. 2).

$$R_f(N) = \frac{\varepsilon_u(N)}{\varepsilon_m} \tag{1}$$

$$R_r(N) = \frac{\varepsilon_m - \varepsilon_p(N)}{\varepsilon_m - \varepsilon_p(N-1)} \tag{2}$$

where N is the number of repetitive thermal cycles, ε_m is the maximum strain, ε_u is the strain after relaxation below T_g" and ε_p is the strain after recovery above T_g.

In cold drawing mode (Figure 3.22 B), the sample film is stretched to at least 150 % of strain at 10°C below its T_g" (Figure 3.22 B, curve 1) and then the stress is released. The sample film is given sufficient time to relax (Figure 3.22 B, curve 2), which is characterized by the strain fixity R_f (Eq. 1). The temperature is then raised to 10°C above its T_g", which triggers strain recovery (Figure 3.22 B, curve 3), which is characterized by the strain recovery R_r (Eq. 2).

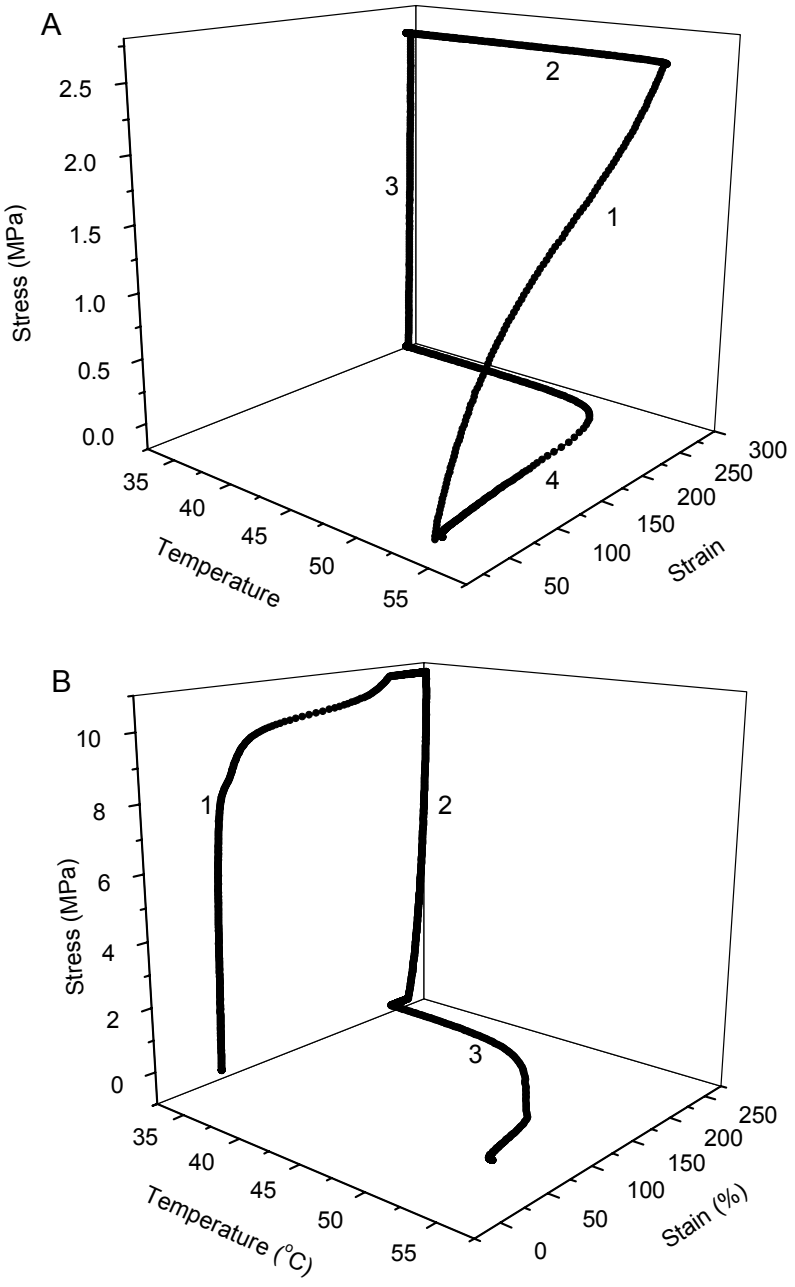

Figure 3.22. Shape memory effect of bile acid-based polymers. (A) Warm drawing, (B) Cold drawing.

The shape memory performance of polymers **1c** and **3-5** for both warm and cold drawing modes was evaluated for at least three cycles (Figure 3.23 and Table 3.5). In the warm drawing mode, the strain fixity and recovery are high, ranging from 90 to 99%. The initial cycle is different than the subsequent ones.[12] This may be caused by the chain relaxation and leads to 1-5 % deviation of R_f and R_r in the following cycles.[2] Strain recoveries in cold drawing mode remained high (above 90%), but strain fixities decreased a lot in comparison with those of warm drawing mode, ranging from 78 to 87%. This may be caused by the slower chain relaxation characteristics of the samples at the low temperature when the samples were stretched.[2] The Young's moduli of copolymers **6a-d** at 25°C shown in Table 3.3, have values ranging from 1.3 to 101.1 MPa. For copolymers **6b-d**, for which T_g is below room temperature, the modulus (E) decreases as the molar percentage of ricinoleic acid increases. The modulus (E) of copolymer **6a** is much higher than those of copolymer **6b-d**, because its T_g is higher than room temperature.

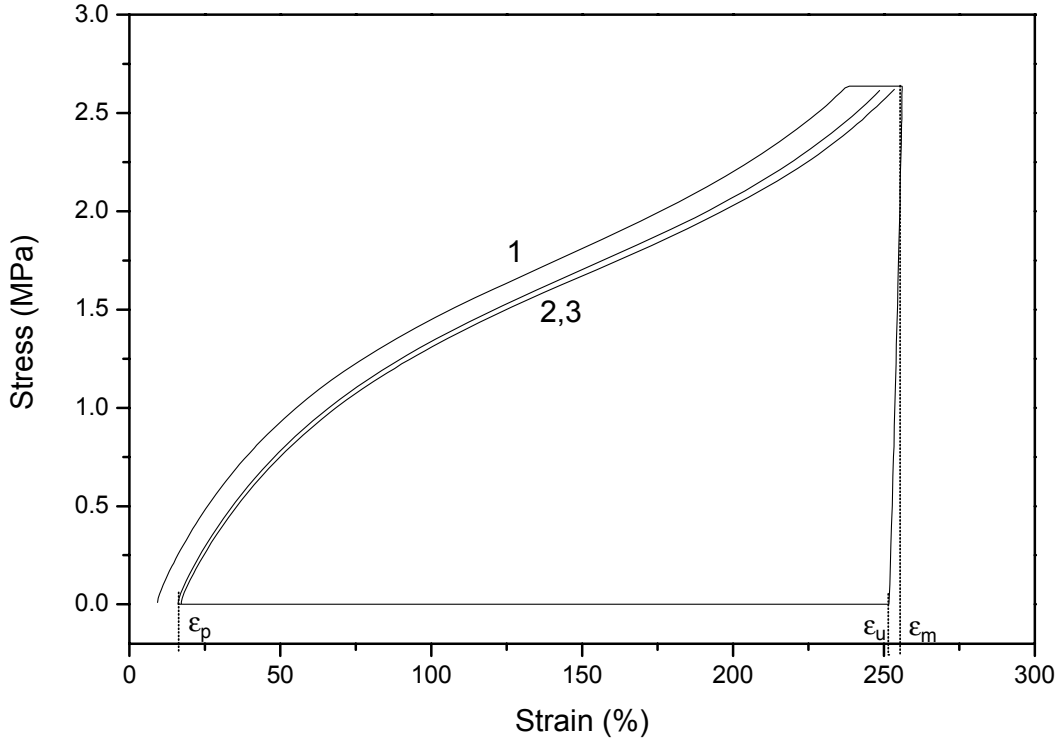

Figure 3.23. Stress-strain plots for the warm drawing of a polymer **1c** sample (respective cycle numbers indicated on the plot).

Table 3.5. Shape memory effect (warm drawing and cold drawing) of bile acid-based polymers.

Polymers		R_r (1)	R_r (2)	R_r (3)	R_f (1)	R_f (2)	R_f (3)
Warm drawing	**1c**	98.0 ± 0.8	99.6 ± 0.1	99.7 ± 0.1	97.4 ± 0.1	97.3 ± 0.1	97.3 ± 0.1
	3	89.9 ± 1.0	94.1 ± 1.3	94.3 ± 1.4	95.4 ± 0.6	95.3 ± 0.9	95.1 ± 0.8
	4	97.1 ± 0.1	99.3 ± 0.1	99.5 ± 0.1	97.9 ± 0.1	97.8 ± 0.1	97.9 ± 0.1
	5	94.7 ± 1.5	99.0 ± 0.3	99.1 ± 0.5	94.5 ± 1.8	94.5 ± 1.8	94.6 ± 2.0
Cold drawing	**1c**	94.2 ± 0.5	99.0 ± 0.2	99.0 ± 0.7	79.1 ± 1.3	77.6 ± 1.4	77.6 ± 1.4
	3	91.0 ± 1.7	98.4 ± 0.4	98.7 ± 0.2	86.8 ± 1.6	86.5 ± 1.2	86.8 ± 1.2
	4	93.9 ± 0.1	98.5 ± 0.1	99.2 ± 0.1	85.8 ± 0.6	83.5 ± 0.9	83.3 ± 0.7
	5	89.5 ± 0.6	98.3 ± 0.1	96.3 ± 0.1	85.4 ± 0.2	84.2 ± 0.6	84.0 ± 0.7

For some samples, the measurements failed due to the slipperiness of the clamps and the sample defects. The standard deviations of R_r and R_f of some polymers are low and the others are high. All standard deviations of R_r and R_f are based on three measurements.

The study of the thermal and mechanical properties of homopolymers **1-5** and copolymers **6a-f** revealed the polymers with shape memory effect and their thermal and mechanical properties could be tuned by adjusting the molar ratio of ricinoleic acid.

3.6 Degradation properties

The degradation of synthetic polymers can be affected by their structure and molecular weight. Different cholic acid-based homopolymers and copolymer **6** (Figure 3.24) were used for the degradation experiments (polymers **7** and **8** were prepared by Dr. Yu Shao in our group). As shown in the structures of the homopolymers **1**, **7** and **8** (Figure 3.24), the only difference between them is the number of the ester and amide bonds in the repeat unit. Polymer **1** has three ester bonds, polymer **7** has two ester bonds

and one amide bond and polymer **8** has one ester bond and two amide bonds. Normally, the cleavage of an amide bond is more difficult than that of an ester bond. The comparison of the degradation properties of these polymers is thus interesting and justifies further investigation.

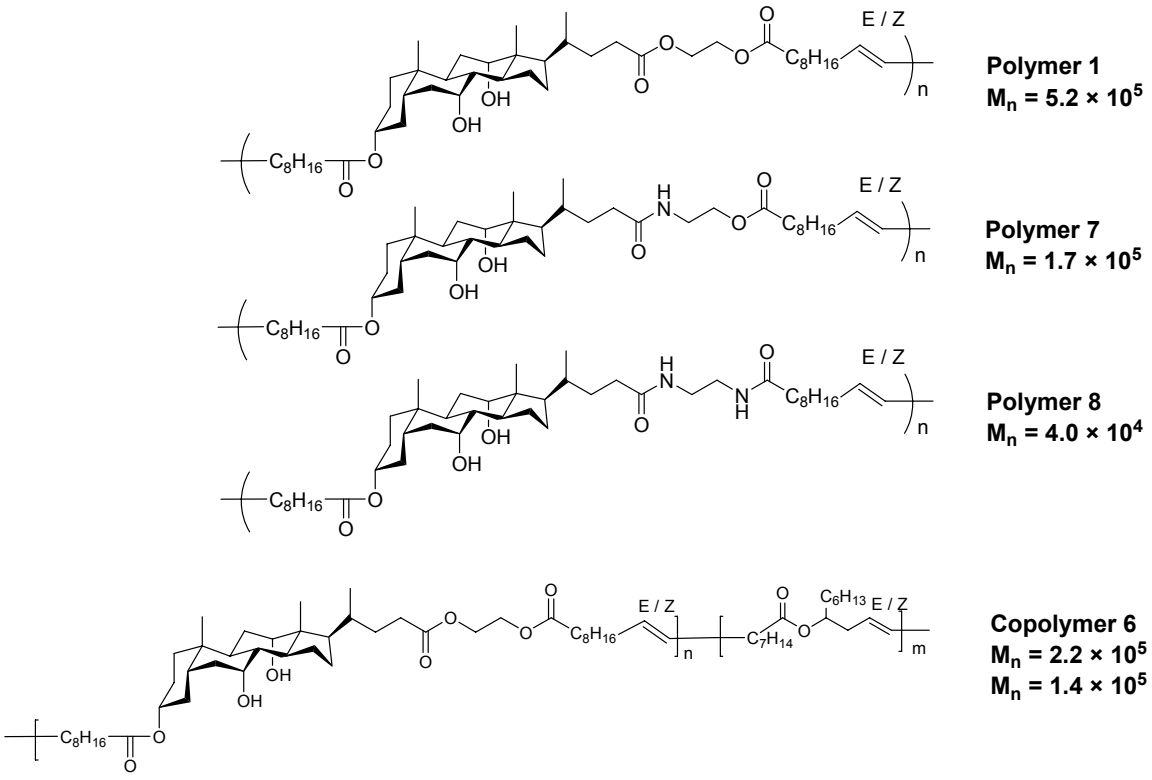

Figure 3.24. The structure of the different polymers used for the degradation experiments. The molecular weights of these polymers are given next to the structure.

The degradation of polymer **1a** (Figure 3.25) at 37°C shows a 17.0% relative weight loss after 168 days. However, the molecular weight remains quite stable (the molecular weight (M_n) of the polymer at the beginning of the degradation is 5.2×10^5) and there is no effect of bulk degradation.

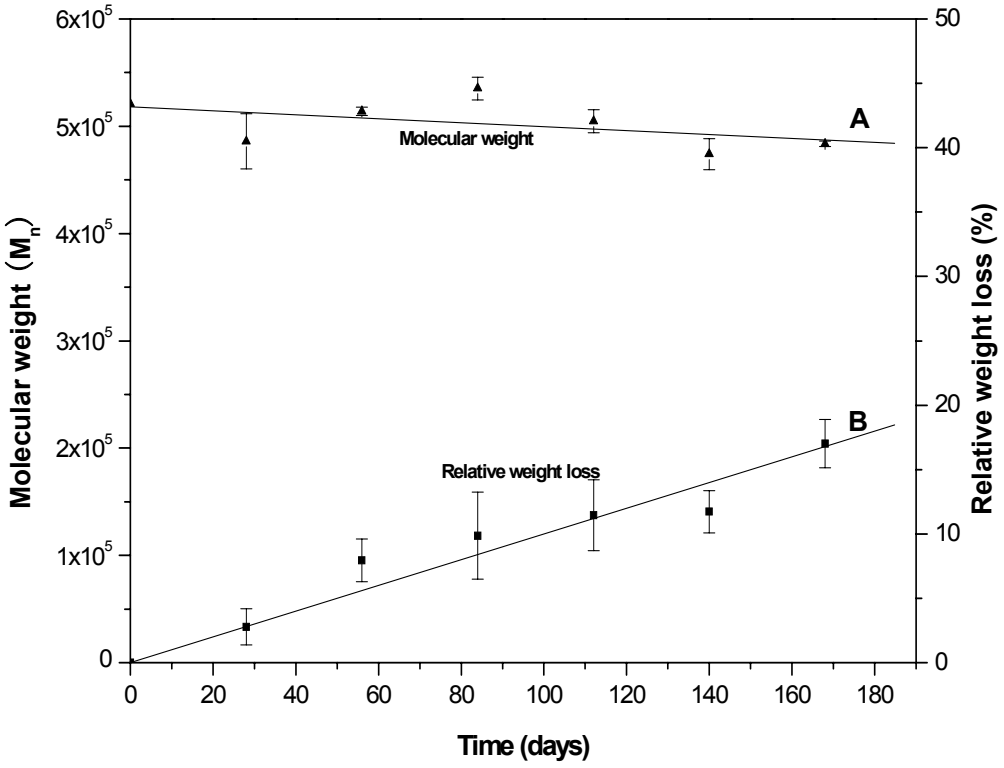

Figure 3.25. Degradation of the polymer **1a** film in PBS at 37°C; (A) Molecular weight (M_n); (B) Relative weight loss.

The degradation of polymer **7** (Figure 3.26) at 37 °C is slower than that of polymer **1a**, with 13.8% relative weight loss after 168 days. The molecular weight decreases slightly, probably due to the presence of the amide group in the repeat unit and the high molecular weight of the polymer. The degradation of polymer **8** (Figure 3.27) at 37 °C shows a 12.8% relative weight loss after 168 days and molecular weight (M_n) decreased from 4.0 to 2.5 × 10^4. The lower starting molecular weight of polymer **8** may be the cause of this faster drop in M_n.

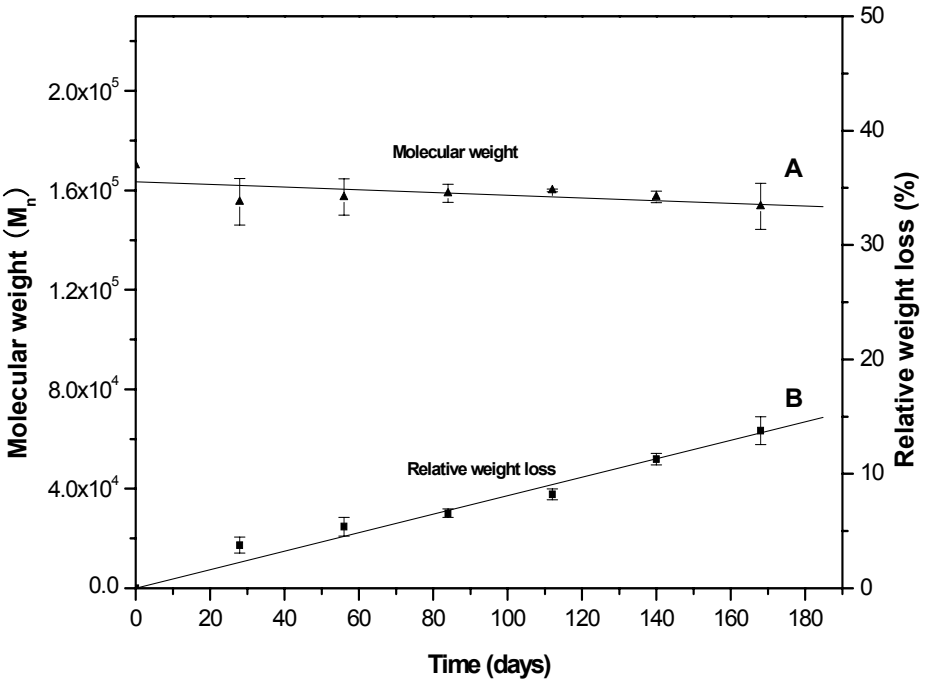

Figure 3.26. Degradation of the polymer **7** film in PBS at 37°C. (A) Molecular weight; (M_n); (B) Relative weight loss.

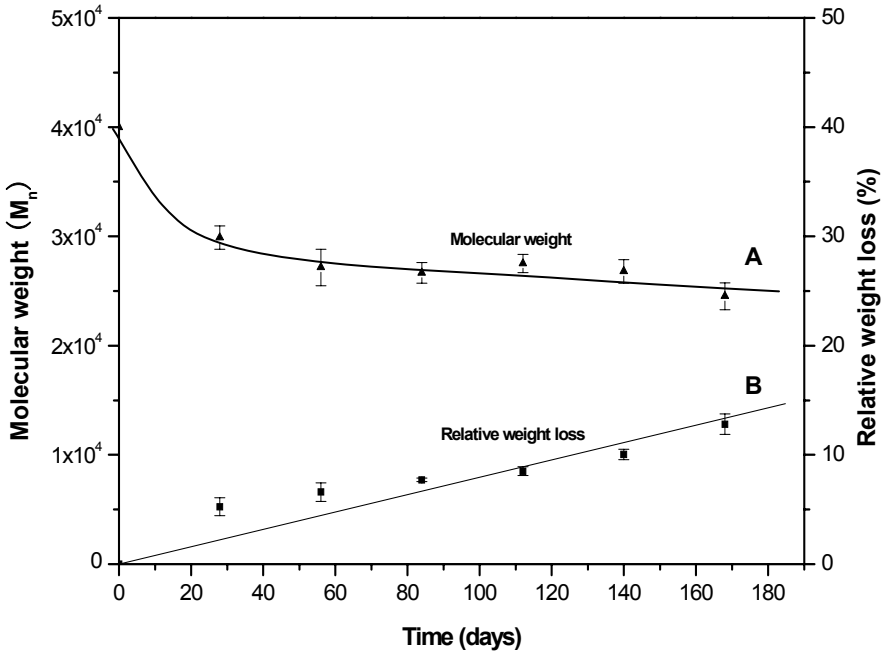

Figure 3.27. Degradation of the polymer **8** film in PBS at 37°C. (A) Molecular weight (M_n); (B) Relative weight loss. The curve of molecular weight serves as a visual guide

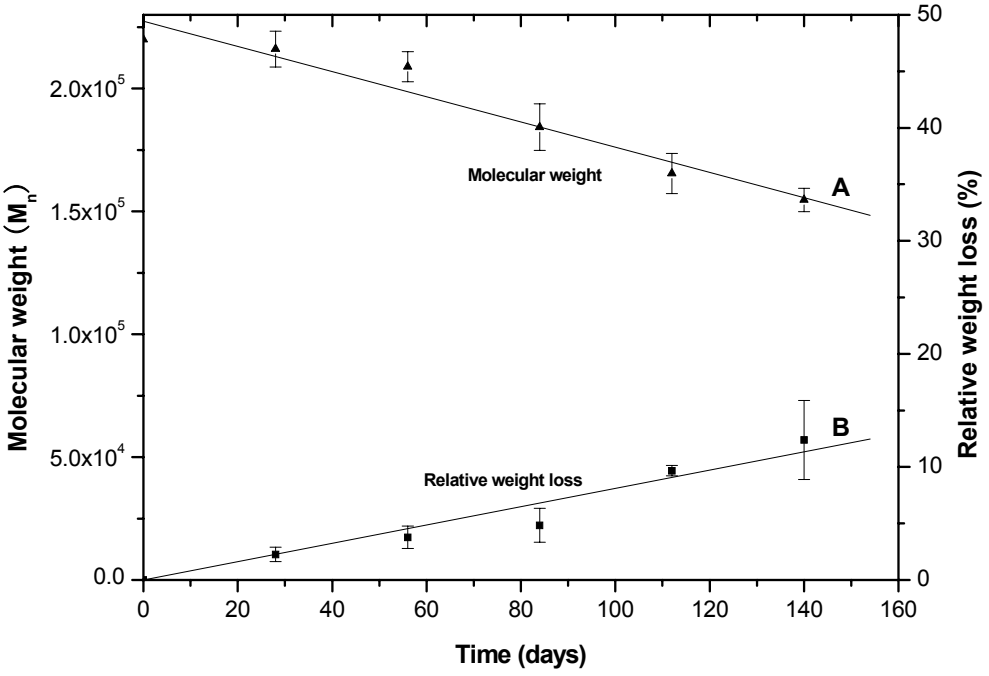

Figure 3.28. Degradation of the copolymer **6a** film in PBS at 37°C. (A) Molecular weight, (M_n); (B) Relative weight loss.

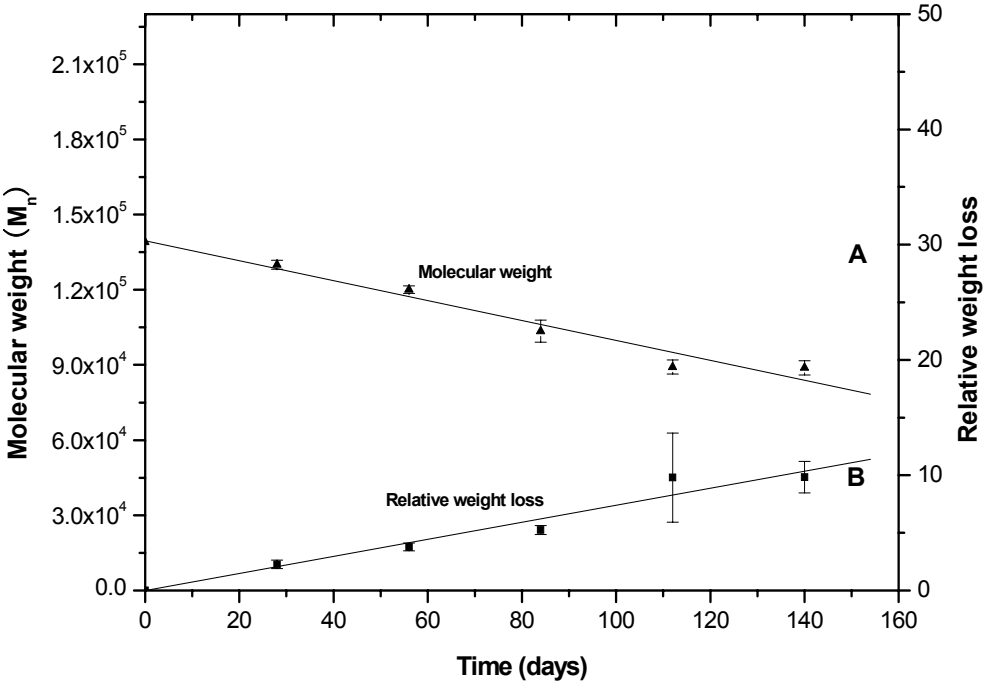

Figure 3.29. Degradation of the copolymer **6c** film in PBS at 37°C. (A) Molecular weight (M_n); (B) Relative weight loss.

The degradation rates of copolymers **6a** and **6c** at 37 ^{o}C show 12.4% (**6a**) and 9.8% (**6c**) relative weight loss after 140 days (Figures 3.28 and 3.29). The molecular weight slowly decreased over time (almost linear). These two copolymers (**6a** and **6c**) were degraded at similar rates, indicating that the copolymerization between cyclic monomer **3a** with ricinoleic acid monolactone does not greatly change the degradation process because no new functionality was introduced into the polymers.

3.7 References

(1) Gautrot, J. E.; Zhu, X. X. *Chem. Commun.* **2008**, *14*, 1674-1676.

(2) Gautrot, J. E.; Zhu, X. X. *Macromolecules*, **2009**, *42*, 7324-7331.

(3) Hu, X. Z.; Zhang, Z.; Zhang, X.; Li, Z. Y.; Zhu, X. X. *Steroids* **2005**, *70*, 531-537.

(4) Gautrot, J. E.; Zhu, X. X. *Angew. Chem. Int. Ed.* **2006**, *45*, 6872-6874.

(5) Biswas, G.; Sengupta, J.; Nath, M.; Bhattacharjya, A. *Carbohydr. Res.* **2005**, *340*, 567-578.

(6) Hodge, P.; Yang, Z.; Ben-Haida, A.; McGrail, C. S. *J. Mater. Chem.* **2000**, *10*, 1533-1537.

(7) Ruddick, C. L.; Hodge, P.; Zhuo, Y.; Beddoes, R. L.; Helliwell, M. *J. Mater. Chem.* **1999**, *9*, 2399-2405.

(8) Colquhoun, H. M.; Lewis, D. F.; Hodge, P.; Ben-Haida, A.; Williams, D. J.; Baxter, I. *Macromolecules* **2002**, *35*, 6875-6882.

(9) Hodge, P.; Kamau, S. D. *Angew. Chem. Int. Ed.* **2003**, *42*, 2412-2414.

(10) Ozcan, H. M.; Sagiroglu, A. *Prep. Biochem. Biotechnol.* **2009**, *39*, 170-182.

(11) Slivniak, R.; Domb, A. J. *Biomacromolecules* **2005**, *6*, 1679-1688.

(12) Rabani, G.; Luftmann, H.; Kraft, A. *Polymer* **2006**, *47*, 4251-4260.

4 Conclusions

4.1 Synthesis

Macrocyclic monomers based on bile acids (lithocholic acid and cholic acid) (Figure 3.1, cyclic monomers **3a-e**) were successfully synthesized via ring-closing metathesis with the first-generation Grubbs catalyst. All cyclic monomers possess one (litho)cholic acid core and a long flexible alkane chain connected to both positions 3 and 24 of the bile acid core through ester and amide linkages. A small linker (ethylene glycol, ethanolamine or ethylene diamine) was incorporated into some of the macrocycles (cyclic monomers **3a-d**) between the bile acid core and the long flexible alkane chain through ester or amide bonds.

A significantly improved yield of the cyclic monomers (from 53 to 90% for cyclic monomer **3a**) was achieved by using a higher reaction temperature (from room temperature to 40^{o}C) and a lower concentration of the starting material (from 13 to 3 mM).

Different main-chain homopolymers based on bile acids were prepared from the corresponding cyclic monomers (compounds **3a-e**) via ring-opening metathesis polymerization with the second-generation Grubbs catalyst. For polymer **1**, molecular weights (M_n) ranged from 6.3×10^4 to 5.2×10^5 depending on the catalyst loadings and polymerization times used. Copolymerization of cyclic monomer **3a** with ricinoleic acid monolactone provided a series of copolymers **6a-f**.

ED-ROMP is a powerful tool in the preparation of polymers with high molecular weights. By controlling the polymerization time and catalyst loading, high molecular weight polymers (up to 5.2×10^5) can be obtained with relative ease. Such high molecular weight may be a challenge for other methods such as acyclic diene metathesis polymerization or polycondensation.

4.2 Characterization

For the polymers**,** direct correlation was observed between the M_n and T_g. T_g increases with increasing M_n and finally reaches a plateau (at $M_n = 2.0 \times 10^5$). For the homopolymers **1-5** having comparable molecular weights, the T_g of the polymer based on cholic acid is higher than that of the polymer based on lithocholic acid when the functional linkages are the same (e.g. $T_{g,\ \text{polymer } \mathbf{1c}} > T_{g,\ \text{polymer } \mathbf{2}}$); the presence of amide linkages in the polymer also increases the T_g (e.g., $T_{g,\ \text{polymer } \mathbf{3}} > T_{g,\ \text{polymer } \mathbf{4}} > T_{g,\ \text{polymer } \mathbf{2}}$); the number of functional groups between the core and the flexible alkane chain (e.g., $T_{g,\ \text{polymer } \mathbf{5}} > T_{g,\ \text{polymer } \mathbf{1c}}$) greatly affects T_g. For the copolymers **6a-f**, the T_g's and Young's modulus (E) decrease with increasing content of ricinoleic acid. The T_g and hardness of the polymer can be thus tuned by copolymerization. This is very useful for the applications of these polymers. Polymers **1c** and **3-5** demonstrated shape memory properties in both warm and cold drawing modes with high strain recovery and strain fixity.

The degradation experiments were carried out on the films prepared from polymers **1**, **7** and **8** and copolymers **6a** and **6c**. The degradation of these polymers was slow, with a relative weight loss of less than 20% after 140 ~ 168 days in PBS solution. The change in molecular weight (M_n) is not evident, except for polymer **8**, which had a lower starting molecular weight.

4.3 Future work

Firstly, further studies on the mechanical properties of the polymers will provide a direct comparison of the different polymers made of bile acids.

Secondly, the degradable shape-memory polymers may find applications in biomedical engineering. The degradation properties of some of these polymers have been studied in PBS at 37^{o}C. It will be of practical importance to study the degradation of these polymers in a biological environment with the presence of bacteria, fungi and/or enzymes.

Thirdly, the liquid crystalline properties of polymer **3** with the presence of THF were observed (Appendix 3). The mechanism of formation of liquid crystalline properties

is still unknown. The probable reason of formation of liquid crystalline properties of this polymer may be related with the hydrogen bond between the solvent and amide group of the polymer. It would be interesting to study the structural effect on such properties by changing the length of spacer group linking the bile acid core and the alkane chain.

APPENDICES

1. Grubbs catalysts

There are three ruthenium-based Grubbs catalysts frequently used, referred as first-, second- and third-generation Grubbs catalysts (Figure A1). All these Grubbs' catalysts are able to initiate the metathesis including ring-closing metathesis (RCM), ring-opening metathesis polymerization (ROMP), acyclic diene metathesis polymerization (ADMET), ring-opening metathesis (ROM), and cross-metathesis (CM).[1]

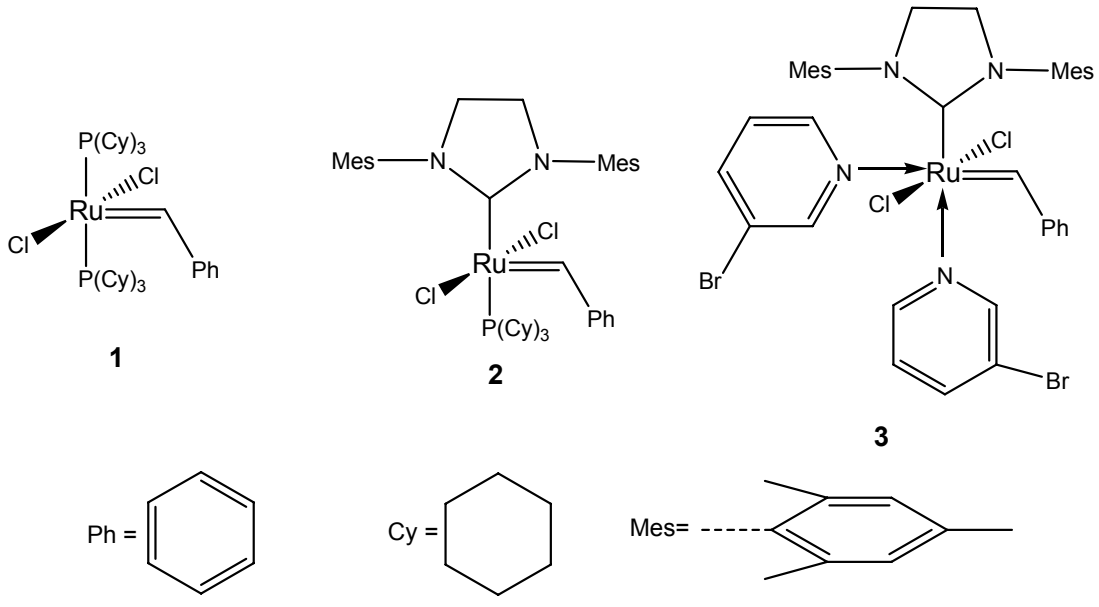

Figure A1. The structure of first- (**1**), second- (**2**) and third- (**3**) generation Grubbs' catalysts.

First-generation Grubbs catalyst (1). This catalyst has been widely used in polymer preparation and ring-closure metathesis. The polymer prepared possesses low PDI. Meanwhile, the synthesis of some large ring carbocycles and heterocycles became

possible with the use of this catalyst (the two examples shown in Figure A2). However, this catalyst is not stable in solution and reacts rapidly with air. It decomposes with the presence of acetonitrile, DMSO and DMF.[2] Furthermore, the polymerization of bulky monomer using this catalyst is not very efficient.[3]

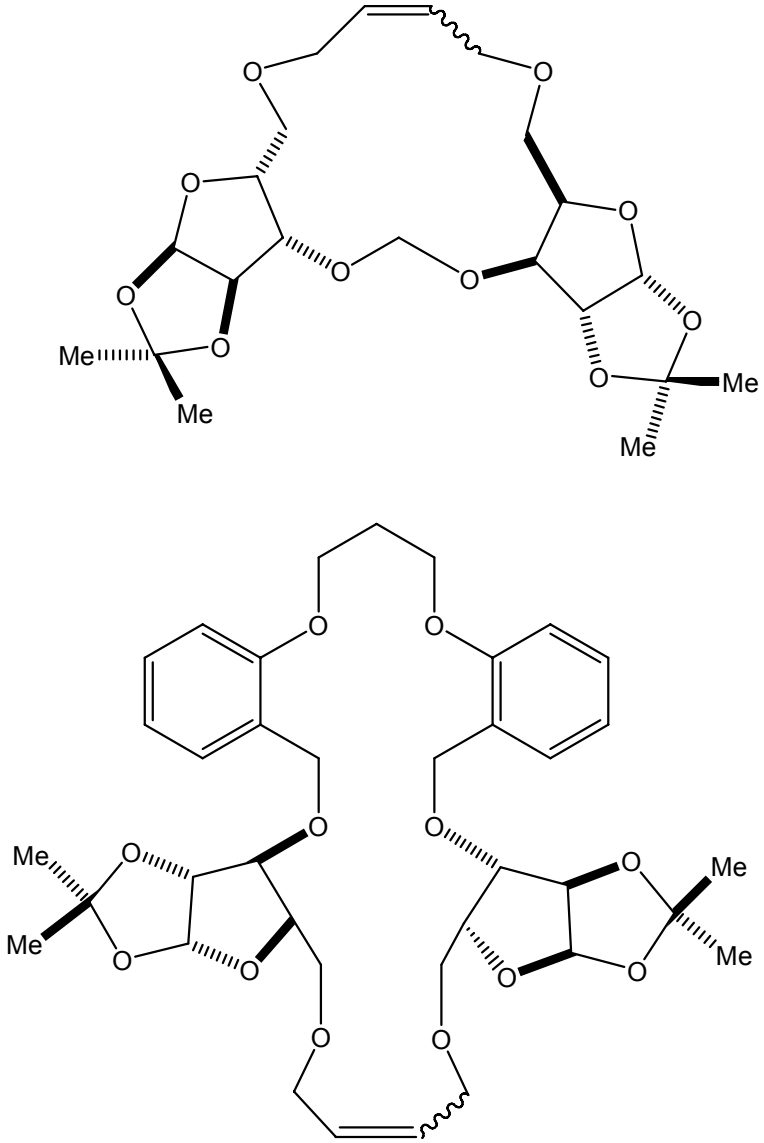

Figure A2. The structures of macrocycles prepared via ring-closure metathesis using first-generation Grubbs catalyst.[4]

Second-generation Grubbs catalyst (2). In the structure of second-generation Grubbs catalyst, one of the phosphine ligands is replaced by an N-heterocyclic carbine, which is a stronger σ-donor, bulkier and less labile. Therefore, this catalyst is more effective than the first-generation Grubbs catalyst for more highly substituted (bulkier) and electron-poor olefins.[5] However, polymers with high PDI are produced using the second-generation Grubbs catalyst because the rate of propagation is increased greatly compared to the initiation rate.[5] One of typical ring-opening metathesis polymerization using the second-generation Grubbs catalyst is shown in Figure A3.

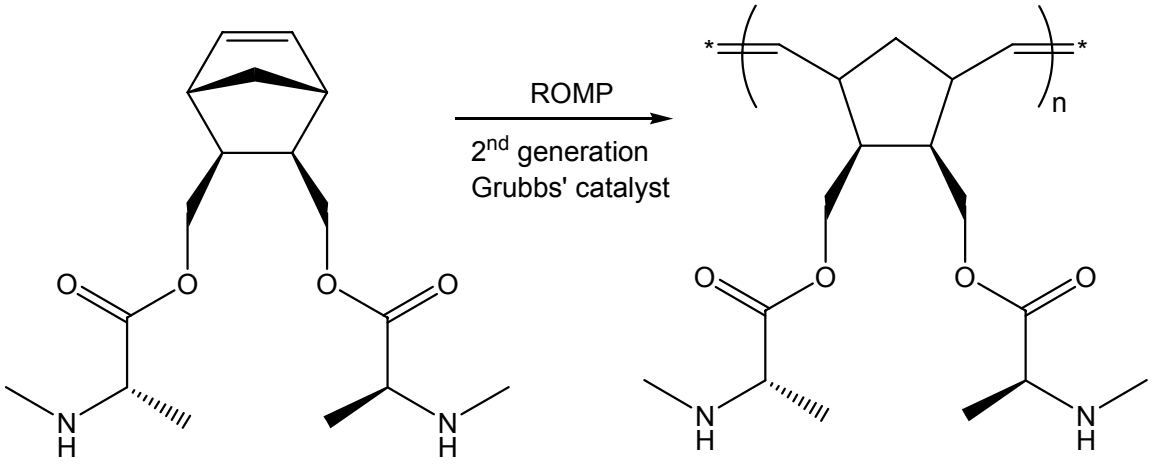

Figure A3. ROMP of amino acid-derived norbornene monomer using second-generation Grubbs' catalyst.[6]

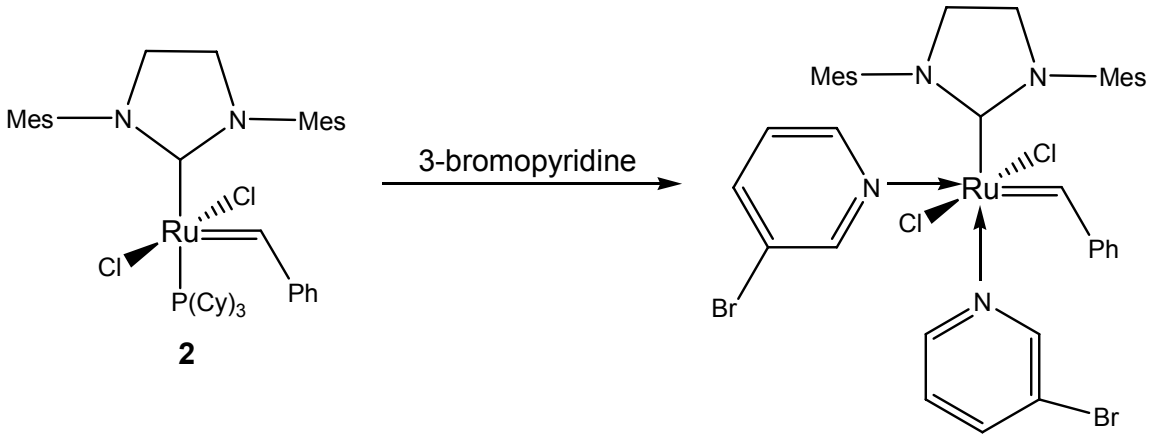

Figure A4. Synthesis of third-generation Grubbs catalyst from second-generation Grubbs catalyst.

Third-generation Grubbs catalyst (3). The third-generation Grubbs catalyst can be easily prepared from the second-generation Grubbs catalyst (Figure A4). This catalyst also contains an N-heterocyclic carbene ligand, but a phosphine ligand is replaced by two bromo-pyridine ligands. Thus, this change makes the third-generation able to initiate quicker than the second-generation and yields polymers with lower PDI.[7-9]

References:

(1) Rybak, A.; Fokou, P. A.; Meier, M. A. R. *Eur. J. Lipid Sci. Technol.* **2008**, *110*, 797-804.

(2) Sanford, M. S.; Love, J. A. *Handbook of Metathesis* **2003**, *1*, 112-131.

(3) Czelusniak, I.; Khosravi, E.; Kenwright, A. M.; Ansell, C. W. G. *Macromolecules* **2007**, *40*, 1444-1452.

(4) Biswas, G.; Sengupta, J.; Nath, M.; Bhattacharjya, A. *Carbohydr. Res.* **2005**, *340*, 567-578.

(5) Bielawski, C. W.; Grubbs, R. H. *Angew. Chem. Int. Ed.* **2000**, *39*, 2903-2906.

(6) Sutthasupa, S.; Sanda, F.; Masuda, T. *Macromolecules* **2009**, *42*, 1519-1525.

(7) Love, J. A.; Morgan, J. P.; Trnka, T. M.; Grubbs, R. H. *Angew. Chem. Int. Ed.* **2002**, *41*, 4035-4037.

(8) Sanford, M. S.; Love, J. A.; Grubbs, R. H. *Organometallics* **2001**, *20*, 5314-5318.

(9) Choi, T. L.; Grubbs, R. H. *Angew. Chem. Int. Ed.* **2003**, *42*, 1743-1746.

2. NMR spectra of intermediates and products

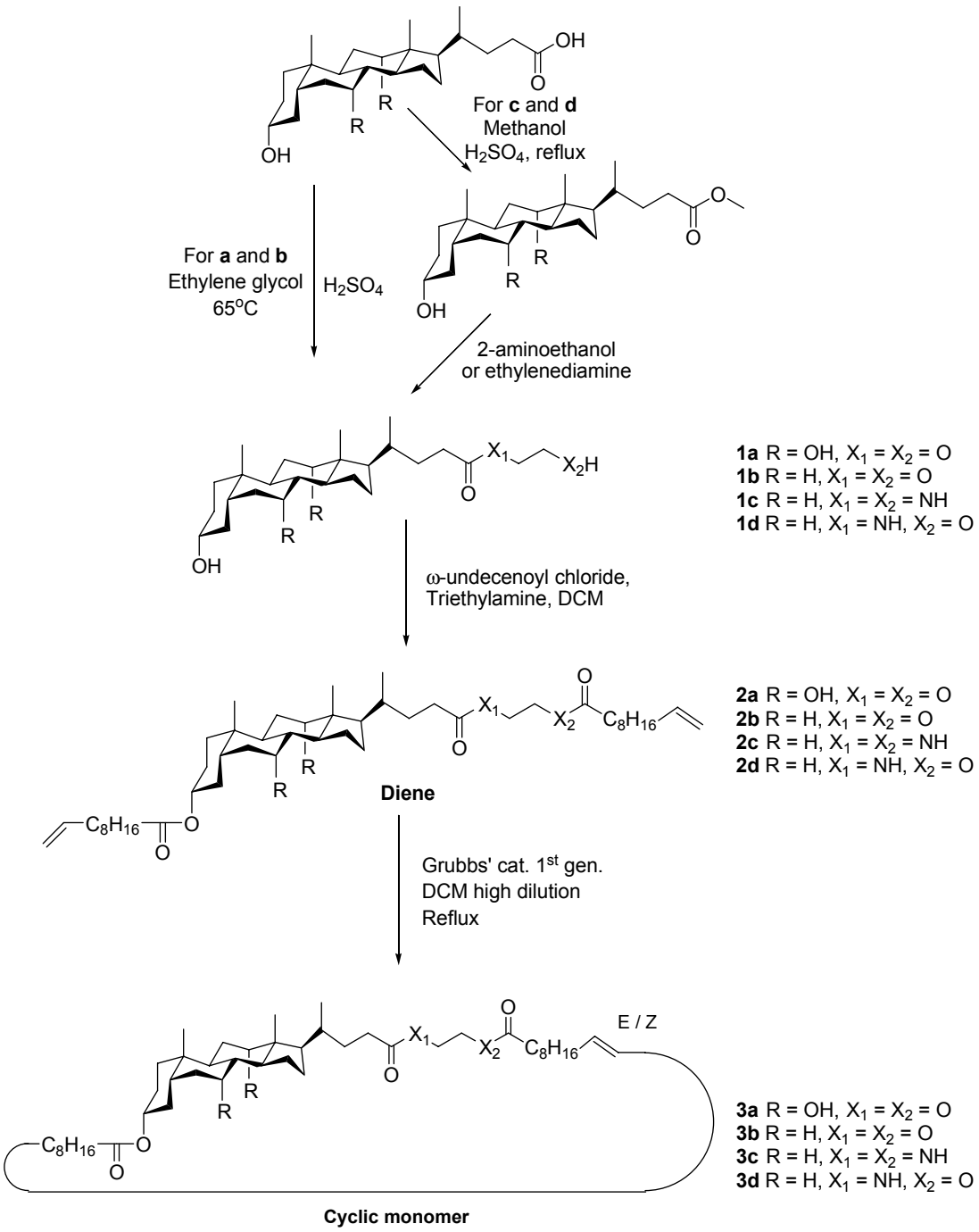

Figure A5. Synthesis of bile acid-based cyclic monomers **3a-d**.

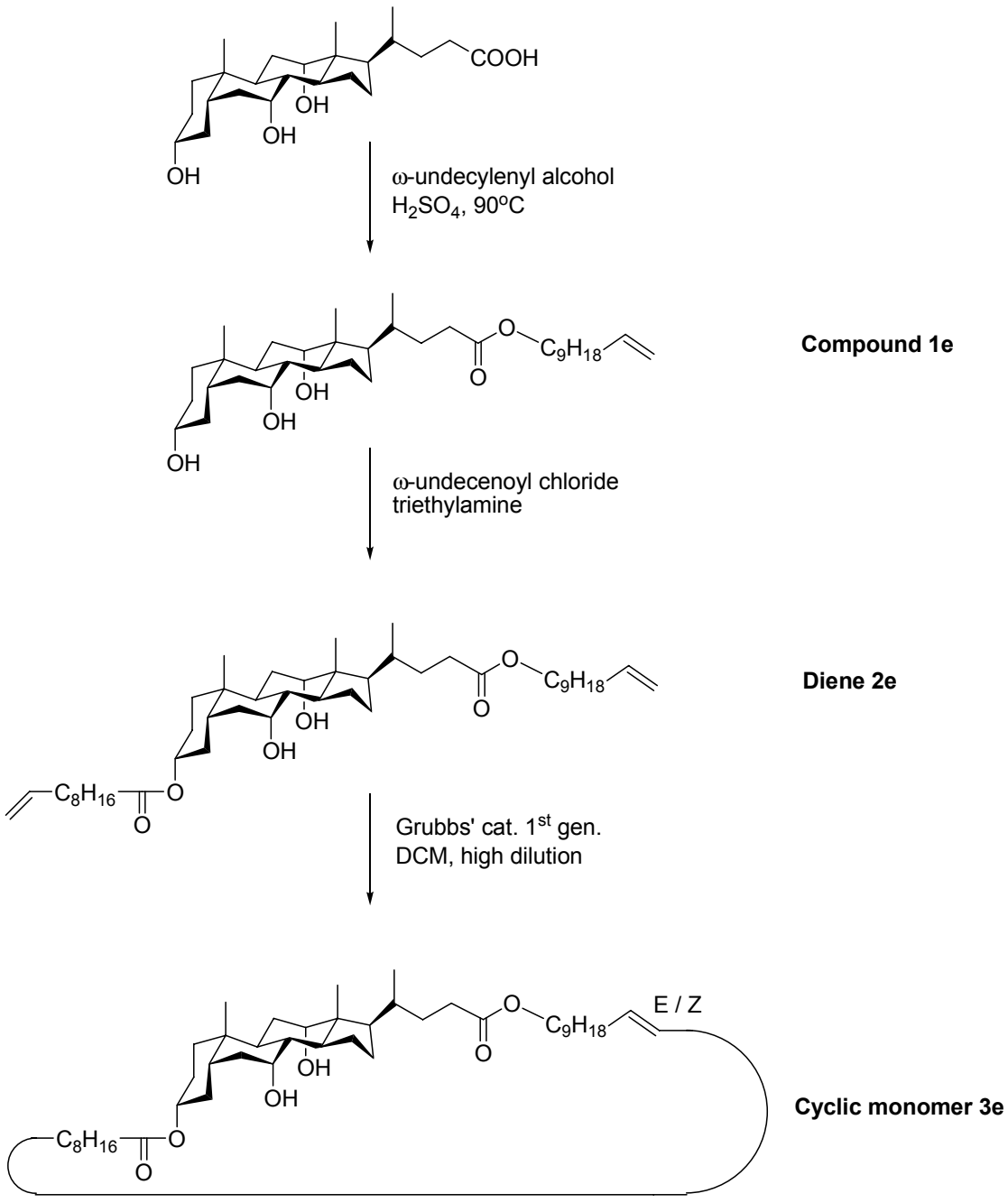

Figure A6. Synthesis of bile acid-based cyclic monomer **3e**.

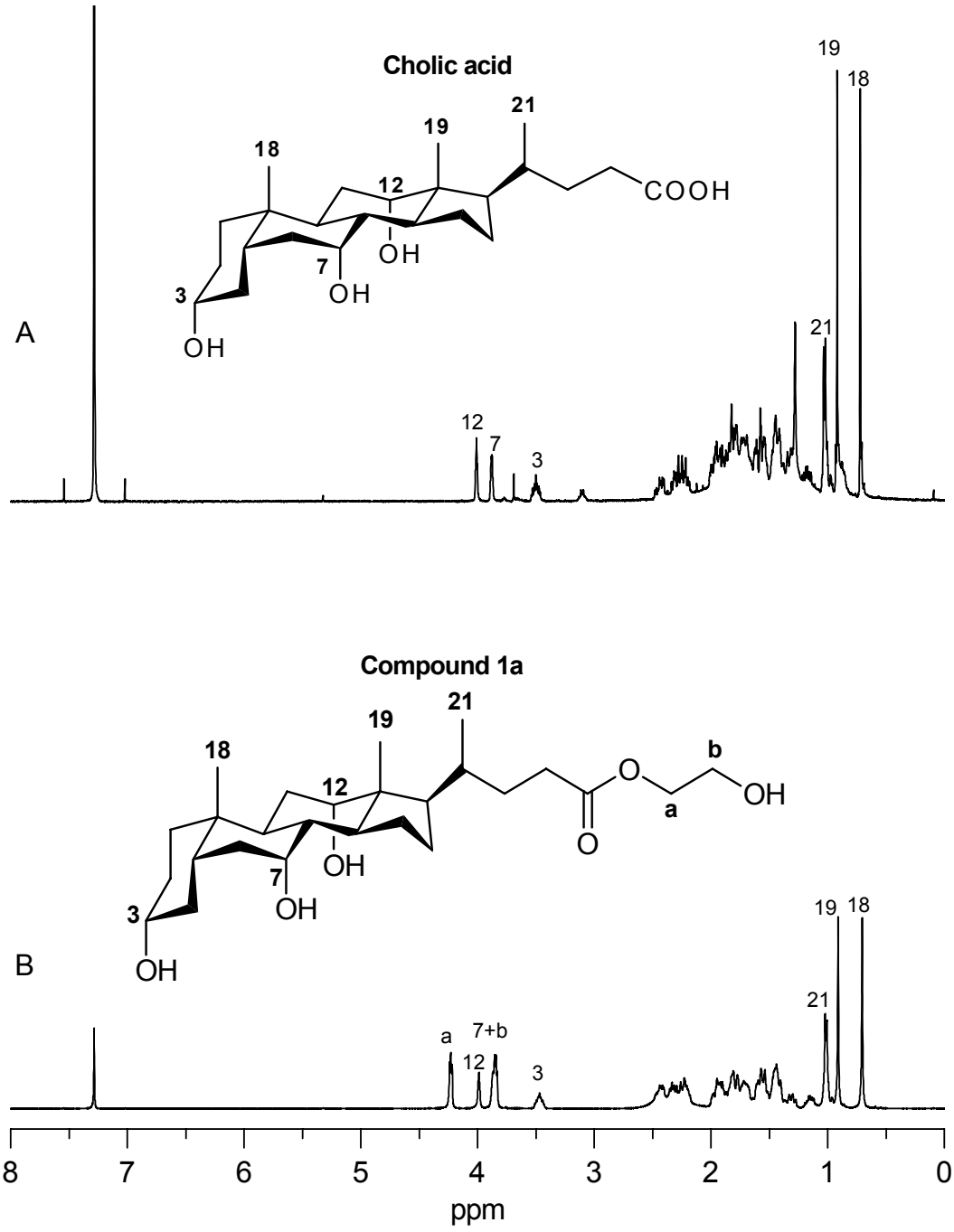

Figure A7. ^{1}H NMR spectra of (A) cholic acid and (B) compound **1a** in $CDCl_3$.

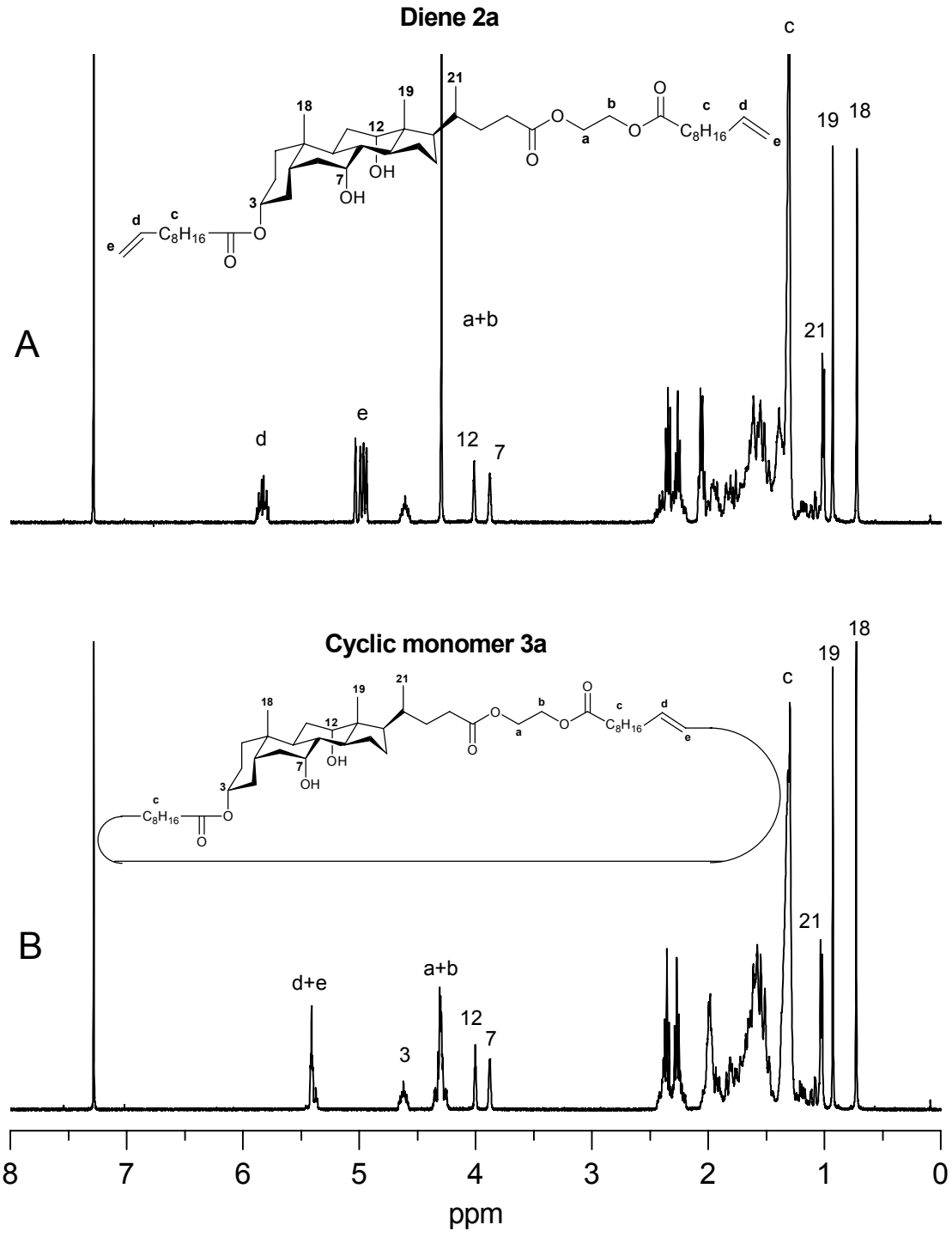

Figure A8. ^{1}H NMR spectra of (A) diene **2a** and (B) cyclic monomer **3a** in $CDCl_3$.

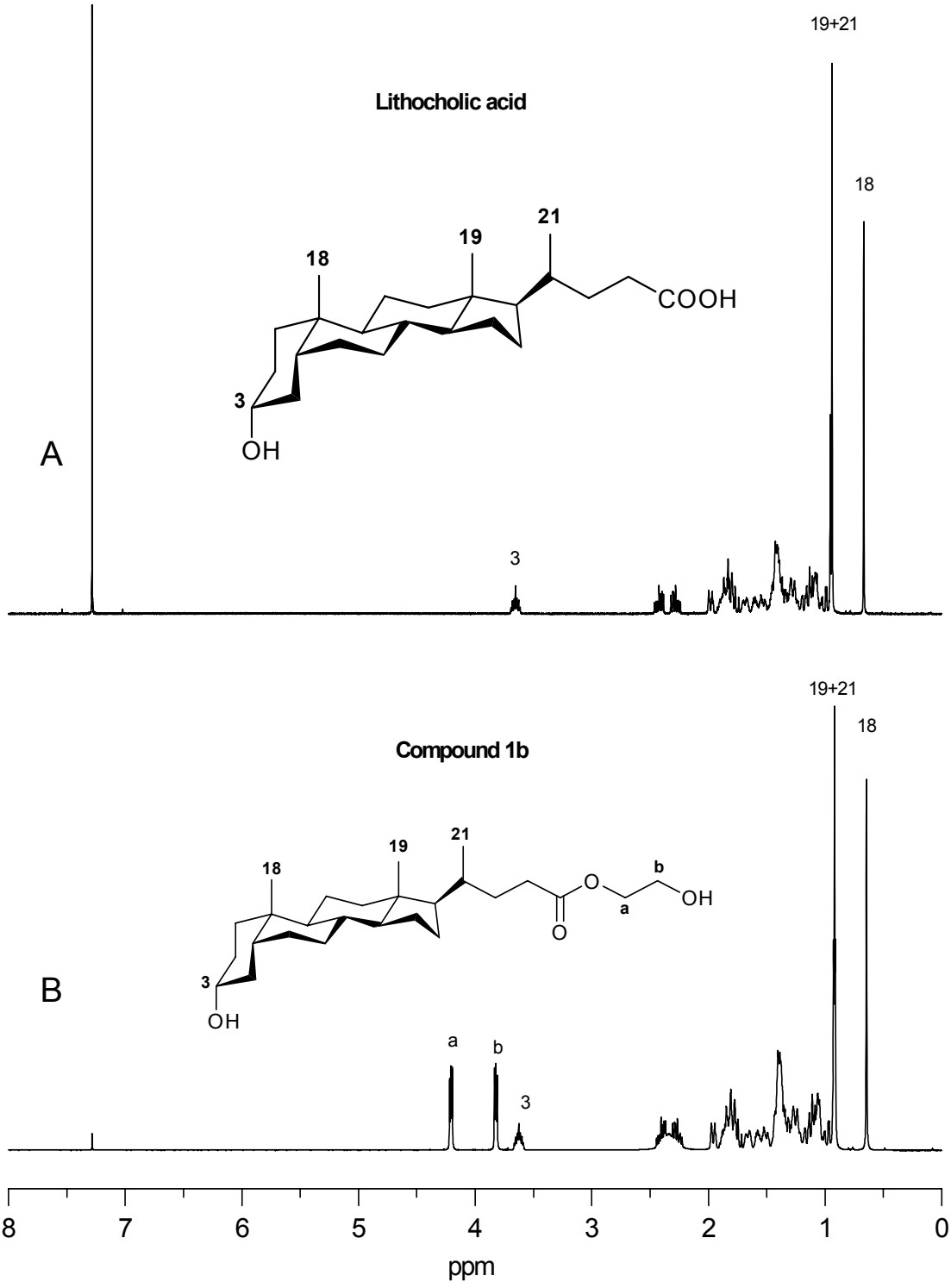

Figure A9. ^{1}H NMR spectra of (A) lithocholic acid and (B) compound **1b** in $CDCl_3$.

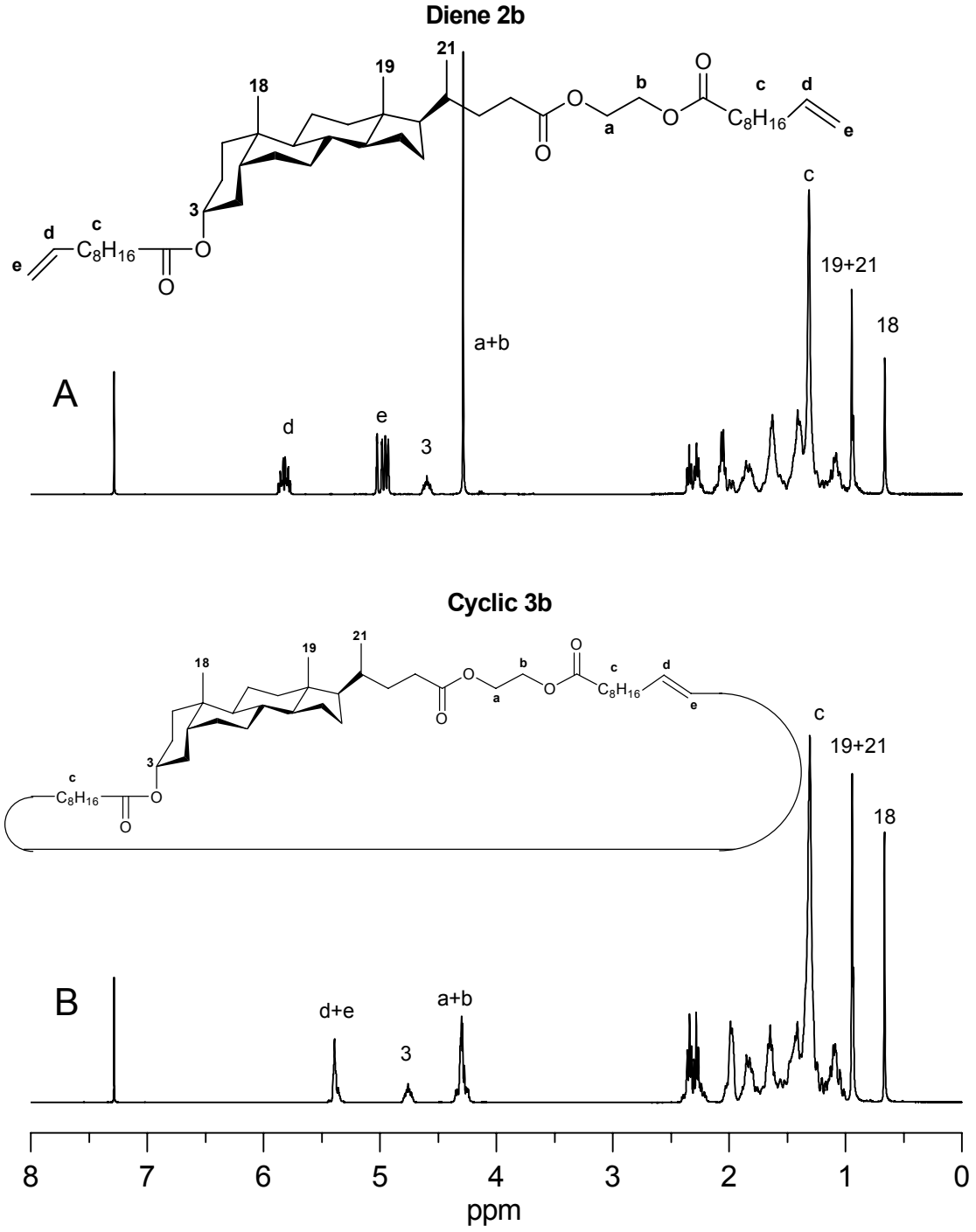

Figure A10. ^{1}H NMR spectra of (A) diene **2b** and (B) cyclic monomer **3b** in $CDCl_3$.

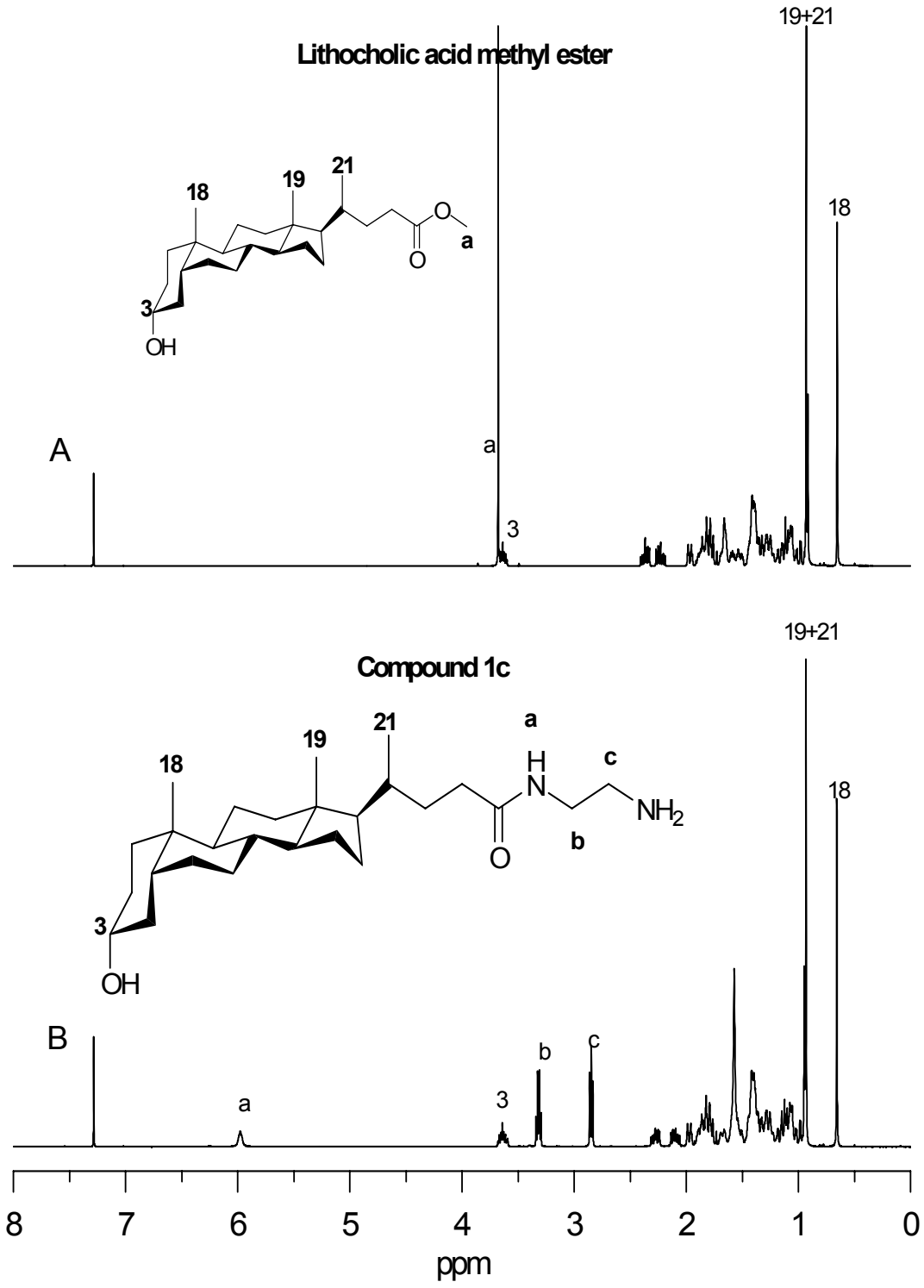

Figure A11. ^{1}H NMR spectra of (A) lithocholic acid methyl ester and (B) compound **1c** in $CDCl_3$.

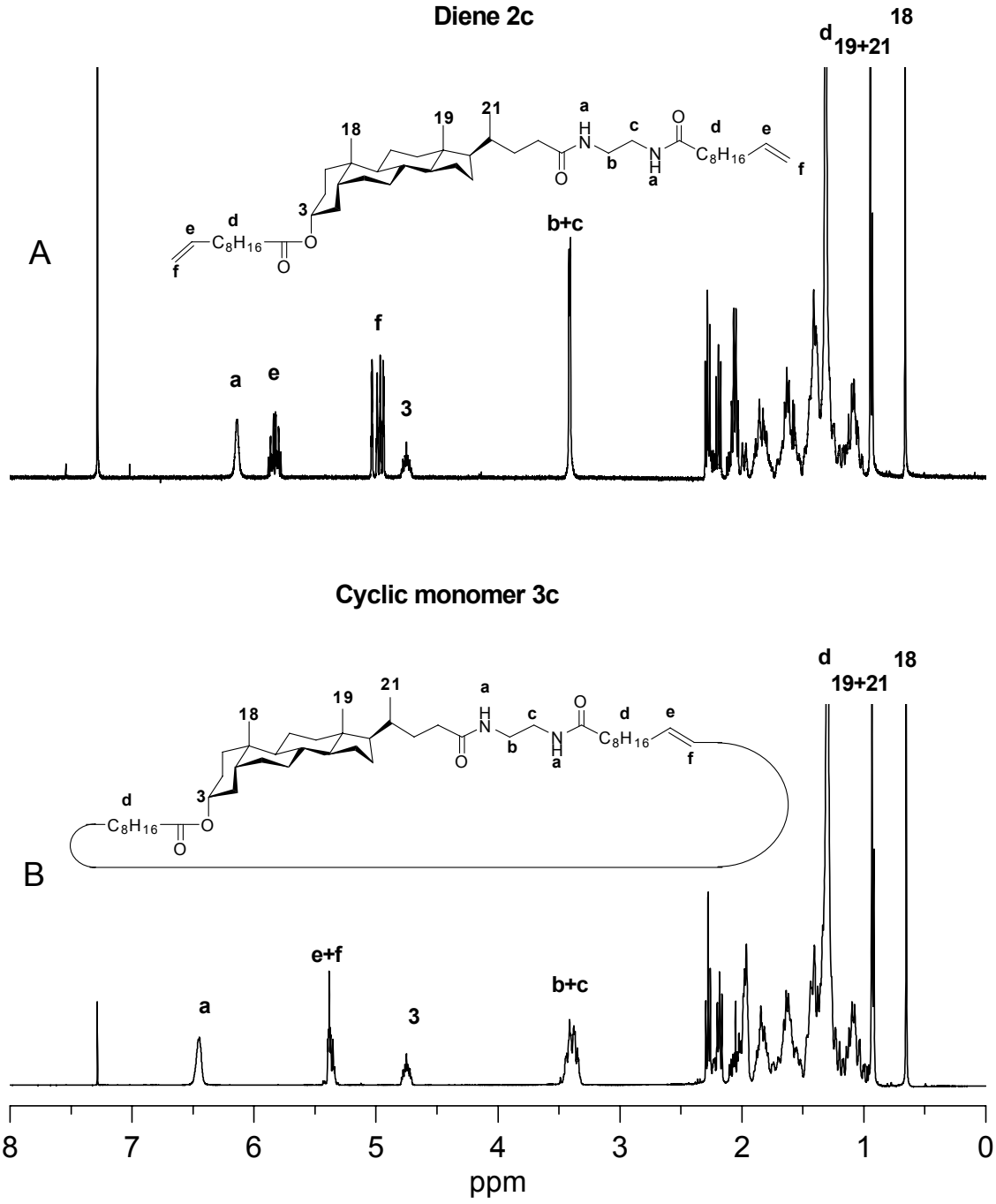

Figure A12. ^{1}H NMR spectra of (A) diene **2c** and (B) cyclic monomer **3c** in $CDCl_3$.

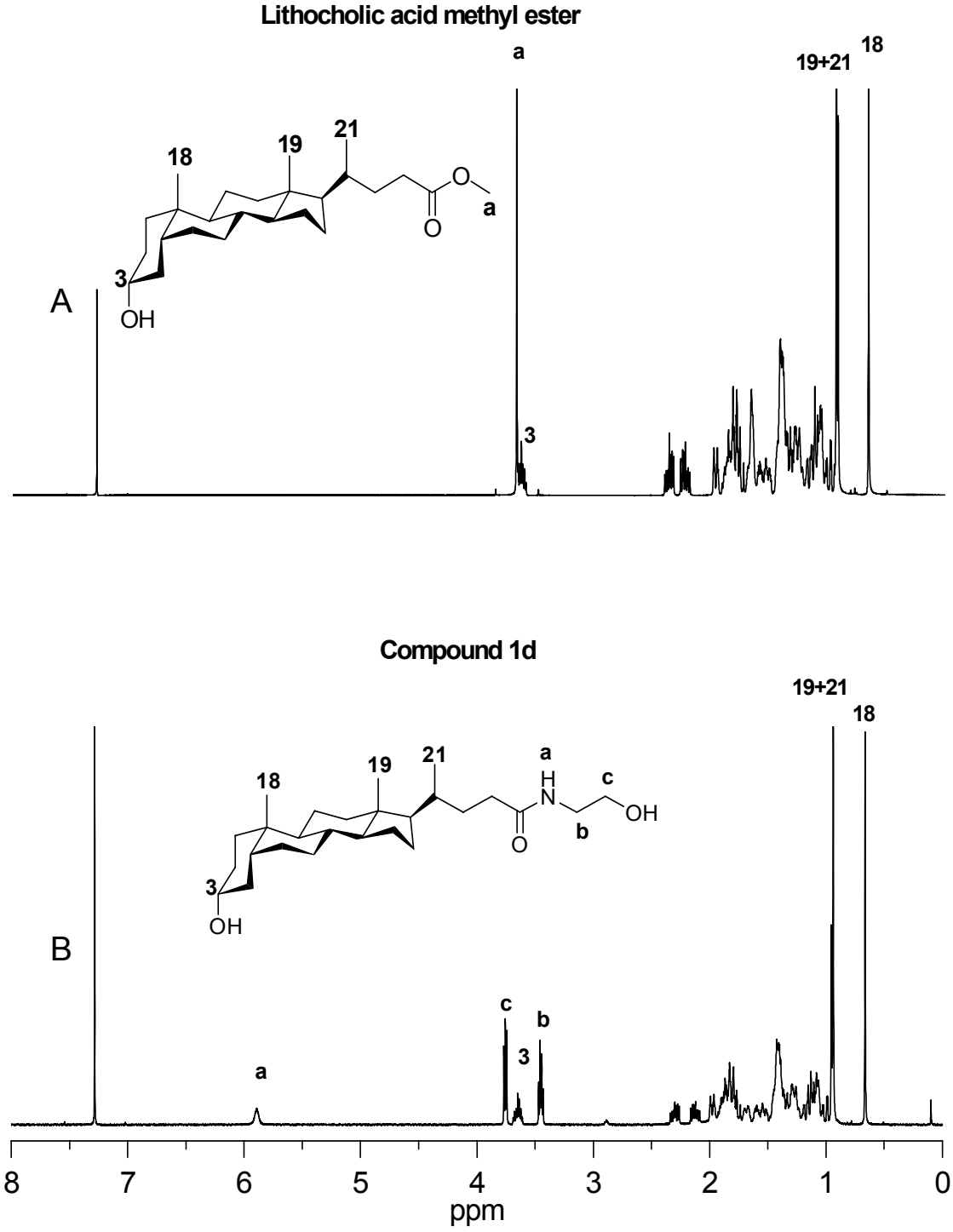

Figure A13. ^{1}H NMR spectra of (A) lithocholic acid methyl ester and (B) compound **1d** in $CDCl_3$.

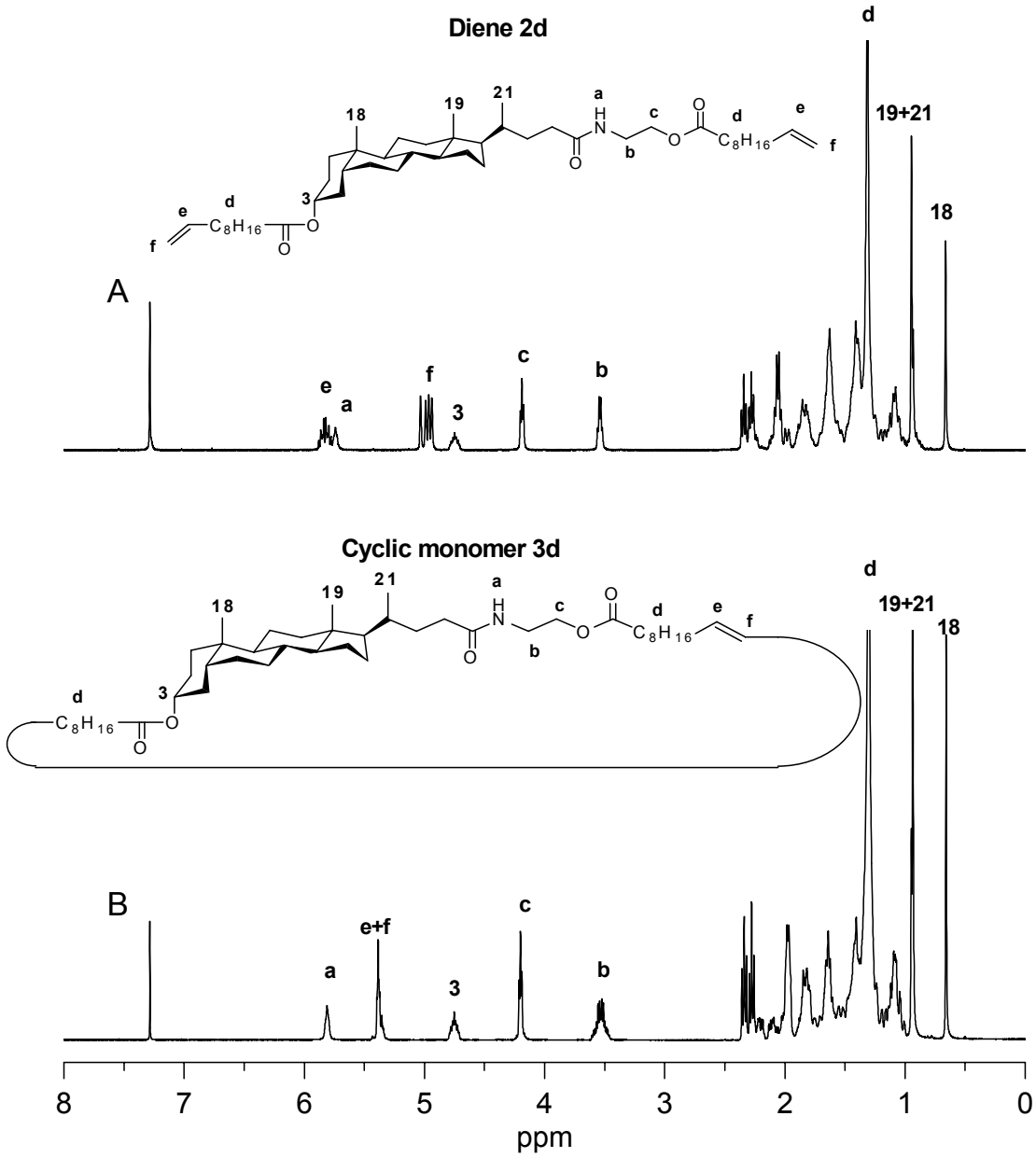

Figure A14. ^{1}H NMR spectra of (A) diene **2d** and (B) cyclic monomer **3d** in $CDCl_3$.

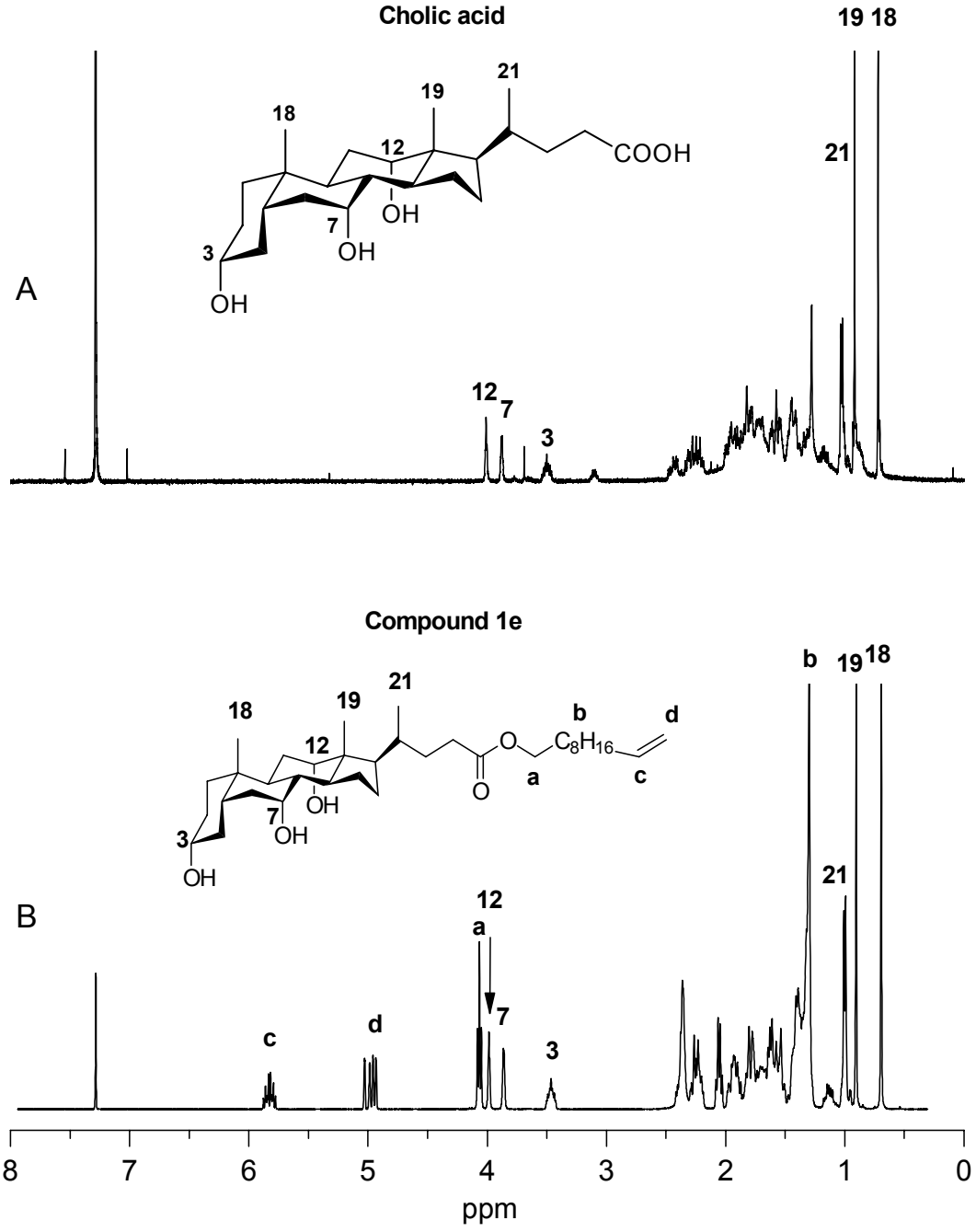

Figure A15. ^{1}H NMR spectra of (A) cholic acid and (B) compound **1e** in $CDCl_3$.

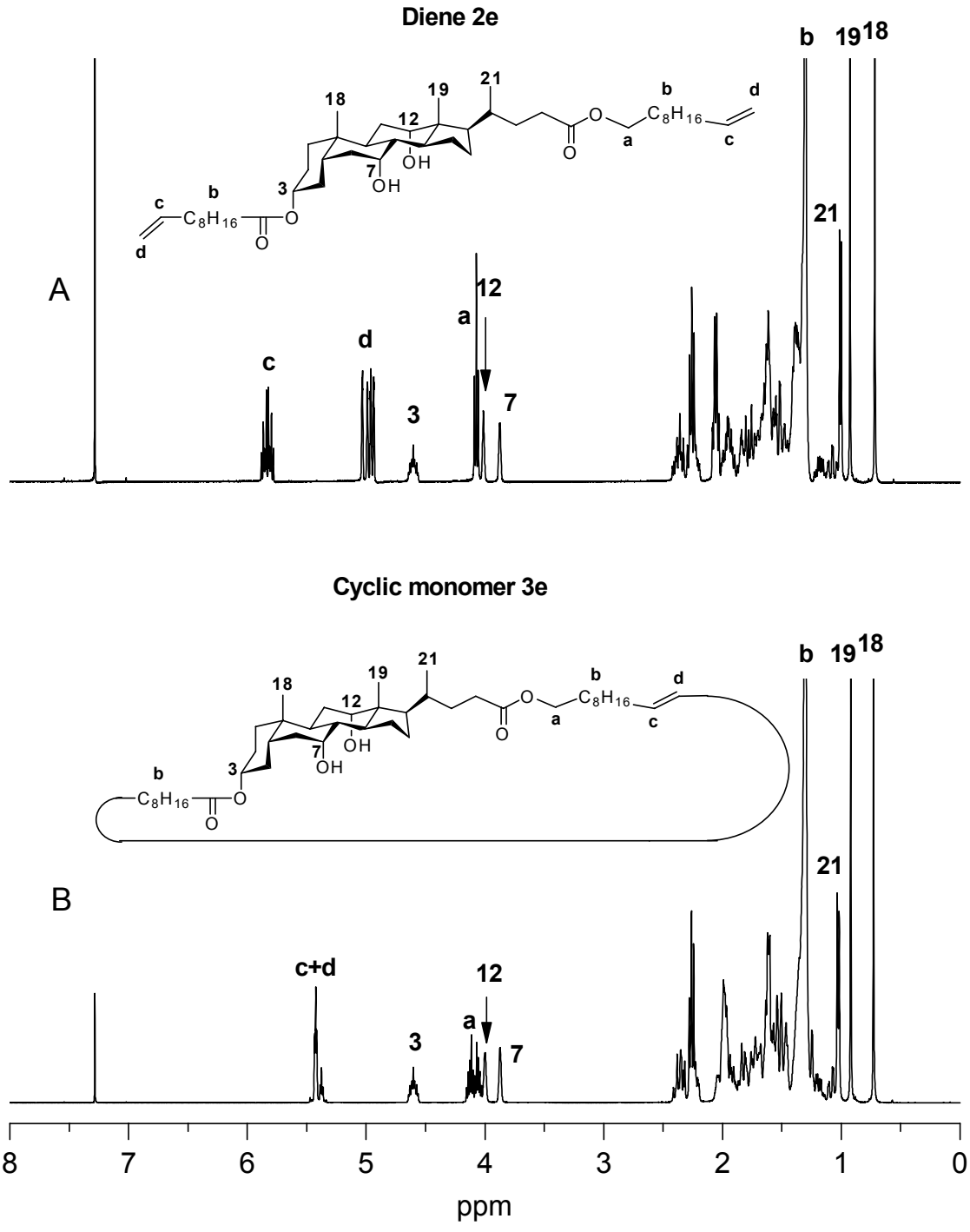

Figure A16. ^{1}H NMR spectra of (A) diene **2e** and (B) cyclic monomer **3e** in $CDCl_3$.

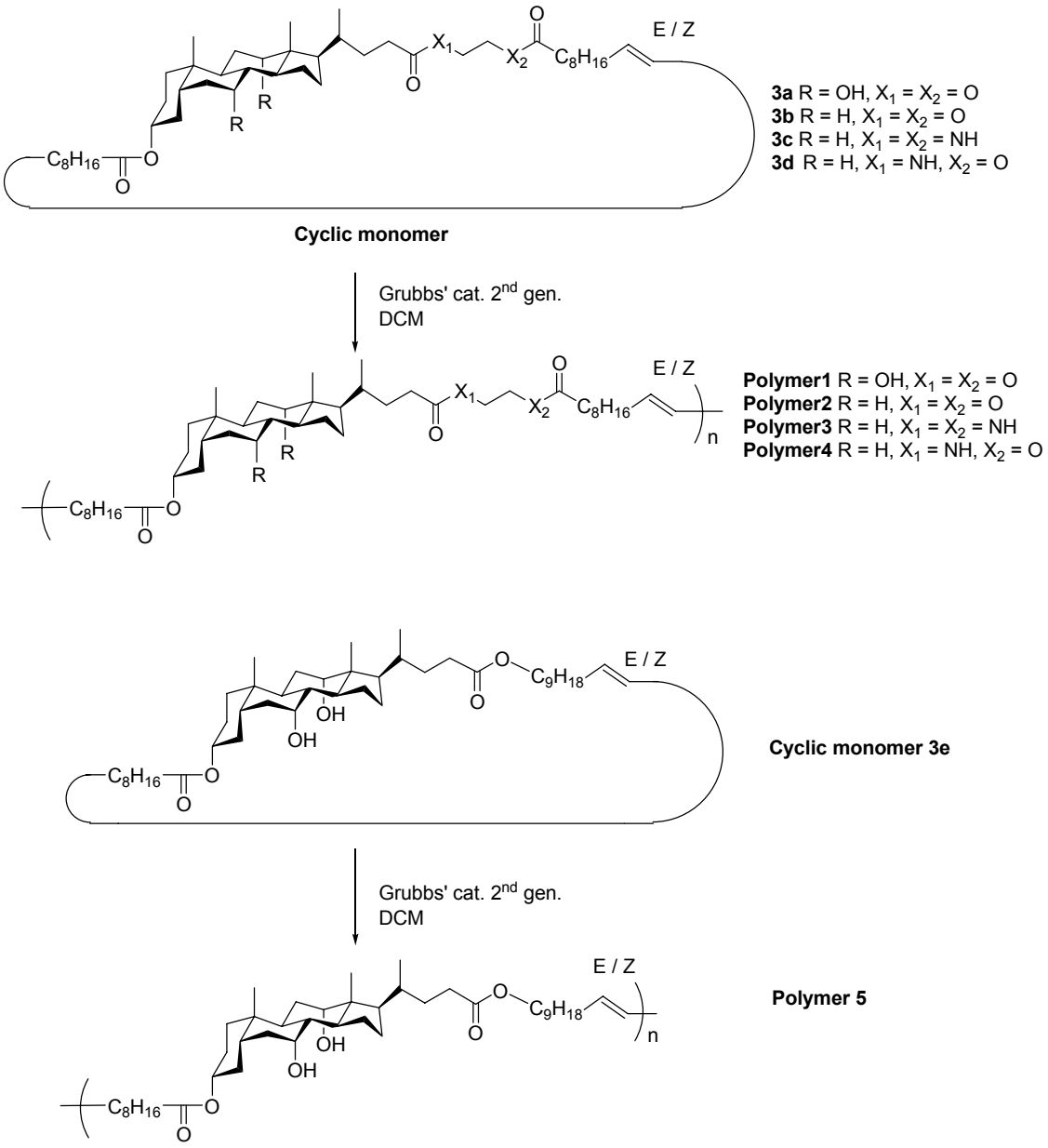

Figure A17. Preparation of polymers **1-5** via ring opening metathesis polymerization.

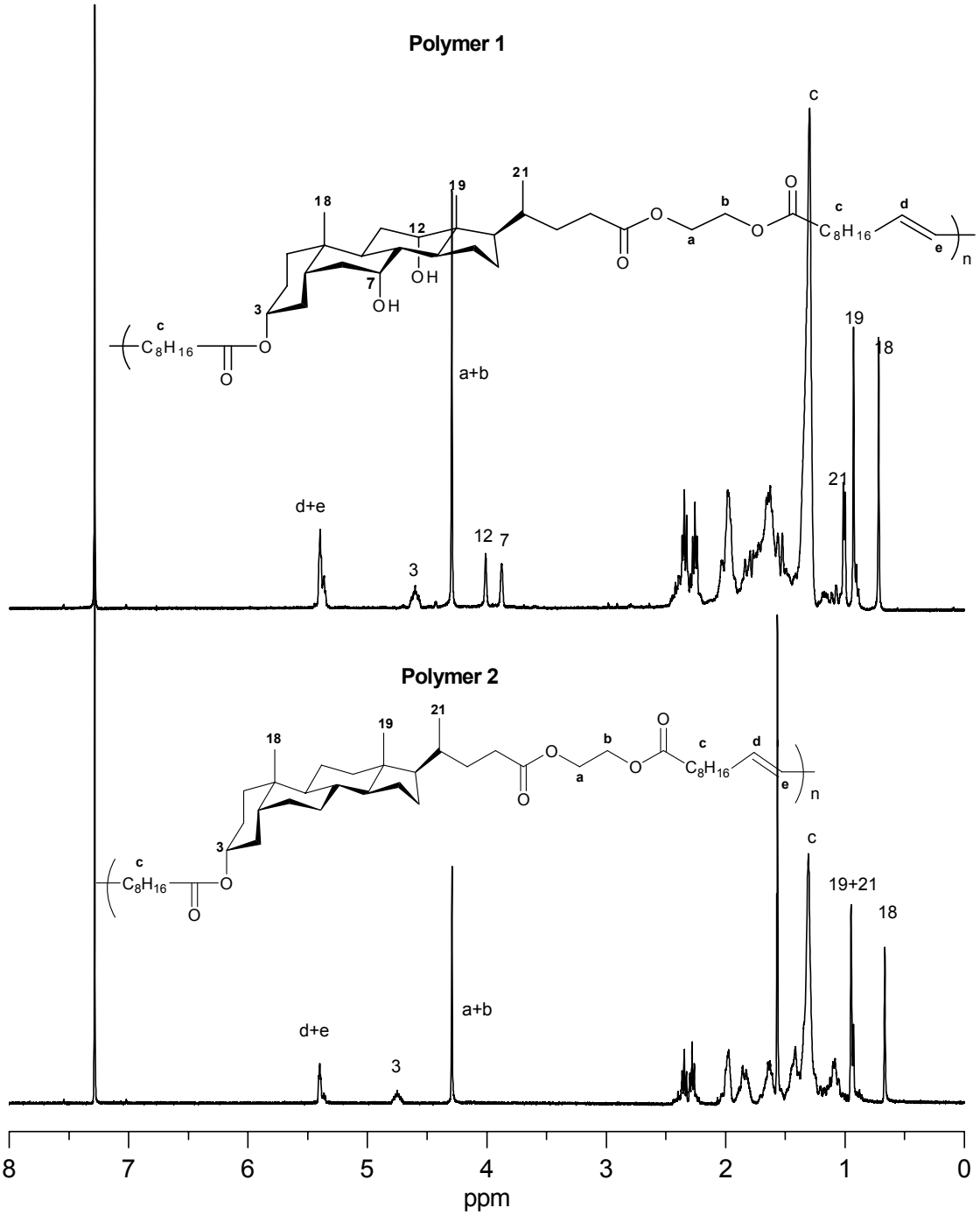

Figure A18. ^{1}H NMR spectra of (A) polymer **1** and (B) polymer **2** in $CDCl_3$.

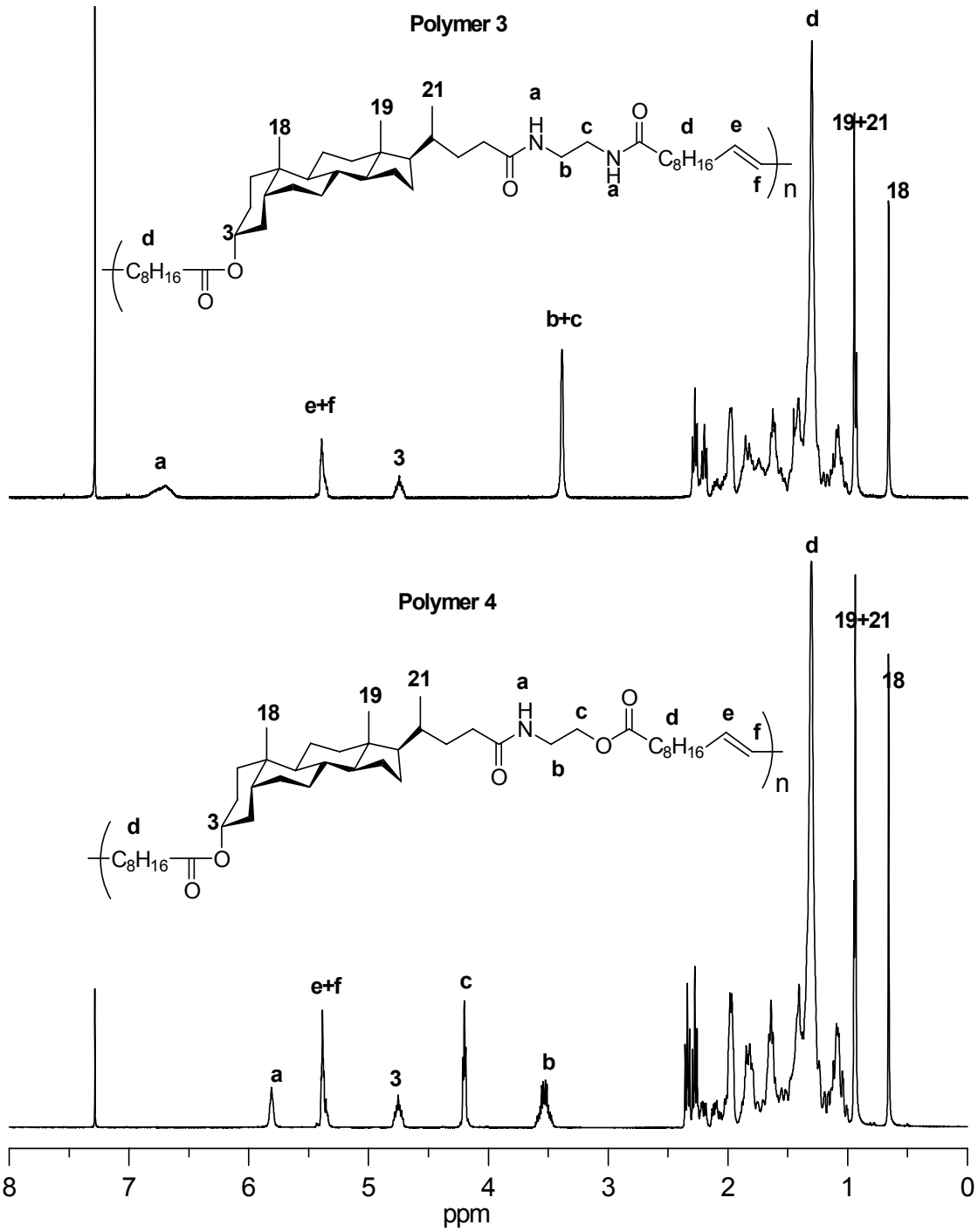

Figure A19. ^{1}H NMR spectra of (A) polymer **3** and (B) polymer **4** in $CDCl_3$.

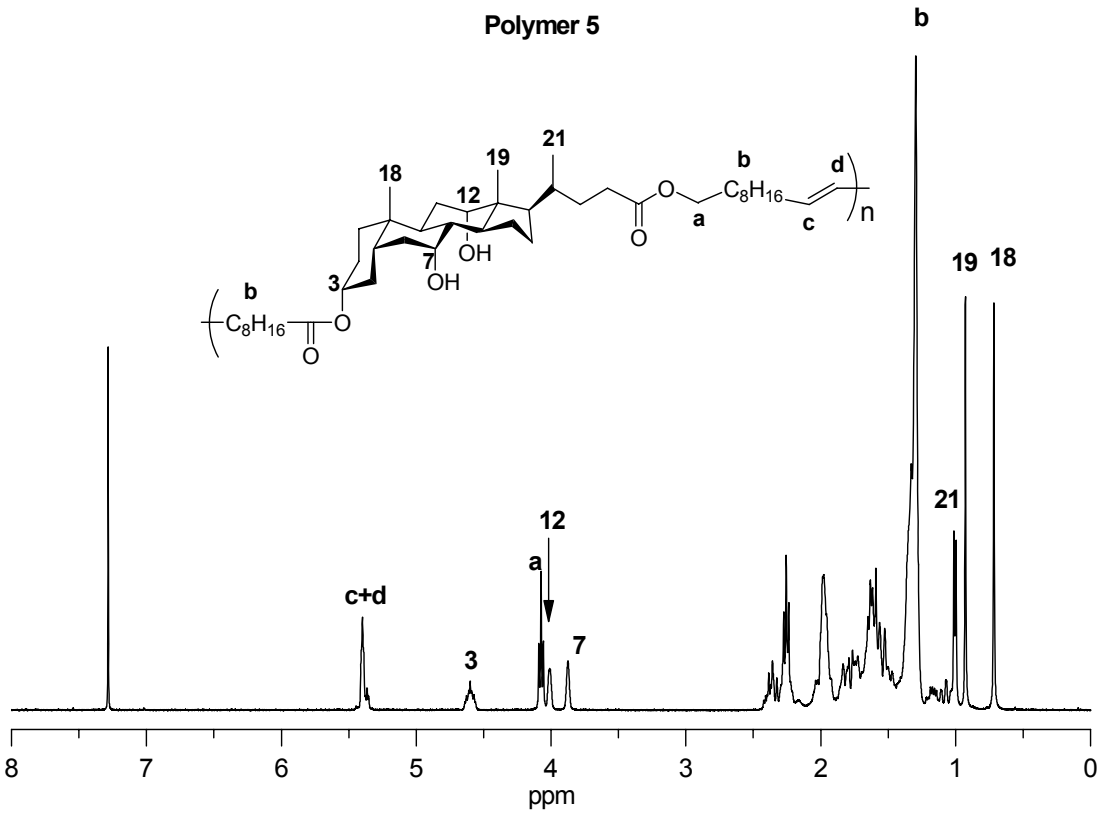

Figure A20. ^{1}H NMR spectra of polymer **5** in $CDCl_3$.

3. Liquid crystalline properties of polymer 3

Polymer liquid crystals have attracted much interest due to their unique properties and applications. Liquid crystalline (LC) polymers based on cholesterol moiety have been widely studied and documented.[1-4] Our recent study of side chain polymers based on cholic acid and its derivatives showed no thermotropic LC properties.[5] This is attributed to the less planar conformation of the bile acids in comparison to cholesterol.[5] It may be interesting to verify also if polymers with bile acids in the main chain present the same behavior. The chemical structure of the polymer shown in Figure 3.30 has been prepared via ROMP as described in Chapter 2.

Polymer **3** is the main-chain lithocholic acid-based polymer with two amide bonds and one ester bond. We found that it is possible to obtain LC phase for the lithocholic acid-based polymer and it was surprising since this polymer was previously thought to be amorphous in its pure form.[5] Interestingly, this polymer was found to show a LC property when treated with THF.

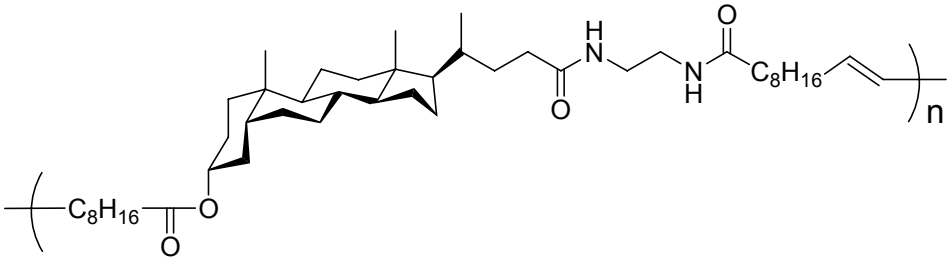

Figure A21. Chemical structure of the lithocholic acid-based polymer **3**.

The sample prepared from THF was studied with polarizing optical microscopy (POM) (Figure 3.31). At room temperature, it showed typical birefringence, suggesting an anisotropic structure. With the increase of the temperature, the birefringence decreased gradually, indicating the loss of intrinsic order with temperature. No abrupt disappearance of birefringence was found. Further annealing at 83 ^{o}C for 24 h did not result in any birefringence. Therefore the structure evolution inside the material may be

thermally irreversible. It should be noted that no birefringence was observed for the sample prepared from chloroform.

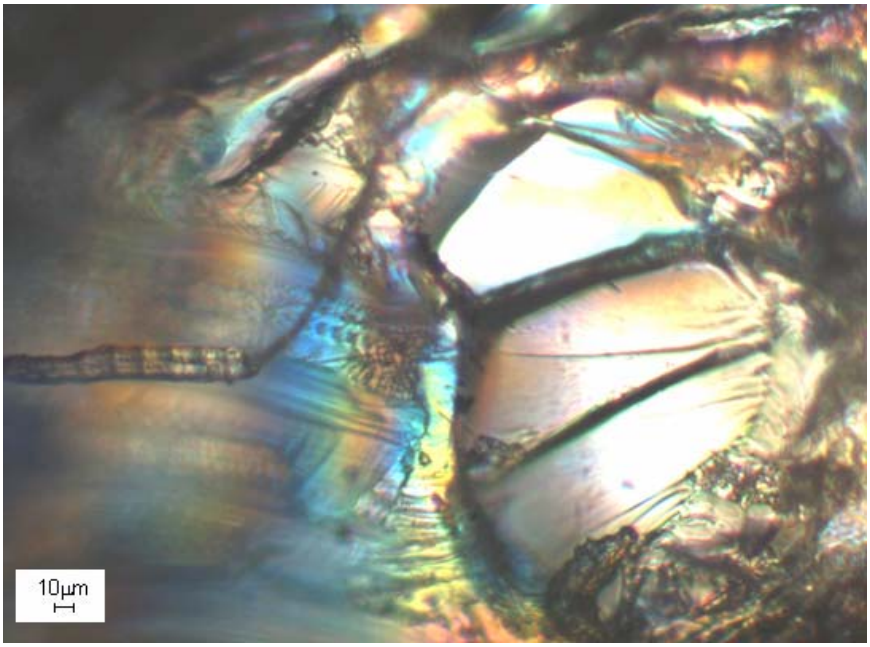

Figure A22. Polarizing optical micrograph taken at room temperature of polymer **3** obtained by precipitation from THF.

The thermal transformation of the samples was studied with DSC. The results are shown in Figure 3.32. The sample prepared from the chloroform solution shows only one glass transition at 83 ^{o}C (Figure 3.32 curve A). In contrast, the sample prepared from THF shows complex endothermal peaks (Figure 3.32 curve B). It is noted that this peak is not reversible in the cooling that followed. Only one glass transition (T_g = 83 ^{o}C) showed up in the following scans whether or not annealing (83 ^{o}C for 24 h) was done. These results in addition to the evidence from POM suggest that the sample obtained from chloroform is amorphous, while that from THF has some ordering.

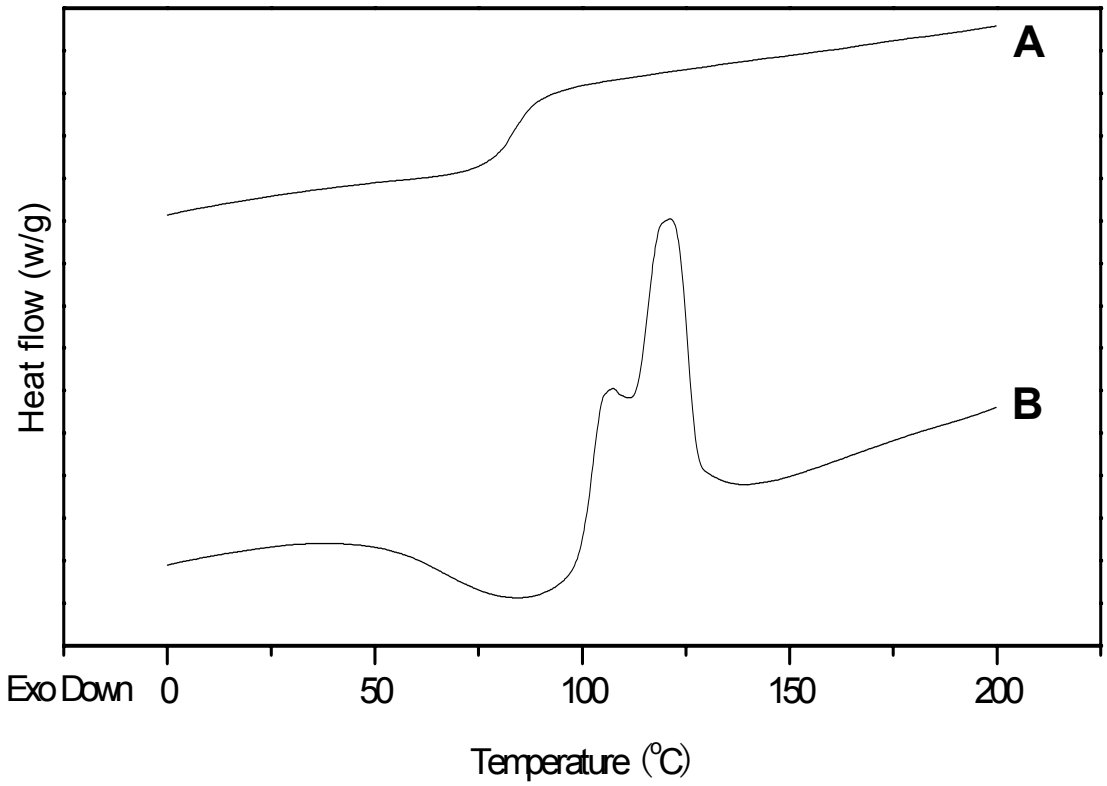

Figure A23. DSC traces of polymer **3**. (A) film cast from $CHCl_3$ solution, (B) precipitated from THF.

To further understand the phase transition in the sample prepared from THF, X-ray diffractograms recorded at various temperatures were taken and the results are shown in Figure 3.33. At room temperature, a diffraction peak, though broad to some extent, appeared at ca. 3° along with a big diffraction halo centered around 18°. This is usually found in liquid crystal structures, although the intrinsic order may not be defined enough here to confirm this. The appearance of only one broad peak at small angles makes it difficult to identify the real LC phase; only one peak at small angle may indicate a nematic phase. As a clear tendency, the intensity of broad peak at small angles decreased with increasing temperature, especially above 100 °C. This corresponds well to the observation in the DSC curve, in Figure 3.32, with the heat peak appearing at about 100 °C. The diffractogram taken at 119 °C shows a complete loss of the diffraction peak at

small angles, which suggests an amorphous state of the polymer. This remained here after cooling the sample to room temperature as well as after annealing at 83 ^{o}C for 24 h.

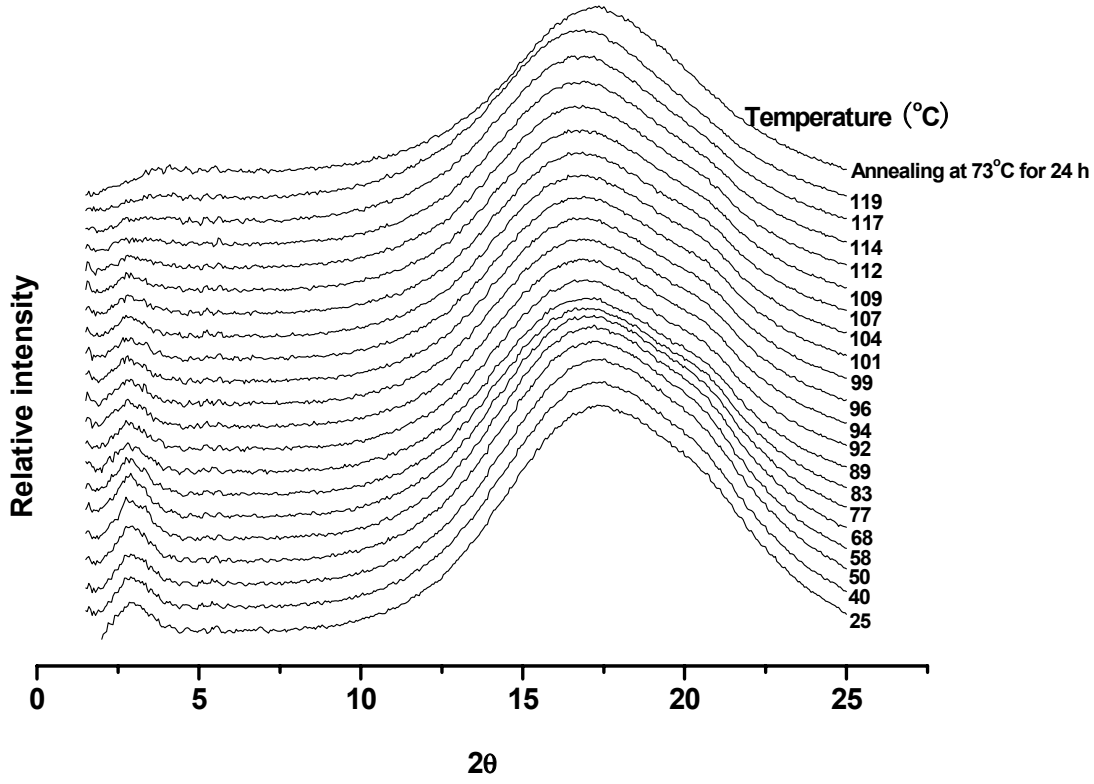

Figure A24. X-ray diffractograms of polymer **3** (LC) measured at different temperatures and at 73^{o}C for 24 h.

Polymer **3** precipitated from THF forms LC phase whereas film of polymer **3** cast from chloroform is amorphous. In order to understand the important role of THF in the formation of LC phase in the material, experiments were done for the comparison of these two samples.

The ^{1}H NMR spectrum of the polymer **3** (Figure 3.34) shows the presence of THF existing in liquid crystalline polymer **3**, as evidenced by the typical peak at 3.77 ppm, even though the material was dried in a vacuum oven at 83^{o}C for 24 h.

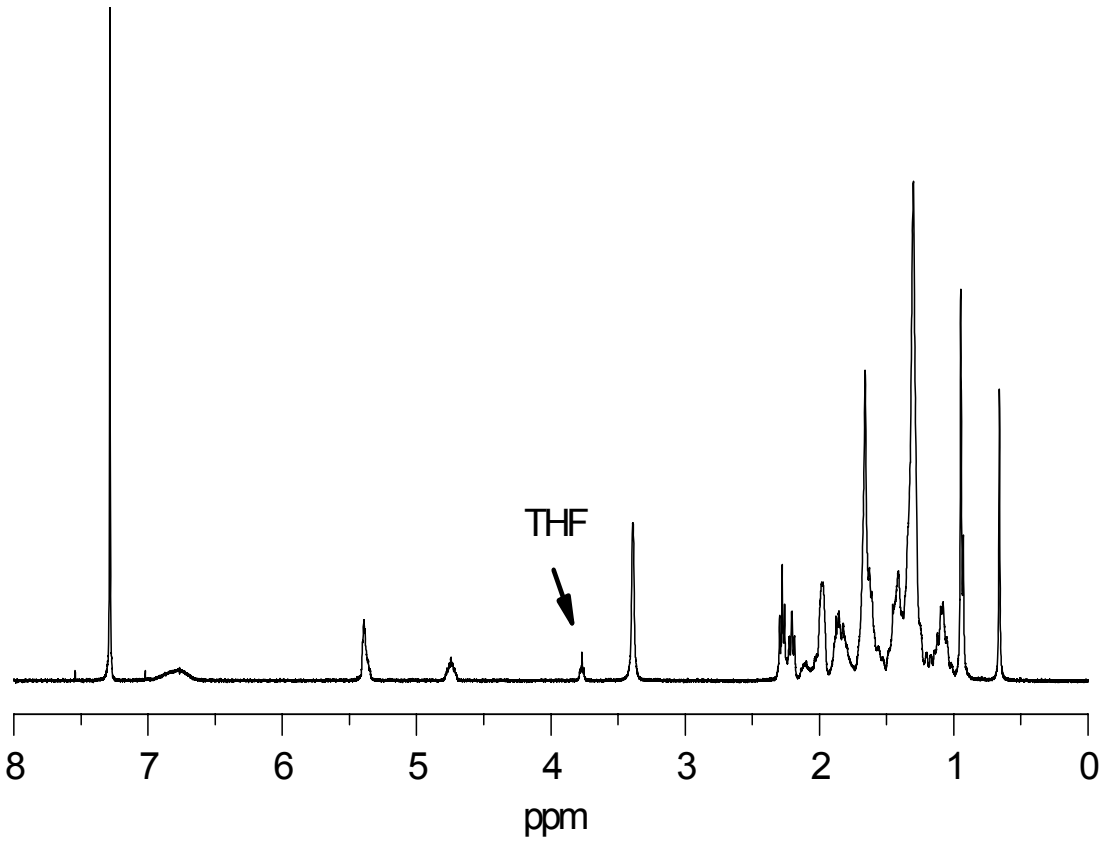

Figure A25. ^{1}H NMR spectrum of polymer **3** (LC, dried in vacuum at 83^{o}C for 24 h) in $CDCl_3$.

Figure 3.35 show the X-ray diffractograms of the precipitation from THF solution, obtained by casting from chloroform, and the same film after being placed in a THF vapor chamber for 72 h. The presence of a diffraction peak at a low angle (2.8^{o}, as indicated by an arrow in Figure 3.35), and a broad halo at high angles (9.6~25.0^{o}) indicate a typical LC structure.[6] Curves **A** and **C** in Figure 3.35 are the same, which indicates that a small amount of THF plays a critical role in the formation of LC phase. The polymers tested include polymers **1**-**5** and **7**-**8**, but only polymer **3** was found to have such a LC property.

In conclusion, te solvent, THF, is very critical for the formation of this LC phase.

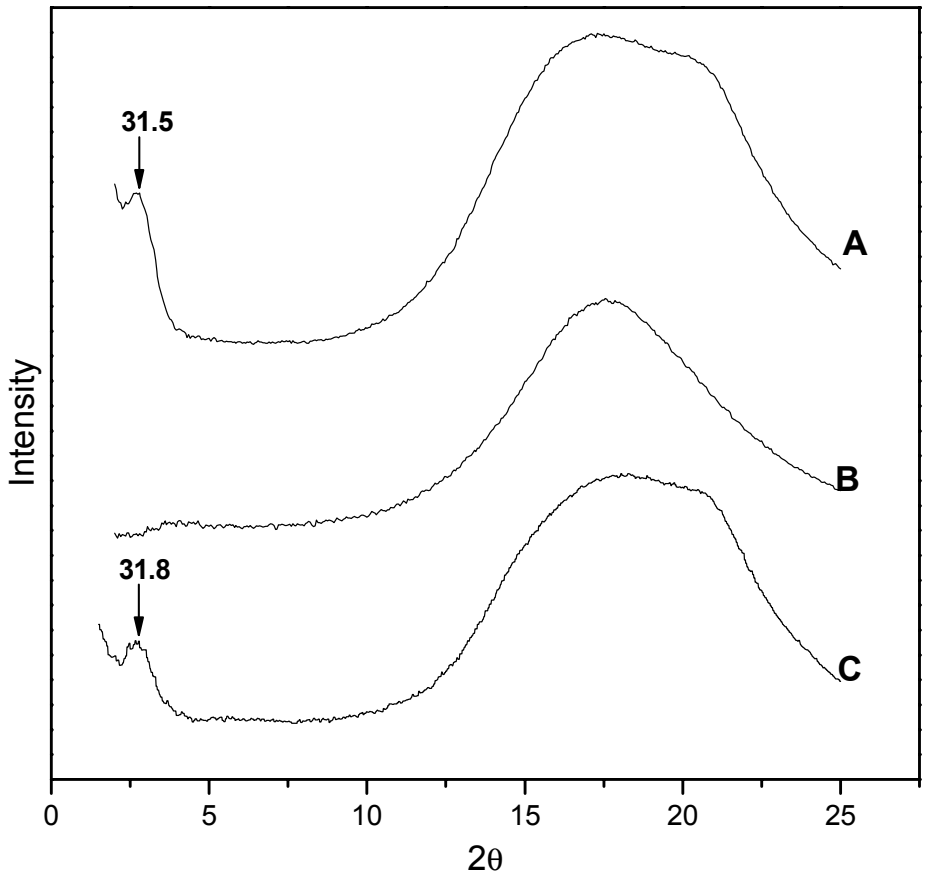

Figure A26. X-ray diffractograms at room temperature of polymer **3**, with Bragg spacings given in angstroms: (A) precipitated from THF; (B) film cast from $CHCl_3$ solution; (C) same film as in B, but equilibrated in THF vapor for 72 h.

References:

(1) Genzer, J.; Sivaniah, E.; Kramer, E. J.; Wang, J. G.; Xiang, M. L.; Char, K.; Ober, C. K.; Bubeck, R. A.; Fischer, D. A.; Graupe, M.; Colorado, R.; Shmakova, O. E.; Lee, T. R. *Macromolecules* **2000**, *33*, 6068-6077.

(2) Krishnan, S.; Kwark, Y. J.; Ober, C. K. *Chem. Rec.* **2004**, *4*, 315-330.

(3) Krishnan, S.; Wang, N.; Ober, C. K.; Finlay, J. A.; Callow, M. E.; Callow, J. A.; Hexemer, A.; Sohn, K. E.; Kramer, E. J.; Fischer, D. A. *Biomacromolecules* **2006**, *7*, 1449-1462.

(4) Youngblood, J. P.; Andruzzi, L.; Ober, C. K.; Hexemer, A.; Kramer, E. J.; Callow, J. A.; Finlay, J. A.; Callow, M. E.; *Biofouling*, **2003**, *19*, 91-98.

(5) Zhang, J. H.; Bazuin, C. G.; Freiberg, S.; Brisse, F.; Zhu, X. X. *Polymer* **2005**, *46*, 7266-7272.

(6) Kumar, S. Liq. Cryst. 2001.